SEISMIC RESISTANT DESIGN OF BUILDING STRUCTURES WITH RIGID BASEMENT LEVELS

by

Navid Abediasl

B.S., Civil Engineering, Islamic Azad University of Central Tehran Branch, 2016

Submitted to the Institute for Graduate Studies in
Science and Engineering in partial fulfillment of
the requirements for the degree of
Master of Science

Graduate Program in Civil Engineering
Boğaziçi University
2019

ACKNOWLEDGEMENTS

As a matter of appreciation it is my pleasure to send my great thanks to those people who had contribution in preparation and writing of this thesis.

I would like to state my gratefulness to my parents not only for their endless support and encouragement but also for the inspiration to choose Structural Engineering.

I would like to express my sincere gratitude to my thesis supervisor, Assoc. Prof. Kutay Orakçal, for his guidance, support, patience, kindness and encouragement throughout this thesis. Without his supports and leading it was almost impossible to accomplish this thesis.

Besides, I would like to express my special thanks to Associate Professor Serdar Soyöz and Professor Alper İlki for accepting to be in my thesis jury and for their valuable comments to my study and suggestions for future works.

I wish to thank dear research assistant Cem Tura who has also been a great teacher to me and without his dedication and effort I would not have been able to finish this work.

I would like to thank dear research assistant Aslı Keser for her guidance and invaluable comments through this study.

I would also like to thank my dear friends Mohsen Azimi, Reza Yari and Pedram Khatamino who always encouraged me, believed in me when I did not even believe in myself and helped me through difficult times.

ABSTRACT

SEISMIC RESISTANT DESIGN OF BUILDING STRUCTURES WITH RIGID BASEMENT LEVELS

In this study, a representative building with laterally-rigid basement levels is analyzed under design earthquake loads, using the latest approaches recommended in the Turkish Building Seismic Code 2018 (TBSC 2018). The same structure is used to apply the earthquake analysis methods suggested in the previous version of the Turkish Seismic Code (TEC 2007), as well as ASCE 7-10 and Eurocode 8, for comparative assessment of analysis results. In TBSC 2018, two main approaches are proposed for strength-based design of building structures with rigid basement levels. In the first approach, for buildings that satisfy the code definition to be considered as buildings with a rigid basement, it is permitted to consider the upper and the lower portion masses separately in the analysis, yet using the same structural model, since the two portions have modal characteristics that are well-separated from each other. This approach is similar to the methodology in the previous 2007 Turkish Seismic Code, as well as the Two-Stage Analysis method in ASCE 7-10. An interesting point about the TBSC 2018 method is the permission to use Modal Response Spectrum Analysis for the rigid lower system, which is not permitted in both TEC 2007 and ASCE7-10. Results obtained using another analysis method specified in TBSC 2018, which involves considering the total mass of the structure including the basement levels, referred to as the Total Structure Approach are also evaluated, using both the Equivalent Lateral Load and Modal Spectral Analysis procedures. Finally, a nonlinear model of the representative building is generated and Nonlinear Response History Analysis results are compared with the response quantities obtained using the TBSC 2018 methods, in order to assess the level of reliability or overconservatism in the different analysis methods specified in TBSC 2018.

ÖZET

RİJİT BODRUM KATLI BİNALARI DEPREME DAYANIKLI TASARIMI

Bu çalışmada, bodrum katları yanal olarak rijit olan örnek bir bina 2018 yılında yürürlüğe giren Türkiye Bina Deprem Yönetmeliği (TBDY 2018)'nin bodrumlu binalar için önerdiği en son yaklaşımları kullanılarak tasarım deprem yükleri altında analiz edilmiştir. Aynı bina bu tip binalar için 2007 yılında yürürlüğe giren Türkiye Bina Deprem Yönetmeliği (TBDY 2007)'nin, ASCE 7-10'un ve Eurocode 8'in deprem analizi için önerdiği yöntemler karşılıklı değerlendirme için kullanılmıştır. 2018 deprem yönetmeliğinde bodrumlu binaların dayanıma göre tasarımı için iki ana yöntem önerilmiştir. Birinci yöntemde yönetmeliğin tanımına uyan bodrumlu binaların alt ve üst bölümü kütlelerinin aynı analiz modelinde ayrı ayrı göz önüne alınmasına izin verilmiştir. Bu yaklaşım TBDY 2007'nin yöntemiyle birlikte ASCE 7-10'da iki aşamalı analiz olarak adlandırılmış yönteme benzerdir. TBDY 2018'e ilişkin ilgi çekici bir nokta ise rijit alt bölümün analizi için mod birleştirme yönteminin kullanılmasına izin verilmesidir; TBDY 2007 ve ASCE 7-10'da rijit alt bölüm için mod birleştirme yönteminin kullanılmasına izin verilmemiştir. TBDY 2018'de belirtilen diğer bir analiz yönteminden elde edilen sonuçlar ayrıca değerlendirilmiştir; bu yöntem bodrum kütlesi dahil tüm bina kütlesini eşdeğer deprem yükü ve mod birleştirme yöntemlerinde hesaba kattığı için tüm yapı yöntemi olarak adlandırılmıştır. Son olarak, örnek binanın doğrusal olmayan modeli hazırlanmıştır ve zaman tanım alanında doğrusal olmayan analizlerden elde edilen sonuçlar TBDY 2018'in farklı yöntemlerinden elde edilen sonuçların güvenilirlik veya aşırı güvenlilik derecesini değerlendirmek üzere karşılaştırılmıştır.

TABLE OF CONTENTS

LIST OF FIGURES

LIST OF TABLES

LIST OF SYMBOLS

A_0	Effective ground acceleration
A_S	Total area of longitudinal reinforcements
a_i	Span length between longitudinal reinforcements
b_0	Width of confined core
D	Overstrength factor
D_{lower}	Structure's lower portion overstrength factor
D_{upper}	Structure's upper portion overstrength factor
$\bar{D}_{lower}^{(X)}$	Structure's lower portion equivalent overstrength factor
$\bar{D}_{n,lower}^{(X)}$	Structure's lower portion equivalent overstrength factor at nth vibration mode
E_c	Tangent modulus of elasticity of concrete
E_{sec}	Secant modulus of elasticity of concrete
f_{cc}	Compressive strength of confined concrete
f_{ce}	Expected compressive strength of concrete
f_{ck}	Characteristic compressive strength of concrete
f_{co}	Compressive strength of unconfined concrete
f_e	Effective confining stress
$f_e(T)$	Linear elastic strength demand on the load-bearing system
f_{ex}	Effective confinement pressure on X direction
f_{ey}	Effective confinement pressure on Y direction
f_{sye}	Expected tensile strength of reinforcements
$f_y(\mu, T)$	Yield strength based on anticipated ductility capacity and period
g	Gravitational constant
G_c	Shear modulus of concrete
H_N	Total height above basement perimeter walls [m]
h_0	Height of confined core
I	Building importance factor
k_e	Confinement effectiveness factor

m_i	ith floor total mass [t]
$m_{ixn}^{(X)}$	ith floor modal efficient floor mass at n^{th} natural vibration mode in X-direction earthquake for the X axis of the building [t]
$m_{iyn}^{(X)}$	ith floor modal efficient floor mass at n^{th} natural vibration mode in X-direction earthquake for the Y axis of the building [t]
$m_{i\theta n}^{(X)}$	ith floor modal efficient floor mass at n^{th} natural vibration mode in X-direction earthquake rotating around the Z axis of the building [tm^2]
$m_j^{(s)}$	Seismic mass at node j
$m_{txn}^{(X)}$	Modal base shear efficient mass at nth natural vibration mode in X-direction earthquake for the X axis of the building [t]
QB	Basement live loads
QN	Superstructure live loads
R	Load-bearing system behavior coefficient
R_{lower}	Structure's lower portion load-bearing system behavior coefficient
R_{upper}	Structure's upper portion load-bearing system behavior coefficient
$R_a(T)$	Earthquake reduction factor based on anticipated ductility capacity
$(R_a)_{lower}$	Equivalent earthquake load reduction factor for the lower portion of the structure
$(R_a)_{n,lower}$	Equivalent earthquake load reduction factor for the lower portion of the structure at nth vibration mode
$(\bar{R}_a)_{lower}$	Equivalent earthquake load reduction factor for the lower portion of the structure in total structure approach
$(\bar{R}_a)_{n,lower}$	Equivalent earthquake load reduction factor applied to the lower portion of the structure at nth vibration mode
$(R_a)_{upper}$	Equivalent earthquake load reduction factor for the upper portion of the structure
$R_y(\mu_k, T)$	Yield strength reduction coefficient based on anticipated ductility

S_1	Spectral acceleration coefficient for 1s period
S_S	Spectral acceleration coefficient for short period
$S_{ae}(T)$	Elastic spectral acceleration at period T [g]
S_{aer}	Record spectral elastic acceleration
S_{aet}	Target spectral elastic acceleration
$S_{aR}(T)$	Reduced design spectral acceleration at period T [g]
S_{D1}	Design spectral acceleration coefficient for 1s period
S_{DS}	Design spectral acceleration coefficient for short period
s	Spacing between confinements
T	Fundamental natural period [s]
T_A	Left corner period of spectrum [s]
T_B	Right corner period of spectrum [s]
T_L	Constant spectral displacement range period limit [s]
T_p	Fundamental period of the structure
u_{max}	Maximum top displacement
u_y	Top displacement at yielding point
$V_{tE}^{(x)}$	Total equivalent earthquake load applied to the overall structure in the X-direction (base shear load) [kN]
$V_{x,total}^{(x)}$	Calculated base shear force under earthquake effect in X-direction for total building (upper + lower portion) [kN]
$V_{x,upper}^{(x)}$	Calculated base shear force under earthquake effect in X-direction for structure's upper portion [kN]
$w_j^{(s)}$	Seismic weight at node j
$w_{G,j}^{(s)}$	Seismic weight at node j from dead loads
$w_{Q,j}^{(s)}$	Seismic weight at node j from live loads
γ_c	Specific weight of concrete
$\Gamma_n^{(X)}$	nth mode modal participation factor for X-direction earthquake
ϵ_{cc}	Strain at compressive strength of confined concrete
ϵ_{co}	Strain at compressive strength of unconfined concrete
ϵ_s	Strain at reinforcing steel

ϵ_{sh}	Strain hardening initiation strain
ϵ_{su}	Ultimate strain capacity
λ_c	Confined concrete strength modifier
μ_k	Anticipated ductility capacity for load-bearing system
$\nu^{(X)}$	A coefficient utilized for the calculation of structure's lower portion equivalent earthquake loads reduction coefficient
ν_c	Poisson's ratio of concrete
$\nu^{(X)}_{lower}$	A coefficient to calculate structure's lower portion reduced internal forces derived from its own vibration
$\nu^{(X)}_{upper}$	A coefficient to calculate transmitted internal forces from upper portion to the lower portion of the structure
ρ	Redundancy factor
ρ_x	Confinement ratio on X-direction
ρ_y	Confinement ratio on Y-direction
ΣX	Total mass participation ratio on X-direction
ΣY	Total mass participation ratio on Y-direction
$\Phi_{i(X)n}$	ith floor n^{th} natural vibration modeshape amplitude in X-direction earthquake
Φ_{ixn}	ith floor n^{th} natural vibration modeshape amplitude in X axis
Φ_{iyn}	ith floor n^{th} natural vibration modeshape amplitude in Y axis
$\Phi_{i\theta n}$	ith floor n^{th} natural vibration modeshape amplitude rotating around Z axis

LIST OF ACRONYMS/ABBREVIATIONS

ASCE	American Society of Civil Engineers
BHC	Building Height Class
BUC	Building Usage Category
CSI	Computers and Structures, Inc.
DOF	Degree of Freedom
EDC	Earthquake Design Class
EL	Earthquake Level
ELF	Equivalent Lateral Force
FEM	Finite Element Modeling
RSA	Response Spectrum Analysis
NLRHA	Nonlinear Response History Analysis
PGA	Peak Ground Acceleration
PGV	Peak Ground Velocity
SDF	Single Degree of Freedom
SRSS	Square Root of Sum of Squares
TBSC	Turkish Building Seismic Code
TEC	Turkish Earthquake Code
TS	Turkish Standard

1. INTRODUCTION

1.1. General

Increase in population, together with industrial and economical developments and insufficient improvements in public transportation means, has tremendously promoted purchasing of private automobiles in Turkey. The continuous increase in the number of privately-owned cars necessitates significant parking space in densely-populated cities. Municipal authorities have recently enforced specifications for new buildings to include parking areas in their basements, which means that new buildings structures will include more basement stories. In the new Turkish Seismic Code (TBSC 2018) particular attention is given to analysis methods for determining the earthquake loads on the rigid basement floors of buildings, through new and alternative analysis approaches, which has motivated this study on comparative evaluation of code-prescribed analysis methods for determining design-level earthquake effects on building structures with laterally-rigid basement levels incorporating perimeter walls [1].

For building structures with basement levels, four linear elastic strength-based analysis methods are offered in the new Turkish Seismic Code, which includes two alternative Equivalent Static Lateral Force methods and two alternative Response Spectrum Analysis Methods. As a case study, a representative 11-story reinforced concrete building structure with two basement levels is investigated in this study. The equivalent lateral force and response spectrum analysis methods are applied on a structural model of the building generated using the widely-used analysis software CSI ETABS, for applying the respective analysis methods specified of the seismic code and comparison of analysis results.

In the new Turkish Seismic Code, for a structure that is categorized as a building with a laterally-rigid basement, it is recommended to consider the upper and lower portion masses of the structure separately, but using a single analysis model, which is called a two-stage loading analysis approach. It means for the first stage only the upper-structure masses are considered to obtain the upper-structure response quantities, while the lower-portion masses are neglected. However, the stiffness of the lower portion is considered in the analysis model because of the existence of the lower-portion structural elements in the model. Similarly, in order to obtain the lower-portion response quantities, the upper-portion masses are neglected in the model of the structure. This method appears to be similar to the two-stage analysis approach in ASCE 7-10; however, it is different in the sense that ASCE 7-10 uses not only a two-stage but also a a two-model approach where the flexible upper structure is first modeled as a fixed-supported separate structure, and the rigid basement is then modeled and analyzed as a second separate structure. On this separate model of the rigid basement, the earthquake effects that are transferred to the basement from the upper structure (the support reactions at the fixed supports of the upper-structure model) are also applied.

Moreover, an alternative method is introduced in TBSC 2018 for analysis of buildings with rigid basement levels, which is called the total structure approach. In this approach, for obtaining the design earthquake forces acting on the basement levels of the building, a specific earthquake load reduction factor called $(\bar{R}_a)_{lower}$ is defined for the basement levels, which can be used in either the Equivalent Lateral Force or the Modal Response Spectrum analysis methods. Calculation of the aforementioned earthquake load reduction factor for the basement levels is based on the ratio of the base shear forces developing at the base of the upper structure (at the top of the perimeter walls) and at the base of the total structure (at the foundation level). As will be demonstrated in this study, although the total structure approach is allowed for the analysis of the structures including basement levels, it is more suitable for the analysis of mixed (along building height) structural systems that have behavior coefficients that are not too separated from each other (e.g., buildings with structural steel stories on top of reinforced concrete stories).

In this study, TBSC 2018 methods of analysis are applied on the aforementioned representative building with rigid basement levels. The analysis results (the story shear forces and the shear forces on structural walls in particular) are compared with each other. Analysis results are also compared with the results of the analysis approaches specified in ASCE 7-10 and Eurocode 8. Furthermore, results of the code-prescribed analysis methods are compared with Nonlinear Response History Analysis results conducted on the building under ground motion records that were scaled to match the design spectrum, in order to assess the accuracy of the different analysis methods in the code, as well as possible lack of safety or over-conservatism incorporated in the methods.

1.2. Background

1.2.1. Strength-Based Seismic Design

Based on TBSC 2018, Strength-Based Design is one of the two main design approaches under earthquake load effects, which considers adequate capacity of the structural elements to resist earthquake forces that are reduced based on code-prescribed reduction factors, which depend on the ductility level of the structural system. In this approach, based on an expected performance level of life safety, reduced earthquake loads are defined with respect to the corresponding system behavior factor. Under reduced earthquake loads, linear elastic structural analysis is conducted to obtain internal forces. Over-strength factor should also be considered for obtaining the internal forces that can lead to non-ductile (e.g., shear) failure modes. Accordingly, the capacities of the elements and the strength demands are compared for design. Furthermore, relative story displacements are compared with the limit values specified in the code. Strength demands should be less than strength capacities while relative story displacements should also be less than the permitted limits. Otherwise, element sections and or-reinforcement should be changed and the aforementioned procedure has to be checked respectively. Finally, the detailing requirements in the seismic code need to applied to make sure the structural elements and the structural system possesses adequate ductility capacity.

It is not feasible to design structures behave linear elastically (with no damage) during severe earthquake scenarios. Therefore, the structures are designed for much lower earthquake loads than those expected on linear elastic structures. In seismic codes, a behavior factor which has an empirical origin is used to reduce linear elastic forces for design purposes in order to consider the nonlinear response of a structure. Due to the fact that inelastic displacements are irreversible, a permanent damage is expected to remain in the structures after an earthquake event [2]. Accordingly, an anticipated level of in-elasticity in structural systems during an earthquake event is defined by the use of behavior factors (R-factors). Definition of R-factors accounts for an inherent ductility level which measures the ability of structural elements to deform in-elastically. Since a flexible upper structure (with ductile detailing) and a rigid lower basement (where most of the earthquake forces are resisted by the perimeter walls, which are not designed and detailed for ductile behavior) have different ductility levels, it is significant to consider an appropriate behavior factor for each portion to be able to expect an adequate deformation level to dissipate earthquake energy through the aforementioned inelastic behavior [3].

Moreover, an over-strength factor of is defined in modern seismic codes, including the new Turkish Seismic Code, which is presented in Figure 1.1 In the strength-based design approach, over-strength factor is defined as the ratio of the expected capacity (e.g., yield strength) over the design-level capacity (which incorporates material strength reduction factors as well as simplifications in capacity calculations) (Equation 1.1).

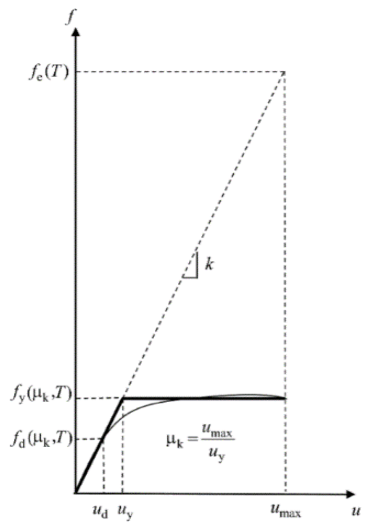

Figure 1.1. Stipulated Ductility Capacity – Strength Demand.

$$f_d(\mu_k, T) = \frac{f_y(\mu_k, T)}{D} \tag{1.1}$$

Respectively, for a constant level of ductility capacity (μ_k) the relation between over-strength factor (D) and load-bearing system behavior factor (R) is defined in Equations 1.2 and 1.3 where I is building importance factor.

$$\mu_k = \frac{u_m ax}{u_y} \tag{1.2}$$

$$\frac{R}{I} = \mu_k D \tag{1.3}$$

On the other hand, in terms of collapse prevention, over-strength factor plays a significant role. Structural over-strength relation with other structural parameters is investigated through an article by Taieb *et al.* (2014) [4]. This paper states that the increase in ductility demand increases the over-strength factor. By taking the advantage of structures over-strength and ductility capacities many seismic codes give the permission to reduce design loads. Besides, the lateral load capacity of structures with vertical geometric irregularity are lower than regular structures. In addition, for a constant ductility value the over-strength factor for beams is higher than that in columns which means the effect of column ductility factors on the over-strength factor is less than beam ductility factors effect. In conclusion, a comparison between moment resisting frame systems and frame-wall systems demonstrates the fact that the more the structures are rigid, the higher over-strength factor is.

1.2.2. Two-Stage Analysis Approach

Due to the fact that the stiffness values of a flexible upper structure is different than a rigid lower portion in terms of dynamics the superstructure modes has a negligible effect on the lower structure while the lower system has almost zero effects on the upper part likewise. Accordingly, the period values are almost the same when the total structure (upper + lower portion) is considered in comparison to the case when only the upper structure is considered. In respect of the dynamic specifications of the rigid lower portion the fundamental period values are close to zero. With regard to SDF response spectrum the effective acceleration for the lower portion is almost equal to PGA.

As mentioned, based on ASCE 7-10 considering the upper and lower portion separately because of their totally different dynamic properties is called two-stage analysis which is almost in the same manner of the new Turkish seismic code guidelines. Although, in the direction of ASCE 7-10 the method is a two-model analysis procedure while a single model approach is introduced by TBSC 2018. Thereby, a literature review is done at this stage to observe the advantages and shortcomings of two-stage analysis method provided by ASCE 7-10 [5].

Two-stage analysis is introduced to the Uniform Building Code in 1988. It has been used by structural engineers because of its simplification to analyze and design of a flexible structure supported by a rigid portion. This method permits a proper base shear scaling using R-factors of the two structures. However, in spite of its purpose for simplicity, implementation of two-stage analysis may be difficult in complicated structures like multi-towers on a mutual rigid podium. Since, it is not mentioned clearly which fundamental period of the overall structure should be used for the seismic analysis of this type of structures.

In the study by Allen *et al.* (2013) through implementation of two-stage analysis on two new hospitals besides the evaluation of an existing hospital building, the advantages and limitations of this method are discussed [6]. To begin with, as an advantage a two model process will save engineers analysis iterations and enable to work in two groups separately while the integrity of the analysis is considered. However, the two model approach may have other shortcomings in comparison to one model which is introduced in the new Turkish Seismic Code. Furthermore, the simplicity of transferring scaled forces from upper structure to the lower system is another convenience provided by two-stage analysis in which seismic load demands from flexible upper portion are assigned statically to the lower portion during the analysis of the lower system no matter which analysis method is performed to obtain upper system responses. In addition, two-stage analysis states that the two structure (upper and lower portion) have different stiffness and structural behaviors so it is acceptable to analyze them independently. However, as a shortcoming in compliance with ASCE 7-10 it is not explained exactly how to utilize proper R-factors respective to the ductility demands for the two portions. However, in the new Turkish Seismic Code it is recommended to consider $(R/I) = 2.5$ for the lower portion. Additionally, it is stated clearly to select appropriate R value in the direction of expected ductility for the upper system from its relative table given in the code. Moreover, another imperfection of two-stage analysis is the lack of provision about the specific elements in the transition part between the upper and lower systems. Plus, there is no requirement to consider over-strength load cases of the lower system. Finally, despite the fact that the intent of ASCE 41-06 Chapter 10 is to provide guidelines for partial retrofits but there is not enough information to check the adequacy of existing structures using two-stage analysis.

In another study by Yuan (2016) where a two-model analysis method was used, it is observed that the stiffness provision of ASCE7-10 for two-stage analysis procedure may be improper [7]. Since in specific cases the underestimation of upper system base shear force may occur. Furthermore, in this document a specific case where upper and lower structure damping ratios were assumed to be different than each other is studied which demonstrates that the approximation of the equivalent modal damping ratio in certain cases may lead to significant errors in seismic load calculation.

In addition, the study by Lee *et al.* shows that excluding the basement in the analytical model of high-rise buildings leads to overestimate the lateral stiffness of the structure which occurs due to the ignorance of the flexibility provided by the basement [8]. By doing so, it not only may shorten the fundamental natural period of the structure but also may cause misestimation in the dynamic response of the structure especially for structures consist of shear wall systems in which basement plays a significant role. Furthermore, this study demonstrates the fact that if rigid diaphragm assumption is done for the basement structure the story shear forces of this portion may extremely overestimated since the flexibility is ignored. Accordingly, an analysis method considering partial rigid diaphragms including the basement effects is proposed for the analysis of high-rise buildings.

Due to the fact that alternative linear elastic analysis methods are introduced by TBSC 2018 for the analysis of mixed in-height structures with different behavior factors, a valuable document by T. Papageorgiou *et al.* is investigated [9]. Accordingly, in respect of most common cases the coexistence of various structural materials (which leads to nonuniform damping as well as elasto-plastic characteristic over the height of the building) is determined. In this case, lower portion is usually a primary concrete structure while a steel upper part is constructed as a secondary system. The various damping characteristics and energy dissipation of the two parts are emphasized since reinforced concrete structures exhibit higher damping which is around 5% in comparison to steel structures with 2% damping in respect of design codes. Therefore, two analysis approaches are investigated for the design of the mixed in-height structures. Firstly, the two structures are decoupled in order to be able to analyze them as separate homogeneous parts. Thereby, concrete part is excited by the ground acceleration and the response is applied as a fictitious excitation at the support level of the upper system. However, decoupling errors are observed due to the fact that the analysis procedure is in contrast to the actual structure. On the other hand, for the cases in which the decoupling errors are above the limits a coupled approach is utilized in respect of equivalent modal damping ratios. Moreover, reference decoupling error levels are defined based on the fundamental eigenfrequencies and the mass ratios of secondary to primary structure in order to help engineers to decide if a convenient decoupled analysis can be used or not.

1.2.3. Scope and Objective

In this study the seismic design approach for a representative building structure with rigid basement levels is investigated through the application of the new Turkish Seismic Code provisions. In general, there are two main approaches recommended by the new code, the first being the Two-Stage approach and the second being the Total

Structure approach. Upon comparison of analysis results, the most practical and reliable approach is identified in this study for the analysis of the structure using the Total Structure methodology. Besides, the representative building is analyzed using ASCE 7 and Eurocode 8 provisions, as well as previous Turkish Seismic Code specifications. Relevant response quantities (story shear forces in particular) obtained for the upper and lower portions of the structure are compared and evaluated. Analysis results are also compared with results of Nonlinear Response History Analyses conducted on a nonlinear model of the structure, under ground motion records scaled to match the design spectrum. Observations and recommendations are presented on the reliability of the code-based analysis methods.

1.2.4. Thesis Outline

In chapter 1 of this thesis, general information on the topic of this study is provided and the motivation of this study is presented. Existing documentation on the topic is cited and the scope of the study is presented. In chapter 2, analysis methods specified in the 2018 Turkish Building Seismic Code, as well as ASCE 7-10 and Eurocode 8, and their application on a representative building structure, are presented. As well, the procedures used for nonlinear structural modeling, selection of appropriate earthquake records, and nonlinear response history analysis of the structure are described. Important response quantities obtained from the code-based analysis methods and those obtained from the nonlinear response history analysis are compared and discussed in chapter 3. Finally, a summary, conclusions and recommendations for future studies are provided in chapter 4.

2. METHODOLOGY

In this chapter, analysis methods specified in the 2018 Turkish Building Seismic Code for building with laterally rigid basement levels are first described. Afterwards, the provisions and analysis methods specified in ASCE 7-10, as well as Eurocode 8 documents are discussed. The application of code-based analysis approaches on a representative building structure are presented. As well, the procedures used for non-linear structural modeling, selection of appropriate earthquake records, and nonlinear response history analysis of the structure are described.

2.1. Building Properties

The representative reinforced concrete building structure used in this study for the application of the seismic-code-based analysis methods consists of 9 stories above and 2 stories below ground level. Total height of the structure is 32.50 m (Figure 2.1, Figure 2.2 and Figure 2.3). The height of normal floors are typically 2.9m while the height increases to 3.8m at basement floors. The lateral load resisting system consists of two U-shaped and two rectangular structural walls. The floor system is flat plate, with perimeter beams. The basement floors are brought into service as parking areas.

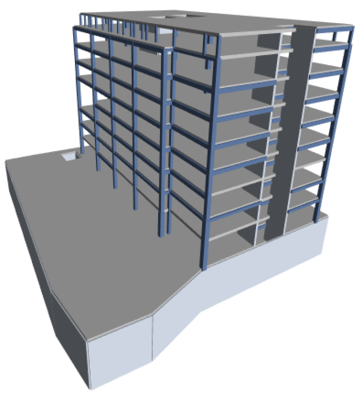

Figure 2.1. 3D view of the structure.

The thicknesses of the U-shaped walls are 350 mm for wall webs and 400 mm for flanges, up to an elevation of +13.0 m. Wall flange thickness reduces to 350 mm above that level. The depth of perimeter beams are generally 500 mm. Ultimately, slabs have a thickness of 240 mm at normal floor levels while it increases to 300 mm at basement levels.

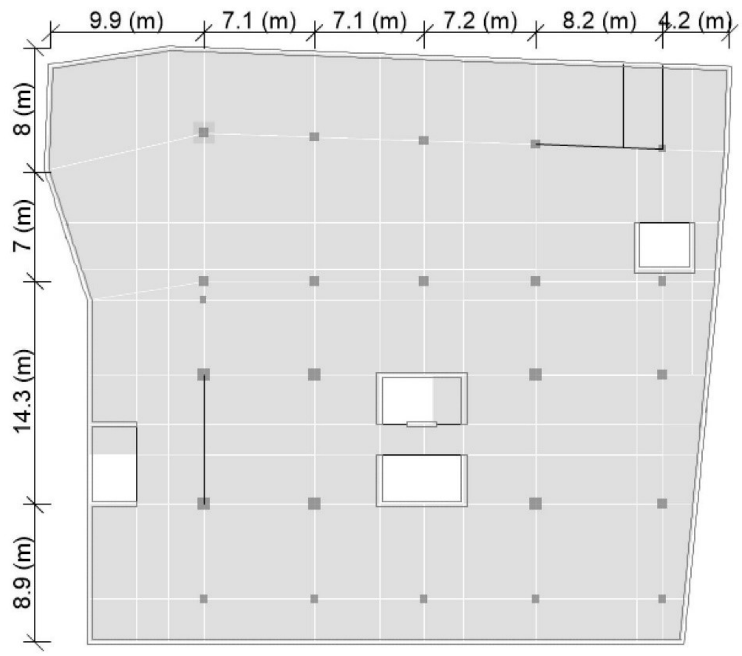

Figure 2.2. Typical basement plan view.

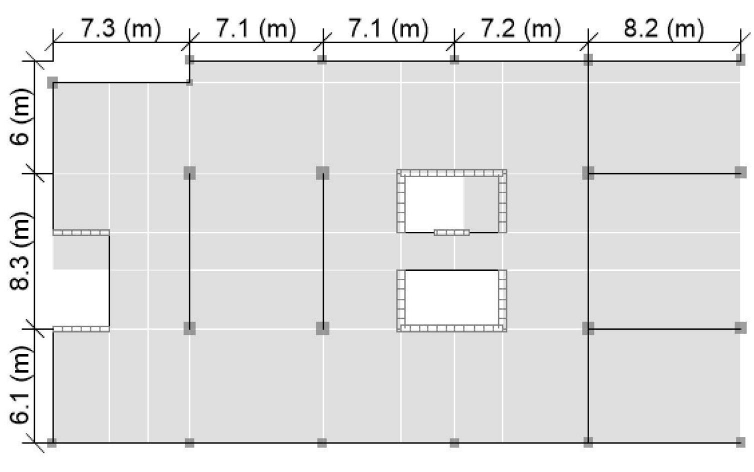

Figure 2.3. Typical superstructure plan view.

2.2. Linear Elastic Modeling

CSI-ETABS software is used to generate linear elastic models of the structure for linear analyses [10]. In accordance with the Requirements for Design and Construction of Reinforced Concrete Structures (TS500) (Turkish Standards Institute, 2000) concrete elastic modulus, shear modulus and Poisson's ratio values are defined. Based on TBSC 2018, damping characteristics, and effective rigidity of the structural elements are determined. In respect of architectural properties corresponding loads are assigned based on Design Loads for Buildings (TS498) (Turkish Standards Institute, 1997) [11].

2.2.1. Materials

In this structure, C40 concrete class is used with characteristic compressive strength $f_{ck} = 40\,MPa$. For C40 class concrete, Modulus of Elasticity of concrete is defined as $E_c = 34000\,MPa$ using Equation 2.1 (TS500) [12]. Shear Modulus of concrete is defined as $G_c = 14167\,MPa$ using Equation 2.2 (TS500) according to Poisson Ratio of concrete $\nu_c = 0.2$ (TS500). In addition, weight per unit volume of the concrete is assumed as $\gamma_c = 25\,kN/m^3$ in respect of common practice.

$$E_c = 3250\sqrt{f_{ck}} + 14000 \tag{2.1}$$

$$G_c = \frac{E_c}{2(1+\nu_c)} \tag{2.2}$$

2.2.2. Structural Elements

The structural members are modeled using corresponding types of elements with respect to the Finite Element Modeling approach. Based on the behavior of the members, beams and columns are defined typically as frame elements. Frame elements can resist axial load, biaxial bending, torsion and biaxial shear. Besides, slabs and walls are defined as shell elements in which membrane and plate behaviors are considered together [13]. Furthermore, in accordance with Table 4.2 of TBSC 2018 for reinforced concrete structures sections are considered to be cracked sections. So, the effective rigidities of reinforced concrete sections should be assigned using the respective table about the stiffness modifiers (Table 2.1).

Table 2.1. Reinforced concrete sections stiffness modifiers.

Reinforced Concrete Structural Elements Stiffness Modifiers		
Walls - Slab (In-Plane)	**Axial**	**Shear**
Structural Walls	0.50	0.50
Basement Walls	0.80	0.50
Slabs	0.25	0.25
Walls - Slab (Out of Plane)	**Bending**	**Shear**
Structural Walls	0.25	1.00
Slab	0.25	1.00
Frame Elements	**Bending**	**Shear**
Coupling Beams	0.15	1.00
Moment Frame Beams	0.35	1.00
Moment Frame Columns	0.70	1.00

2.2.3. Gravity Loads

Gravity loads which are considered as permanent loads are automatically calculated by the software based on self-weights of the elements. On the other hand, live loads which are classified as temporary loads are applied in the character of uniform distributed loads on floor slabs according to its corresponding table in TS498 (Table 2.2). In addition, floor finishings are assigned to their corresponding floor slabs as presented in Table 2.3.

Table 2.2. Uniform live loads.

Load Type	**Uniform Load** (kN/m^2)
Live Load Residential	2.00
Live Load Basement	5.00

Table 2.3. Uniform finishing loads.

Load Type	**Uniform Load** (kN/m^2)
Floor finishes and ceilings plaster of basement	2.50
Floor finishes and ceilings plaster of normal floors	3.70

2.2.4. Seismic Masses

One of the significant points to obtain more realistic analytical responses is to consider mass magnitudes precisely which directly affect the dynamic behavior of the structure. Accordingly, the presence of dead loads are fully considered. However, live loads contribution is determined using reduction factors since there is a low probability to have an earthquake event and live loads simultaneously. Consequently, in terms of the occupancy of the building proper live load contribution factors are used subsequent to this probabilistic approach (Table 2.4).

Table 2.4. Live load mass contribution factors.

Load Type	**Live load contribution**
Live Load Residential	0.30
Live Load Parking Area	0.30

$$w_j{}^{(s)} = w_{G,j}{}^{(s)} + n.w_{Q,j}{}^{(s)} \tag{2.3}$$

$$m_j{}^{(s)} = \frac{w_j{}^{(s)}}{g} \tag{2.4}$$

2.3. Analysis Methods

2.3.1. TBSC 2018 Methodology

2.3.1.1. Seismic Parameters. The elastic design spectrum for structure are obtained by using the building's location in the new Turkish Seismic Hazard Map (Figure 2.4), and the Soil Class is Z2 [14].

Figure 2.4. Building location in the new Turkish seismic map.

The spectrum parameters are obtained for the EL-2 (design) ground motion level (Table 2.5). In accordance with the given information horizontal elastic spectrum is obtained using Equations 2.5 to 2.8 for EL-2 ground motion level (Figure 2.5.).

Table 2.5. Spectrum Parameters for EL-2 earthquake.

Spectrum Parameters	**Magnitude based on the location**
S_s	0.895
S_1	0.248
S_{DS}	1.022
S_{D1}	0.522
PGA	$0.367(g)$
PGV	$22.761(cm/s)$

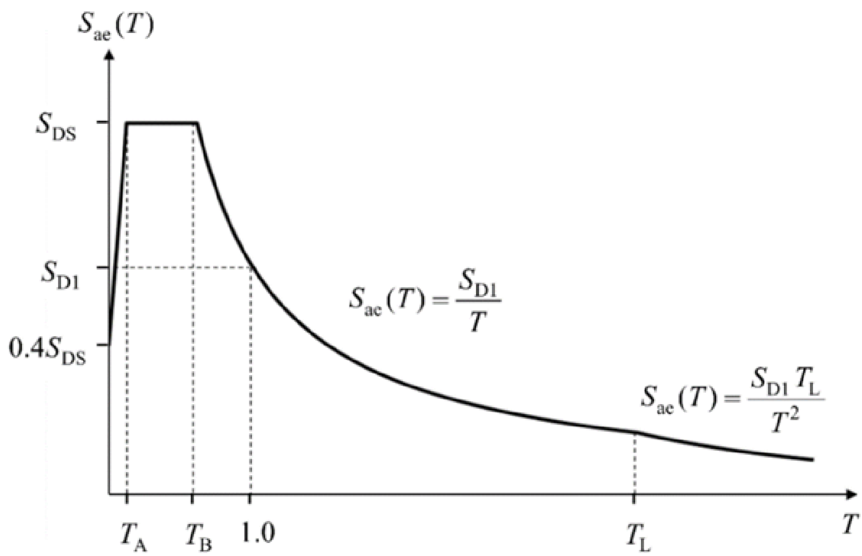

Figure 2.5. Horizontal elastic spectrum based on TBSC 2018.

$$S_{ae}(T) = (0.4 + 0.6\frac{T}{T_A})S_{DS} \qquad (0 \leq T \leq T_A) \tag{2.5}$$

$$S_{ae}(T) = S_{DS} \qquad (T_A \leq T \leq T_B) \tag{2.6}$$

$$S_{ae}(T) = \frac{S_{D1}}{T} \qquad (T_B \leq T \leq T_L) \tag{2.7}$$

$$S_{ae}(T) = \frac{S_{D1}T_L}{T^2} \qquad (T_L \leq T) \tag{2.8}$$

$$T_A = 0.2\frac{S_{D1}}{S_{DS}} \Rightarrow T_A = 0.102s \qquad T_B = \frac{S_{D1}}{S_{DS}} \Rightarrow T_B = 0.511s \qquad T_L = 6s$$

In compliance with TBSC 2018, four types of ground motion levels are determined. The probability of exceedance in 50 years and earthquake return periods of each are defined (Table 2.6). According to EL-2 ground motion level which is called standard earthquake ground motion level, EDC (Earthquake Design Class) is selected to obtain corresponding seismic parameters of the building (Table 2.8). On the other hand, since the building occupancy is residential the BUC factor (Building Usage Category) is selected as $BUC = 3$ and the importance factor $I = 1$ subsequently (Table 2.7).

Table 2.6. Earthquake ground motion levels.

Earthquake ground motion level	**Abbreviation**	**Probability of Exceedance in 50 Years**	**Earthquake Return Periods**
The Greatest Earthquake ground Motion Level	EL-1	2%	2475 Years
Standard Design Earthquake Ground Motion	EL-2	10%	475 Years
Frequent Earthquake Ground Motion Level	EL-3	50%	72 Years
Service Earthquake Ground Motion Level	EL-4	68%	43 Years

Table 2.7. Building Usage Category and Building Importance Factor.

Building Usage Category	**Building Usage Objective**	**Building Importance Factor (I)**
BUC=1	Frequently used structures for long duration after earthquake events and buildings include valuable articles and toxic materials like hospitals, fire services, schools, prisons, museums, toxic material warehouses	1.5
BUC=2	Frequently used structures for short duration like shopping malls, theatres, mosques, sport facilities	1.2
BUC=3	All other structures excluding BUS = 1, BUS = 2 like residential buildings, hotels, offices, industrial buildings	1

In accordance with $S_{DS} = 1.022$ and $BUC = 3$ the Earthquake Design Class is selected as $EDC = 1$ based on Table 2.8. Afterwards, in order to determine Building Height Class (BHC) the code stipulations for buildings with a basement should be checked. If the building satisfies two conditions of the code simultaneously the base of the structure should be assumed as such that starts from an elevation above the perimeter walls. Therefore, total height of the structure is considered in respect of this base (H_N). Firstly, the building should have perimeter walls in at least three sides of the basement floors. Secondly, the ratio between fundamental period of the total structure over the upper structure period has to be less than 1.1. In compliance with these two conditions the elevation of the base is considered as +6.30m since the building satisfies the conditions simultaneously, It has perimeter walls at four sides and $T_{total} = T_{upper} = 1.472s$ (Table 2.11) So, the total height is $H_N = 26.15m$.

Table 2.8. Earthquake Design Classification.

Short Period Design Spectral Acceleration Coefficient (S_{DS}) Based on EL-2	**BUC=1**	**BUC=2,3**
$S_{DS} \prec 0.33$	EDC=4a	EDC=4
$0.33 \leq S_{DS} \prec 0.50$	EDC=3a	EDC=3
$0.50 \leq S_{DS} \prec 0.75$	EDC=2a	EDC=2
$0.75 \leq S_{DS}$	EDC=1a	EDC=1

As mentioned before, because of the very large lateral stiffness of the basement floors compared to the upper structure, fundamental natural period of the total structure is almost the same as superstructure. Therefore, the second condition of the code will generally be satisfied and the first condition will control the total height definition for the building.

Table 2.9. Building Height Category Based on Earthquake Design Class and Height Gaps.

<table>
<tr><th>Building Height Category</th><th>EDC=1, 1a, 2, 2a</th><th>EDC=3,3a</th><th>EDC=4,4a</th></tr>
<tr><td>BHC=1</td><td>$H_N \succ 70$</td><td>$H_N \succ 91$</td><td>$H_N \succ 105$</td></tr>
<tr><td>BHC=2</td><td>$56 \prec H_N \leq 70$</td><td>$70 \prec H_N \leq 91$</td><td>$91 \prec H_N \leq 105$</td></tr>
<tr><td>BHC=3</td><td>$42 \prec H_N \leq 56$</td><td>$56 \prec H_N \leq 70$</td><td>$56 \prec H_N \leq 91$</td></tr>
<tr><td>BHC=4</td><td>$28 \prec H_N \leq 42$</td><td colspan="2">$42 \prec H_N \leq 56$</td></tr>
<tr><td>BHC=5</td><td>$17.5 \prec H_N \leq 28$</td><td colspan="2">$28 \prec H_N \leq 42$</td></tr>
<tr><td>BHC=6</td><td>$10.5 \prec H_N \leq 17.5$</td><td colspan="2">$17.5 \prec H_N \leq 28$</td></tr>
<tr><td>BHC=7</td><td>$7 \prec H_N \leq 10.5$</td><td colspan="2">$10.5 \prec H_N \leq 17.5$</td></tr>
<tr><td>BHC=8</td><td>$H_N \leq 7$</td><td colspan="2">$H_N \leq 10.5$</td></tr>
</table>

Finally, BHC of the building should be selected from its respective Table (Table 2.9). By doing so, the structural behavior factor can be destinated based on Table 2.10. BHC = 5 is selected from the corresponding table in consequence of $H_N = 26.15m$ and EDC = 1. Moreover, in compliance with the load-bearing system of the structure A13 load-bearing system category is used for the earthquake analyses of the superstructure in which the behavior factor is R=6 and over-strength factor D = 2.5 (Table 2.10). On the other hand, for the rigid lower system it is asserted to consider $(R/I) = 2.5$ and $D = 1.5$.

Table 2.10. Load-Bearing System Behavior Coefficient , Over-strength Factor and Permitted Building Heights for Building Load-Bearing Systems.

Building Load-Bearing System	**Behavior Factor R**	**Over-strength Factor D**	**Permitted BHC**
Cast-in-Place Concrete Structures			
A1. Load-Bearing Systems with High Ductility			
A11. High Ductility Moment Frame Systems	8	3	BHC $\geq$ 3
A12. High Ductility Shear Wall System Including Coupled Beams	7	2.5	BHC $\geq$ 2
A13. High Ductility Shear Wall System	6	2.5	BHC $\geq$ 2
A14. Combined High Ductility Frame System together with Shear Wall System Including Coupled Beams	8	2.5	BHC $\geq$ 2
A15. Combined High Ductility Frame System together with Shear Wall System	7	2.5	BHC $\geq$ 2
A16. Single-Story Buildings with less than 12m Height in which Lateral Loads are Resisted by Columns	3	2	-

2.3.1.2. Assembled Model. Foundation of the structure is not considered with regard to common practice; therefore, fixed supports are designated to joints at the foundation level. In addition, slabs at floor levels are determined to behave as rigid diaphragms for the upper portion while they are considered as elastic diaphragms for lower system in order to consider back-stay effects in structural walls. In compliance with TBSC 2018, an additional eccentricity of 5% is included which is applied automatically by ETABS. By the completion of the structural model, based on eigenvalue analysis natural free vibration analysis of the model is done and the dynamic properties of the model is given in Table 2.11 to 2.13. The acceptable modal mass participation in respect of TBSC 2018 part 4.8.1.2 is 95%. Therefore, a least mutual value of almost 95% mass participation is expected in order to consider the number of modes adequately in each of three modal cases.

Table 2.11. Natural vibration periods and corresponding mass participation ratios (Total Structure).

Total Structure Modal Mass Consideration					
Mode Number	**Period (S)**	**Mass Participation on X direction**	**Mass Participation on Y direction**	ΣX	ΣY
1	1.472	0.000	0.179	0.000	0.179
2	1.243	0.000	0.337	0.000	0.516
3	1.009	0.508	0.000	0.508	0.516
4	0.402	0.000	0.029	0.508	0.545
5	0.307	0.000	0.105	0.508	0.650
6	0.227	0.160	0.000	0.668	0.650
7	0.202	0.001	0.007	0.669	0.656
8	0.146	0.000	0.070	0.669	0.726
9	0.128	0.000	0.001	0.669	0.727
10	0.106	0.085	0.000	0.754	0.727
...	...	...	...	...	...
26	0.044	0.000	0.000	0.944	0.947
27	0.044	0.000	0.002	0.944	0.949
28	0.043	0.000	0.001	0.944	0.949
29	0.043	0.000	0.000	0.944	0.950
30	0.042	0.000	0.001	0.945	0.951
31	0.040	0.004	0.001	0.948	0.951
32	0.039	0.000	0.000	0.949	0.952
33	0.037	0.002	0.010	0.950	0.961
34	0.037	0.000	0.002	0.950	0.963
35	0.036	0.007	0.005	0.957	0.968

Table 2.12. Natural vibration periods and corresponding mass participation ratios (Superstructure).

Superstructure Modal Mass Consideration					
Mode Number	**Period (S)**	**Mass Participation on X direction**	**Mass Participation on Y direction**	ΣX	ΣY
1	1.472	0.000	0.273	0.000	0.273
2	1.243	0.000	0.513	0.000	0.786
3	1.009	0.774	0.000	0.774	0.786
4	0.402	0.000	0.037	0.774	0.823
5	0.306	0.000	0.121	0.774	0.944
6	0.225	0.181	0.000	0.955	0.944
7	0.202	0.001	0.005	0.956	0.949
8	0.142	0.000	0.033	0.956	0.983
9	0.128	0.000	0.001	0.956	0.983
10	0.103	0.030	0.000	0.986	0.983
11	0.095	0.000	0.000	0.986	0.983

Table 2.13. Natural vibration periods and corresponding mass participation ratios (Lower Structure).

Lower Structure Modal Mass Consideration					
Mode Number	**Period (S)**	**Mass Participation on X direction**	**Mass Participation on Y direction**	ΣX	ΣY
1	0.099	0.005	0.749	0.005	0.749
2	0.083	0.769	0.007	0.775	0.756
3	0.059	0.000	0.039	0.775	0.795
4	0.057	0.002	0.003	0.777	0.797
5	0.056	0.002	0.042	0.779	0.840
6	0.050	0.002	0.000	0.780	0.840
7	0.049	0.063	0.002	0.844	0.842
8	0.044	0.000	0.011	0.844	0.853
9	0.044	0.002	0.003	0.845	0.856
...	...	...	...	...	...
57	0.019	0.002	0.001	0.952	0.950
58	0.019	0.000	0.000	0.952	0.950
59	0.019	0.001	0.000	0.953	0.950
60	0.019	0.000	0.000	0.953	0.951

2.3.2. TBSC 2018 Analysis Approaches

In compliance with TBSC 2018, four different analysis methods are recommended for strength-based design of structures including two portions with different R and D values. Respectively, two Equivalent Static Lateral Force (ELF) methods and two Modal Response Spectrum Analysis (RSA) methods are provided. In the analysis, selection of the ELF method or the RSA method is defined based on the total height of the structure. The total height definition described previously must be made considering whether or not the structure satisfies the conditions for buildings incorporating by a rigid basement. Since, the representative building is in $BHC = 5$ category as well as $EDC = 1$, it is permitted to analyze the structure using ELF analysis approach.

Two alternative analysis approaches are provided in the seismic code will be described herein. The two analysis methods (ELF and RSA) using the Two-Stage analysis approach are discussed first, and the alternative two methods (ELF and RSA) based on Total Structure analysis approach are presented subsequently. The methods are presented in the following sections of the code:

- Two-Stage Analysis Approach
  (i) Section 4.7.5 (ELF Method)
  (ii) Section 4.8.5 (RSA Method)
- Total Structure Analysis Approach
  (i) Section 4.3.6.1 (ELF Method)
  (ii) Section 4.3.6.2 (RSA Method)

2.3.2.1. Two-Stage Analysis Approach - 4.7.5 ELF Method. In the direction of 4.7.5 method, a linear elastic analysis procedure is performed in two stage. First stage is to conduct an ELF procedure based on upper portion dynamic properties including its fundamental natural period, R_{upper} and D_{upper} while only upper mass is considered. By doing so, reduced internal forces of upper and lower portion are obtained. Subsequently, the second stage is to multiply floor masses at each floor elevation of the lower portion by the reduced spectral acceleration corresponding to T=0. Although, reduced internal forces of the lower system are calculated in accordance with $(R_a)_{lower} = D_{lower} = 1.5$. Finally, design internal forces has to be determined as follows:

- For the Upper Structure
  (i) Ductile Behavior: Internal Forces Obtained from the first stage.

(ii) Non-Ductile Behavior: Internal Forces Obtained from the first stage magnified by D_{upper}.

- For the Lower Structure
  (i) Ductile Behavior: Linear summation of internal forces derived from first stage and second stage in the lower portion elements.
  (ii) Non-Ductile Behavior: Linear Summation of internal forces obtained from the first stage magnified by $0.6D_{upper}$ and internal forces derived from second stage magnified by D_{lower}.

Furthermore, the upper structure internal forces whether based on ductile or non-ductile behavior has to be magnified in respect of base shear amplification factor and second-order effects coefficient if necessary.

2.3.2.2. Two-Stage Analysis Approach - 4.8.5 RSA Method. In compliance with 4.8.5 method which is a Modal Response Spectrum Analysis method, the structure is permitted to be analyzed in the same manner as 4.7.5 method. Accordingly, in the first stage, using the common structural model, a Modal Response Spectrum Analysis is performed in which only the upper mass is considered. The spectrum is reduced in accordance with R_{upper} while D_{upper} is utilized as over-strength factor for non-ductile behavior of the upper portion. Moreover, sufficient number of natural vibration modes is considered in respect of upper portion mass participation ratio which has to be at least 95%. By doing so, the internal forces of upper and lower portion are obtained. Subsequently, for the second stage in the common model only the lower mass is determined to perform a modal response spectrum analysis using a behavior factor of $(R_{lower}/I) = 2.5$ while $D_{lower} = 1.5$ is used to amplify the quantities for non-ductile internal forces. In addition, sufficient number of natural vibration modes in the same manner of the former stage is determined in accordance with the lower portion mass participation ratios.

2.3.2.3. Total Structure Analysis Approach - 4.3.6.1 ELF Method. As an alternative to two-stage analysis approach, the so-called total structure analysis approach is first introduced in the 2018 code. In respect of the 4.3.6.1 method, the mass of the total structure (upper + lower portion) has to be considered in the application of the ELF method, although the total height in accordance with the code conditions has to be specified as well. Based on this method the following four methodologies are specified to obtain internal forces in structural elements:

- For the Upper Portion:
  - (i) Element internal forces based on ductile behavior.
  - (ii) Element internal forces based on non-ductile behavior.
- For the Lower Portion:
  - (i) Element internal forces based on ductile behavior.
  - (ii) Element internal forces based on non-ductile behavior.

As mentioned before, $R = 6$ and $D = 2.5$ are used for the calculations of the superstructure while $R/I = 2.5$ and $D = 1.5$ can be considered for the lower portion calculations. The code intent for the upper portion internal force calculations is to consider total structure in spite of the fact that the base elevation has to be assumed as above the lower portion perimeter walls. However, there is not a clear clarification that which masses should be taken into account in order to obtain upper portion internal forces. Thereby, the total structure mass is considered to obtain the upper structure internal forces, which means basement masses are also included in the lateral force calculations of the superstructure. Based on Equation 2.12 in the code, which is used for the calculation of base shear in the ELF procedure, it shows that base shear is affected by two parameters. Existing mass and reduced spectral acceleration (which is dependent on the fundamental natural period of the structure) are the two variables to calculate base shear. Correspondingly, another unclear point is the selection of fundamental natural period. However, the fundamental natural period of total structure is almost the same as superstructure and the difference can be neglected. Hence, the total structure fundamental natural period is used in the calculations, which is also recommended by the TBSC 2018 handbook [15].

$$R_a(T) = \frac{R}{I} \qquad T > T_B \tag{2.9}$$

$$R_a(T) = D + (\frac{R}{I} - D)\frac{T}{T_B} \qquad T \leq T_B \tag{2.10}$$

$$S_{aR}(T) = \frac{S_{ae}(T)}{R_a(T)} \tag{2.11}$$

$$V_{tE}^{(X)} = m_t.S_{aR}(T_p^{(X)}) \geq 0.04.m_t.I.S_{DS}.g \tag{2.12}$$

Lastly, in order to obtain reduced internal forces $(R_a)_{upper}$ has to be calculated (Equation 2.9 or 2.10). By doing so, the reduced spectral acceleration can be obtained to calculate the base shear applied to the upper portion (Equations 2.11 and 2.12). Thus, element internal forces for ductile behavior are obtained. However, for non-ductile response quantities, the code intends to magnify the values by D_{upper}.

On the other hand, the code intent for the lower portion internal force calculations is to obtain a $(\bar{R}_a)_{lower}$ value for the lower portion (Equation 2.13). This coefficient should be used instead of the R_a coefficient in the corresponding equations to calculate the base shear applied to the basement. Furthermore, there is not an obvious implication about which masses to consider. Therefore, total mass of the structure is considered for the lower portion internal force calculations. Respectively, for each direction of the earthquake the ratio of superstructure base shear over total structure base shear is calculated to be able to obtain $(\bar{R}_a)_{lower}$ of that direction using Equation 2.15.

$$(\bar{R}_a)_{lower} = \frac{(R_a)_{upper}}{\nu^{(X)}} \tag{2.13}$$

$$\nu^{(X)} = \nu^{(X)}_{upper} + \nu^{(X)}_{lower} \tag{2.14}$$

$$\nu^{(X)}_{upper} = \frac{V^{(X)}_{x,upper}}{V^{(X)}_{x,total}} \tag{2.15}$$

$$\nu^{(X)}_{lower} = (1 - \nu^{(X)}_{upper})\frac{(R_a)_{upper}}{(R_a)_{lower}} \tag{2.16}$$

$$\bar{D}^{(X)}_{lower} = \frac{0.6\nu^{(X)}_{upper} D_{upper} + \nu^{(X)}_{lower} D_{lower}}{\upsilon^{(X)}} \tag{2.17}$$

In compliance with Equation 2.13, the code intent is to consider the structural behavior factor (R) varies between the value of upper portion which is determined as 6 and the lower portion as 2.5. Correspondingly,$(\bar{R}_a)_{lower}$ is observed in respect of different base shear ratios in Table 2.14. Based on this observation several conclusions can be reached. Firstly, considering $\nu_{upper} = 0$ means there is no upper structure and the system behaves as same as a rigid lower system. Likewise, considering $\nu_{upper} = 1$ means the system behaves identical to a flexible and ductile upper portion. Secondly, according to this method, increasing the ratio of the upper structure mass over the total structure mass leads to a more ductile behavior in the lower portion, which may not be physical. For many building structures with basement levels, this method can result in unrealistically large values for the earthquake load reduction coefficient $(\bar{R}_a)_{lower}$ for the lower portion, as will be demonstrated in the following chapter of this thesis.

In conclusion, despite the fact that the 4.3.6.1 method is provided as an alternative method for the design of buildings having a basement levels, it is more suitable for the analysis of mixed in height structures in which the upper and lower portion R and D values are close to each other. For instance, a steel frame upper structure with behavior and over-strength coefficients of $R = 8$ and $D = 3$, above a reinforced concrete lower structure for which the coefficients are $R = 6$ and $D = 2.5$. The use of 4.3.6.1 method for the analysis of a flexible upper structure with $R = 6$ supported by a very rigid lower portion (basement) with $R = 1.5$ leads to unreasonably small

Table 2.14. Observation based on various base shear ratios.

ν_{upper}	ν_{lower}	$(_a)_{lower}$
0	2.40	2.50
0.1	2.16	2.65
0.2	1.92	2.83
0.3	1.68	3.03
0.4	1.44	3.26
0.5	1.20	3.53
0.6	0.96	3.85
0.7	0.72	4.23
0.8	0.48	4.69
0.9	0.24	5.26
1.0	0.00	6.00

response quantities (e.g., story shear forces) for the lower portion compared to other methodologies, which will be demonstrated in chapter 3. As well, the 4.3.6.1 ELF Method also gives an abnormal distribution of the earthquake loads and story shear forces on the upper structure, since the base of the structure is taken at the foundation level in the Equivalent Lateral Force calculations, and the very high lateral rigidity of the basement levels are ignored in the equivalent lateral force distribution, as will also be demonstrated in the next chapter.

2.3.2.4. Total Structure Analysis Approach - 4.3.6.2 Method. Lastly, 4.3.6.2 is an alternative RSA method for the procedure discussed for 4.3.6.1, where the calculations are repeated for each vibration mode in each direction of the building in order to obtain the base shear ratios of the upper structure over total structure (Equation 2.13, 2.14, 2.15 and 2.16). Due to the fact that there is not a clear definition of how to consider the direction of modes, all of the vibration modes are determined in both directions to calculate base shear ratios in order to obtain $(\bar{R}_a)_{lower}$ values for each mode. By doing so, $(\bar{R}_a)_{lower}$ quantities are calculated (Figure 2.6 and 2.7). As mentioned before, for a RC wall building, the upper and lower portions have behavior factors (R) of 6 to 2.5, respectively. Thus, the $(\bar{R}_a)_{lower}$ values are expected to be between the limit of $R_a = 1.5$ and $R_a = 6$. Therefore, for the calculated quantities of $(\bar{R}_a)_{lower}$ obtained beyond these limits, an assumption made. If the calculated value (for a specific mode) is larger than 6, it is assumed to be equal to 6, and if the value is less than 1.5, it is considered to be equal to 1.5.

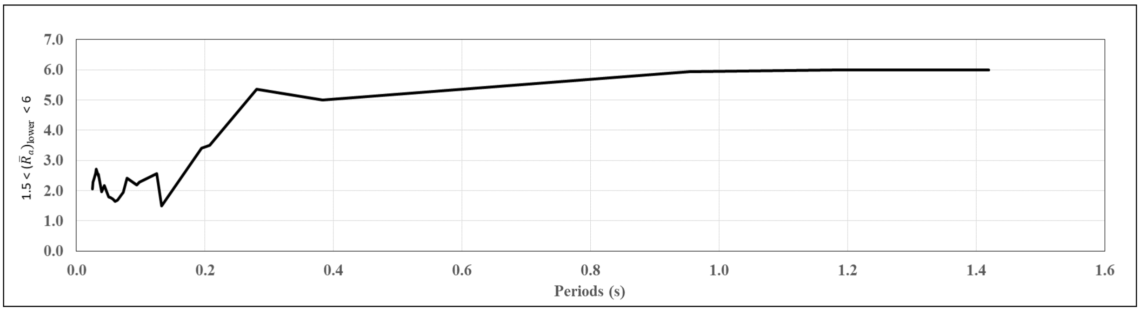

Figure 2.6. $(\bar{R}_a)_{lower}$ obtained from each mode at X-direction.

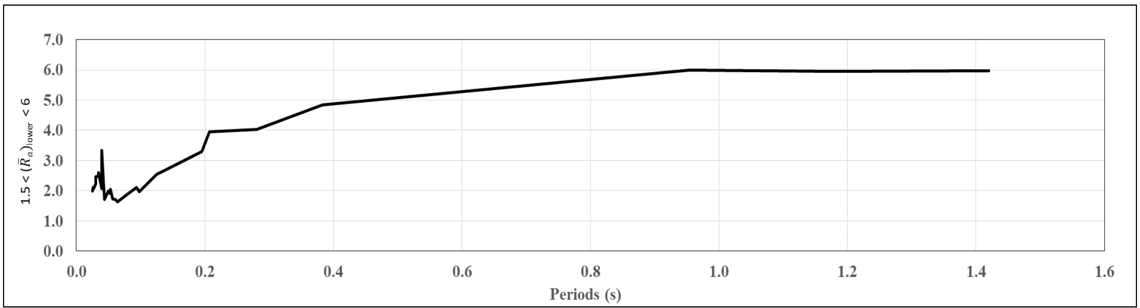

Figure 2.7. $(\bar{R}_a)_{lower}$ obtained from each mode at Y-direction.

The reduced response spectra based on the obtained $(\bar{R}_a)_{lower}$ quantities are presented in Figure 2.8 and 2.9 for each direction. It is observed in the figures that in the 4.3.6.2 RSA method, in which a complex calculation of $(\bar{R}_a)_{lower}$ is made for each mode in each direction, the use of base shear ratios for the calculation of the reduction factor ($(\bar{R}_a)_{lower}$), which should actually represent the ductility and over-strength of the structure, is not consistently meaningful. The calculated reduced spectral acceleration values corresponding to the basement vibration modes (small periods) are supposed to have values that are compatible with the behavior coefficient defined for the basement ($R = 2.5$), whereas it is observed in Figures 2.8 and 2.9 that the reduced spectral acceleration values for small periods may occasionally correspond to behavior coefficients closer to $R = 6$, which is more representative of the superstructure, contrary to what is expected.

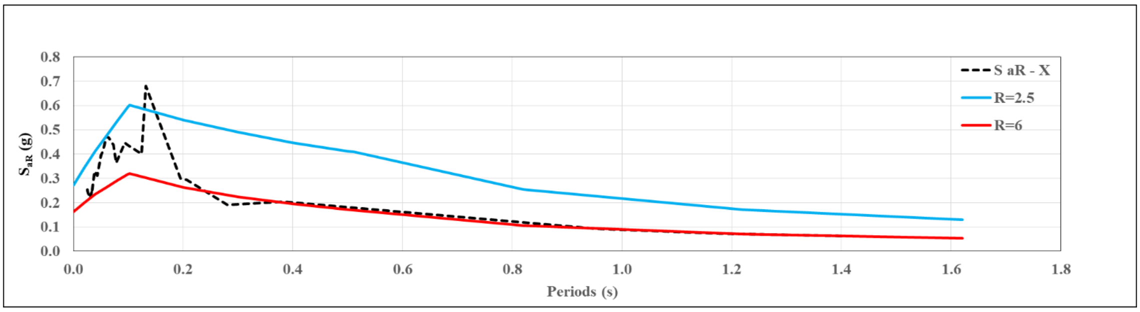

Figure 2.8. Reduced response spectrum based on 4.3.6.2 for X-direction.

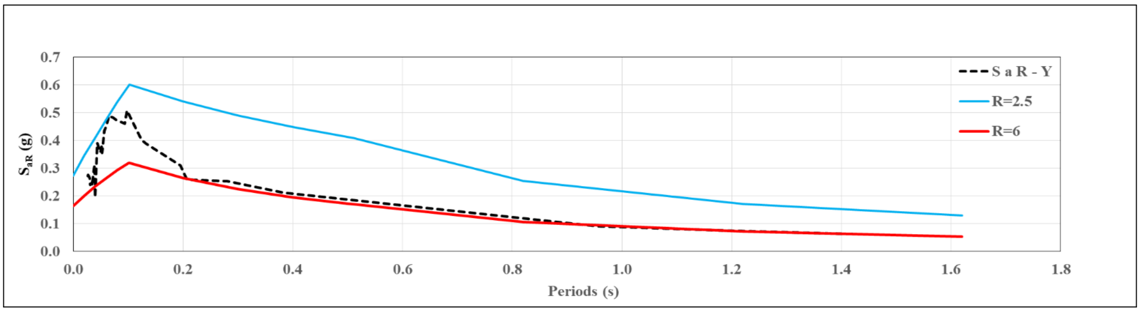

Figure 2.9. Reduced response spectrum based on 4.3.6.2 for Y-direction.

Furthermore, in the seismic code it is asserted that instead of base shear ratios for each mode, the effective modal mass ratios, which is effectively equal to base shear ratios can be used. Base shear effective modal mass ratios are obtained from fundamental structural dynamics equations (Equation 2.18 and 2.20). Therefore, their values are different than mass participating ratios provided by the CSI-Etabs software.

$$\Gamma_n{}^{(X)} = \frac{\sum_{i=1}^{N} m_i \Phi_{i(X)n}}{\sum_{i=1}^{N}(m_i\Phi_{ixn}^2 + m_i\Phi_{iyn}^2 + m_i\Phi_{i\theta n}^2)} \quad ; \quad m_{txn}^{(X)} = \Gamma_n{}^{(X)} \sum_{i=1}^{N} m_i \Phi_{ixn} \tag{2.18}$$

$$m_{ixn}^{(X)} = m_i \Phi_{ixn} \Gamma_n{}^{(X)} \quad ; \quad m_{iyn}^{(X)} = m_i \Phi_{iyn} \Gamma_n{}^{(X)} \quad ; \quad m_{i\theta n}^{(X)} = m_i \Phi_{i\theta n} \Gamma_n{}^{(X)} \tag{2.19}$$

On the other hand, the code states that if $R_{upper} < R_{lower}$ condition is satisfied (for a structure with a rigid basement) the code allows a conservative simplification for the calculations of lower system element internal forces. In this case, for all vibration modes the base shear ratio is considered as $\nu_{n,upper}^{(X)}$. Accordingly, the lower portion reduction coefficient and over-strength factor can be assumed to be as follows for simplicity:

$$(\bar{R}_a)_{n,lower} \cong (R_a))n, lower \quad , \quad \bar{D}_{n,lower}^{(X)} \cong D_{lower} \quad , \quad D_{lower} = 1.5 \tag{2.20}$$

In summary, according to the 4.3.6.2 RSA method, in order to obtain the upper structure internal forces corresponding to ductile behavior, a modal response spectrum analysis is first performed. Total mass of the structure is considered while spectral accelerations are reduced by $(R_a)_{upper}$ defined in Equation 2.9 and 2.10. Internal forces corresponding to non-ductile behavior are amplified by D_{upper}. In order to obtain the lower structure ductile internal forces, two options are provided. The first option involves calculation of $(\bar{R}_a)_{n,lower}$ values for each mode of vibration of the structure, for obtaining the reduced spectra provided in Figure 2.8 and 2.9 for each direction, using a modal response spectrum analysis including the total structure mass. This is a very complicated approach which is very susceptible to errors in the calculations. As the second option, the conservative simplification can be considered where the spectral acceleration values are reduced by $(\bar{R}_a)_{n,lower} \cong (R_a)_{lower} = 2.5$ for the lower portion. In addition, when the first option is used, $\bar{D}_{n,lower}^{(X)}$ is calculated as 1.5 for all modes; therefore the non-ductile internal force quantities should be amplified by 1.5 for the lower portion. Similarly, in the latter case (second option), the code states that the over-strength factor for the lower portion can be directly taken as $D_{lower} = 1.5$. In the following chapter, it will be demonstrated that the first option in 4.3.6.2 RSA method results in unreasonably small response quantities (e.g., story shear forces) for the lower portion compared to other methodologies (similar to the 4.3.6.1 ELF method); however, the response quantities for the upper portion are reasonable.

2.3.3. TEC 2007 Method

In terms of the analysis procedure main differences between the new seismic code in comparison to previous Turkish seismic code are discussed in this section. On contrary to TBSC 2018, reinforced concrete sections are considered to be uncracked in the TEC 2007. Moreover, in compliance with TBSC 2018, R_a values are calculated with respect to Equation 2.8 or 2.9 while according to TEC 2007 R_a quantities are obtained using Equation 2.21 or 2.22 [16].

$$R_a(T) = 1.5 + (R - 1.5)\frac{T}{T_A} \qquad 0 \leq T \leq T_A \tag{2.21}$$

$$R_a(T) = R \qquad T_A < T \tag{2.22}$$

Furthermore, a comparison between Equation 2.8 and 2.21 demonstrates the fact that based on TEC 2007, T_a is determined as a criterion to differentiate $R_a(T)$ and R coefficients. However, in TBSC 2018,T_b is the limiting period (for the equal displacement rule) to choose which equation has to be applied for the calculation of $R_a(T)$. The cracked section assumption (the use of effective cross section rigidity in Table 2.1) in the new code decreases the lateral stiffness and increases the fundamental natural period of the structure. Additionally, elastic and reduced response spectra obtained from each code provisions are compared in Figure 2.10, 2.13. Accordingly, a behavior factor of $R = 6$ is used to obtain reduced response spectrum corresponding to the design of a flexible superstructure while $R = 2.5$ is recommended for the lower basement. Z2 soil type properties are used for the TEC 2007 acceleration spectrum while $A_0 = 0.4$ is assumed.

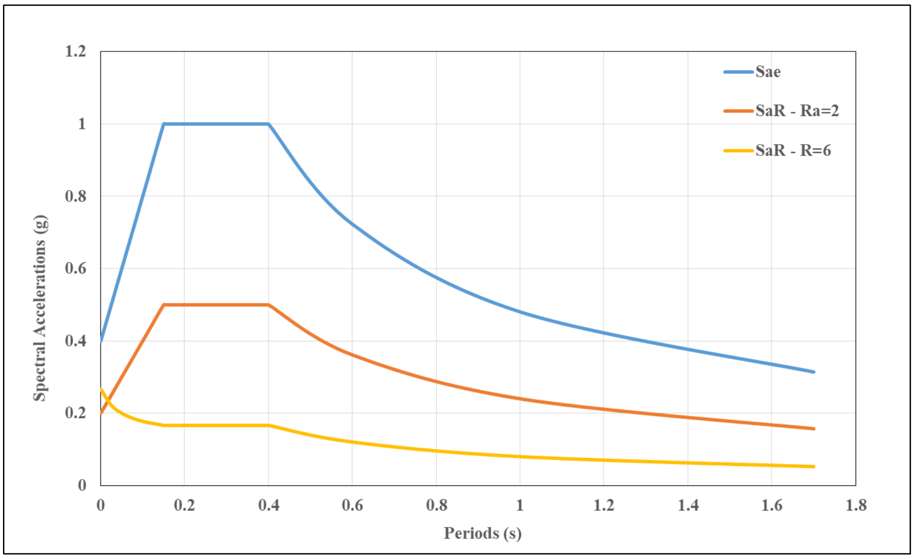

Figure 2.10. Response spectra based on TEC 2007.

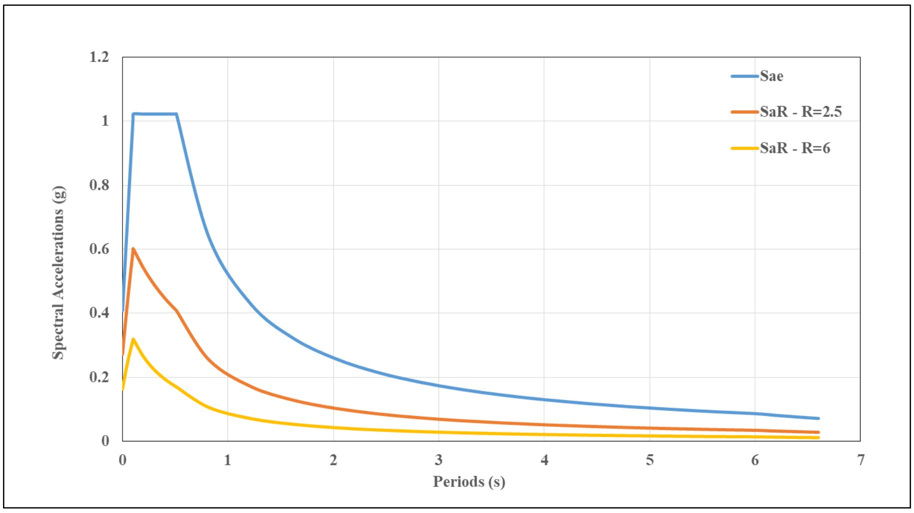

Figure 2.11. Response spectra based on TBSC 2018.

As compared in Figure 2.12 and 2.13, in the new seismic code a great increase in the peak point of the reduced design spectrum is observed which corresponds to the range of rigid basement periods.

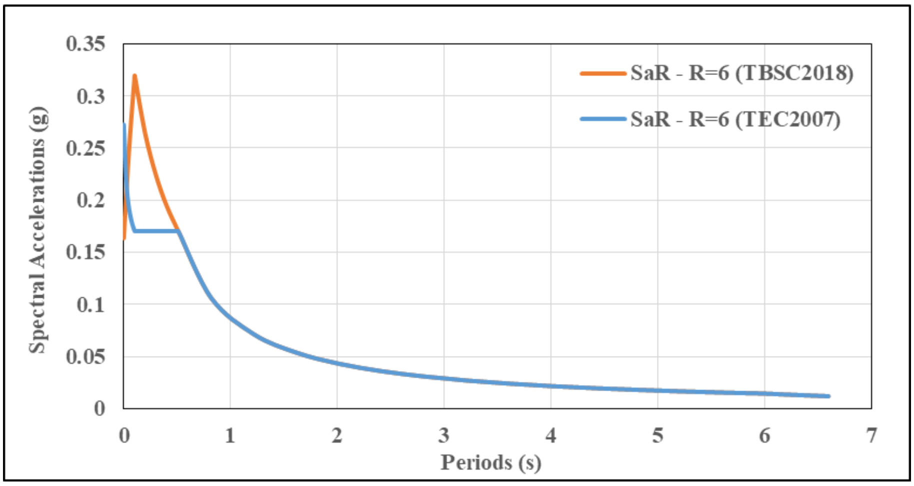

Figure 2.12. Comparison of reduced design spectra TBSC 2018 vs. TEC 2007 for the flexible superstructure.

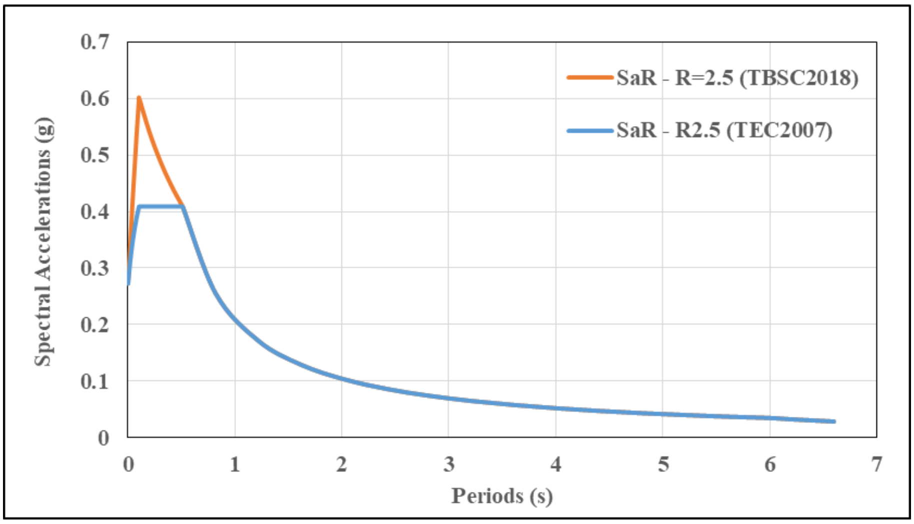

Figure 2.13. Comparison of reduced design spectra TBSC 2018 vs. TEC 2007 for rigid basement.

Moreover, in TEC 2007, the code intent for non-ductile behavior of the upper portion structural elements is to reduce the elastic spectral acceleration by $R_a(T) = 2$, which means the response quantities should be amplified by 3 when the upper structure reduction factor is considered to be 6. In contrast with TBSC 2018, there is not a clear clarification to apply any specific over-strength factor for the non-ductile behavior of the lower system in TEC 2007. Therefore, for non-ductile behavior of the lower system elements the effect of the forces on the upper portion on the lower portion elements are are calculated considering a value of $R_a(T) = 2$ for the upper system, whereas all earthquake forces acting on the lower system are calculated considering $R_a(T) = 1.5$ and $S(T) = 1$ for the lower system.

In TEC 2007, for low and medium-rise buildings, it is permitted to perform either an ELF or a RSA method to obtain flexible upper structure internal forces supported by a rigid basement. However, the rigid lower system internal forces should be obtained by an ELF approach in the same manner as in TBSC 2018 section 4.7.5. Modal response spectrum analysis is not allowed for the analysis of lower portion. Therefore, two analysis approaches specified by TEC 2007 are performed. Firstly, for the upper structure an ELF procedure based on $R = 6$ is applied where only the upper mass is considered. Then, the lower portion masses at each floor elevation are multiplied by elastic spectral acceleration value corresponding to $T = 0(S(T) = 1)$ and the calculated loads are reduced by $R_a(T) = 1.5$. By doing so, the lateral loads obtained from the former case together with the latter case forces are applied simultaneously to the total structure. Therefore, the structure is analyzed under this combination of lateral load application which is exactly in the same procedure as the TBSC 2018 4.7.5 method. Secondly, a RSA procedure is done in which only the upper mass is included. Similar to the previous section the upper structure loads are combined with the lateral loads calculated for the lower system using a linear combination in the analysis software. Moreover, sufficient number of natural vibration modes is determined in respect of at least 90% mass participation ratio based on TEC 2007.

2.3.4. ASCE $7-10$ Method

Based on ASCE 7-10, in terms of response modification factor (R) for structures composed of a vertical combination of a flexible upper system which is supported by a rigid lower system it is permitted to perform a two-step equivalent lateral force method called Two-Stage Analysis [5]. However, there are some limitations in which the structure has to comply with all. The specifications are as follows:

- The stiffness of the lower portion shall be at least 10 times the stiffness of the upper portion.

- The period of the entire structure shall not be greater than 1.1 times the period of the upper portion considered as a separate structure supported at the transition from the upper to the lower portion.

- The upper portion shall be designed as a separate structure using the appropriate values of R and ρ (Redundancy Factor).

- The lower portion shall be designed as a separate structure using the appropriate values of R and ρ. The reactions from the upper portion shall be those determined from the analysis of the upper portion amplified by the ratio of R/ρ of the upper portion over R/ρ of the lower portion. This ratio shall not be less than 1.0.

- The upper portion is analyzed with the equivalent lateral force or modal response spectrum procedure, and the lower portion is analyzed with the equivalent lateral force procedure.

As mentioned, the main difference between the two-stage approach of TBSC 2018 in comparison to ASCE 7-10 is the single-model approach of the new Turkish seismic code, while ASCE 7-10 follows a two-model approach. Furthermore, similar to TEC 2007, the lower portion is not permitted to be analyzed using a modal response spectrum procedure in ASCE 7-10. The reaction forces obtained from the upper portion are applied statically to the lower portion in a separate model in accordance with the R/ρ ratios of the two portion (ρ is the redundancy factor which is selected based on 12.3.4 provisions of ASCE 7-10). In order to perform this procedure the response quantities of 6 DOFs at every joint of the base level in the superstructure model are applied statically to the corresponding joints at the top elevation of the lower portion model, applied in the opposite direction. Therefore, the structure is analyzed in two separate models and the upper portion base is assumed to be fixed supported. Lastly, in contrast with TEC2007 or TBSC2018, in which the lower portion lateral forces are obtained using a simple spectral acceleration multiplication by the story masses in the ELF approach, in ASCE 7-10 specifications the ELF procedure for the lower portion is performed based on the conventional inverse triangle lateral force distribution.

In order to apply the two-stage analysis in compliance with ASCE 7-10 the structural model of the building investigated is divided into two parts as shown in Figure 2.14 and 2.15.

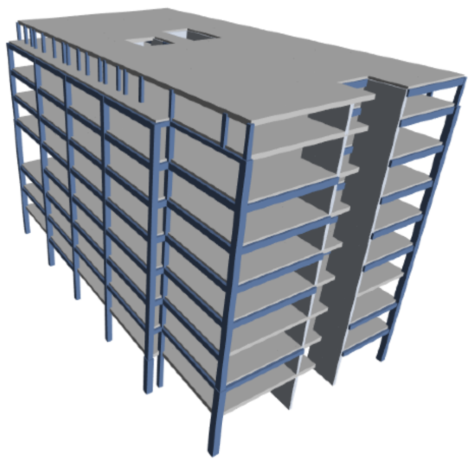

Figure 2.14. Upper portion fixed supported in transition.

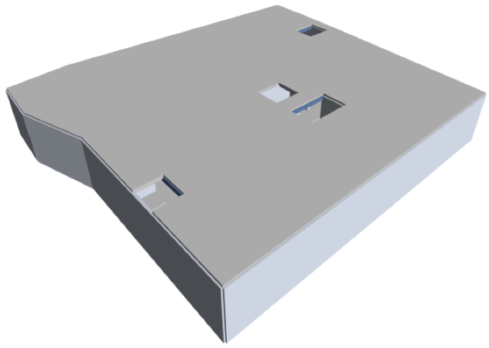

Figure 2.15. Lower portion model in a separate model.

By doing so, the upper structure is analyzed independently using ELF and RSA procedures. Sufficient number of vibration modes is considered to achieve at least 90% of modal mass participation ratios as per ASCE 7-10. The response modification factor is selected as $R = 6$ for both portions based on the Seismic Force-Resisting System from Table 12.2.1 of ASCE 7-10 (Special Reinforced Concrete Shear Walls). As discussed, in order to be able to use two-stage analysis procedure the behavior factor of the lower system shall not exceed the superstructure behavior factor. When the overall structure has the same system (for instance concrete shear wall building) the R/ρ ratios of the upper and lower portion is generally considered as 1.

Reactions from the upper portion are applied in the opposite direction to the corresponding joints at the top elevation of the lower portion model as mentioned. However, an absolute value assumption is done for the application of these forces which neglects the direction of statically applied forces from the upper portion. Accordingly, it is observed that absolute value assumption leads to obtain the same quantities as the opposite direction consideration. Finally, an ELF procedure is performed for the lower portion as well and the internal forces are obtained based on a linear combination of statically applied forces plus the lateral loads derived from lower portion model's ELF procedure itself.

2.3.5. Eurocode 8 Method

2.3.5.1. Mass Considerations. In Eurocode 8, for structures including rigid basement levels, the code clearly states that only masses above the top of the basement have to be taken into account during the analysis for design of the structural elements of the building [17]. This implies that the additional earthquake loads arising from the mass of the basement floors are assumed to be fully resisted by the perimeter basement walls. Similarly, for the calculation of the fundamental period of vibration of the structure, only masses above the top of the rigid basement are considered. Emphasis is directed in Eurocode 8 towards the fact that basement level masses do not influence seismic demands on the structural elements, due to the extremely small lateral deformations of the building basement. Therefore, due to assumed negligible seismic deformations of the basement levels, only the superstructure mass is used in the analysis for design of the structural elements. Due to the fact that lower portion masses are neglected, identical shear forces at the base level of the upper portion of the structure are assumed to be transferred to the lower floors.

2.3.5.2. Basement Level Behavior Factor. It is asserted that the transition slab above the basement serves as a floor of the lower basement which helps to create a rigid-box foundation system together with the peripheral walls and the slab at the roof of the upper basement. In accordance with Eurocode 8, there are two options to design rigid-box foundation elements. Firstly, in terms of dissipative structures (with regard to Eurocode 8 dissipative structural behavior is considered for a behavior factor of $R \leq 4$) the rigid box elements can be designed using a behavior factor corresponds to superstructure ductility class while the design shear forces have to be derived on the basis of capacity design. Secondly, design actions of foundation elements can be derived from a behavior factor regarding to a low dissipative behavior (based on Eurocode 8 low dissipative structural behavior is $R = 1.5$ in concrete buildings and $R = 2$ in steel or composite steel-concrete buildings). Lastly, the action effects of the foundation elements need to not exceed the response of structure under seismic design of the structure in accordance with an elastic behavior ($R = 1$).

2.3.6. Nonlinear Response History Analysis of the Representative Building

In addition to the aforementioned linear analysis procedures, NLRHA of the representative building structure is conducted using CSI–Perform3D software [18]. Due to complexities of nonlinear modeling only primary structural members (walls, beams, and columns) are included in the nonlinear behavior while secondary members (basement slabs, perimeter basement walls) are modeled linear elastically. Superstructure slabs are not included in the analysis models, and are replaced by rigid diaphragm constraints, as is common practice. Moreover, in spite of the fact that material characteristic strengths are used for the linear analysis but expected strengths are utilized for the nonlinear modeling. Therefore, expected compressive strength of concrete is defined as $f_c e = 52MPa$ MPA and expected steel reinforcement is defined as $f_s ye = 504MPa$ MPA in accordance with TBSC 2018 Table 5.1 provisions.

2.3.6.1. Materials. Basement walls are not expected to undergo nonlinear deformations under axial and in-plane flexural demands, therefore nonlinearity under the aforementioned demands are not considered for these elements. Accordingly, basement walls are modeled using Elastic Material for Fiber Sections in Perform3D. $E_{ce} = 36076MPa$ MPA is defined as effective elastic modulus for this material with respect to TBSC 2018 definition. In addition, adequate shear capacity is considered for the design of structural walls; therefore they are not expected to have nonlinear behavior under shear forces. Respectively, the shear behavior of walls are assigned as Elastic Shear Material in the software. G_{ce} = 15032 MPA is calculated using Equation 2.23.

$$G_{ce} = \frac{E_{ce}}{2(1+\nu_c)} \tag{2.23}$$

Nonlinear stress-strain behavior of concrete in structural walls is modeled with regard to TBSC2018 specifications which is similar to concrete stress-strain relationships advanced by Mander *et al.* (1988). In addition, cyclic degradation as well as tensile strength of concrete is neglected. Accordingly, based on the geometry and confining reinforcement of walls in the boundary as well as web regions different materials are defined according to TBSC 2018 equations. Firstly, k_e (confinement effectiveness coefficient) is calculated according to Equation 2.24.

$$k_e = (1 - \frac{\Sigma {a_i}^2}{6 b_0 h_0})(1 - \frac{s}{2 b_0})(1 - \frac{A_s}{b_0 h_0})^{-1} \tag{2.24}$$

Subsequently, f_{ex} and f_{ey} (which are defined as confining pressures) are calculated using Equations 2.25 and 2.26 at two perpendicular directions.

$$f_{ex} = k_{ex} f_{sye} \tag{2.25}$$

$$f_{ey} = k_{ey} f_{sye} \tag{2.26}$$

Then, λ_c (compressive strength modifier of confined concrete) is obtained using Equation 2.27 and 2.28.

$$\lambda_c = 2.254 \sqrt{1 + 7.94 \frac{f_e}{f_{co}}} - 2 \frac{f_e}{f_{co}} - 1.254 \tag{2.27}$$

where

$$f_e = \frac{f_{ex} + f_{ey}}{2} \tag{2.28}$$

Next, confined concrete modified compressive strength is derived from Equation 2.29.

$$f_{cc} = \lambda_c f_{co} \tag{2.29}$$

In addition, modified strain is obtained using Equation 2.30 in respect of confined concrete compressive strength modifier.

$$\epsilon_{cc} = \epsilon_{co}[1 + 5(\lambda_c - 1)] \tag{2.30}$$

where

$$\epsilon_{co} = \frac{f_{co}^{0.25}}{1150} \tag{2.31}$$

Unconfined concrete modulus of elasticity is calculated using Equation 2.32

$$E_c = 5000\sqrt{f_{co}} \tag{2.32}$$

While confined concrete secant modulus of elasticity is defined in accordance with Equation 2.40.

$$E_{sec} = \frac{f_{cc}}{\epsilon_{cc}} \tag{2.33}$$

Lastly, linearization of the stress-strain relationship of the concrete is done using Equations 2.34to 2.36.

$$x = \frac{\epsilon_c}{\epsilon_{cc}} \tag{2.34}$$

$$r = \frac{E_c}{E_c - E_{sec}} \tag{2.35}$$

$$f_c = \frac{f_{cc}xr}{r - 1 + x^r} \tag{2.36}$$

Respectively, linearized concrete stress-strain curve is defined for corresponding structural wall fibers in Perform3D as shown in Figure 2.16.

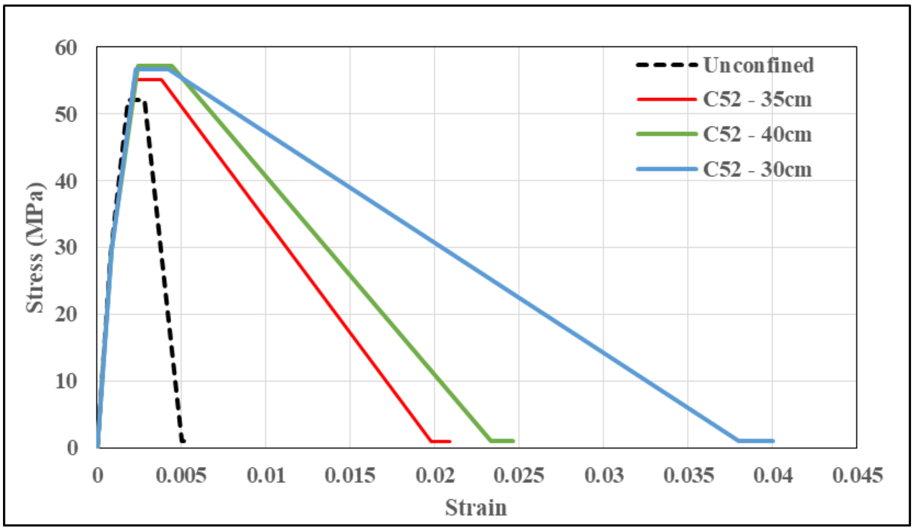

Figure 2.16. Linearized stress-strain relationship of concrete material.

On the other hand, reinforcing steel model is defined based on Equations 2.37, 2.38 and 2.39 while cyclic degradation is neglected. Besides, Non-buckling steel material is used for the steel reinforcement in Perform3D model.

$$f_s = E_s \epsilon_s \qquad (\epsilon_s \leq \epsilon_{sy}) \tag{2.37}$$

$$f_s = f_{sy} \qquad (\epsilon_{sy} \leq \epsilon_s \leq \epsilon_{sh}) \tag{2.38}$$

$$f_s = f_{su} - (f_{su} - f_{sy}) \frac{(\epsilon_{su} - \epsilon_s)^2}{(\epsilon_{su} - \epsilon_{sh})^2} \qquad (\epsilon_{sy} \leq \epsilon_s \leq \epsilon_{sh}) \tag{2.39}$$

The stress-strain relationship derived from the aforementioned equations is presented in Figure 2.19.

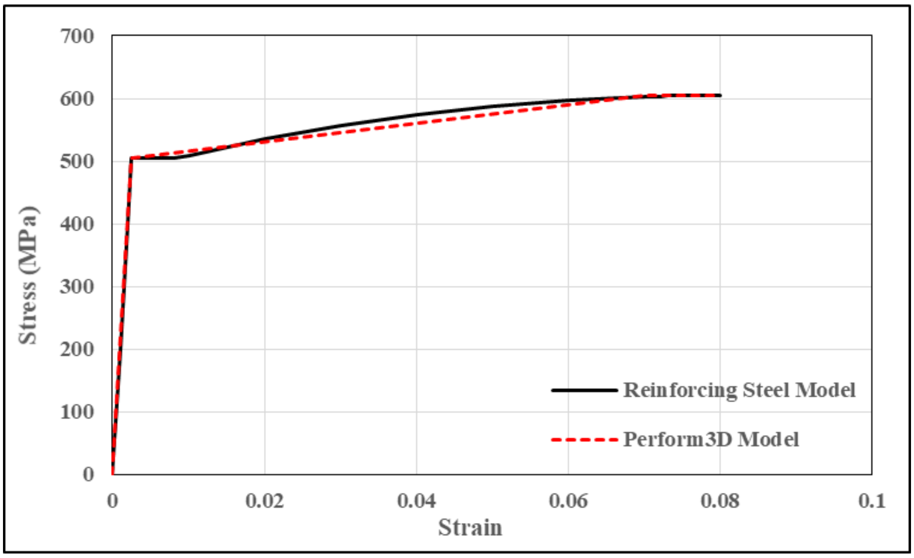

Figure 2.17. Reinforcing steel stress-strain relationship.

2.3.6.2. Modeling of Structural Members. There are two main approaches to consider nonlinear behavior of structural members. Firstly, lumped plasticity (also known as plastic hinge model) is used to consider columns nonlinear flexural behavior. In this approach concentrated PMM hinges is modeled for the possible inelasticity regions of columns which considers biaxial bending under axial loads (Figure 2.18).

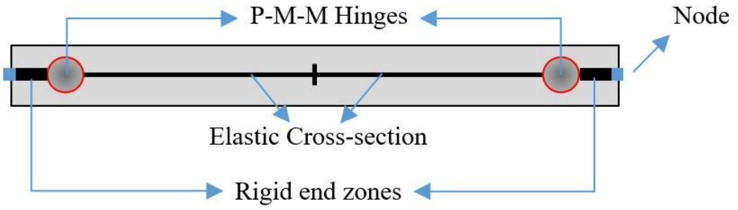

Figure 2.18. Modeling of columns using PMM hinges.

Plastic rotation capacities which accounts for nonlinear behavior of the columns are defined in compliance with ASCE 41-13 as presented in Table 2.15 [19].

Table 2.15. Acceptance criteria and nonlinear modeling parameters of columns.

Conditions			Plastic Rotation (rad)		Strength Loss Ratio	Performance Criteria (rad)		
$\frac{P}{A_g f_{ce}}$	$\rho_{sh} = \frac{A_{sh}}{b_w s}$	$\frac{V}{b_w h \sqrt{f_{ce}}}$	a	b	c	IO	LS	CP
≤ 0.10	≥ 0.0060	≤ 0.25	0.032	0.060	0.20	0.005	0.045	0.060
≤ 0.10	≥ 0.0060	≥ 0.50	0.025	0.060	0.20	0.005	0.045	0.060
≥ 0.60	≥ 0.0060	≤ 0.25	0.010	0.010	0.0	0.003	0.009	0.010
≥ 0.60	≥ 0.0060	≥ 0.50	0.008	0.008	0.0	0.003	0.007	0.008
≤ 0.10	≤ 0.0005	≤ 0.25	0.012	0.012	0.20	0.005	0.010	0.012
≤ 0.10	≤ 0.0005	≥ 0.50	0.006	0.006	0.20	0.004	0.005	0.006
≥ 0.60	≤ 0.0005	≤ 0.25	0.004	0.004	0.0	0.002	0.003	0.004
≥ 0.60	≤ 0.0005	≥ 0.50	0.0	0.0	0.0	0.0	0.0	0.0

In accordance with the given nonlinear modeling parameters, backbone curves are obtained with regard to Figure 2.19.

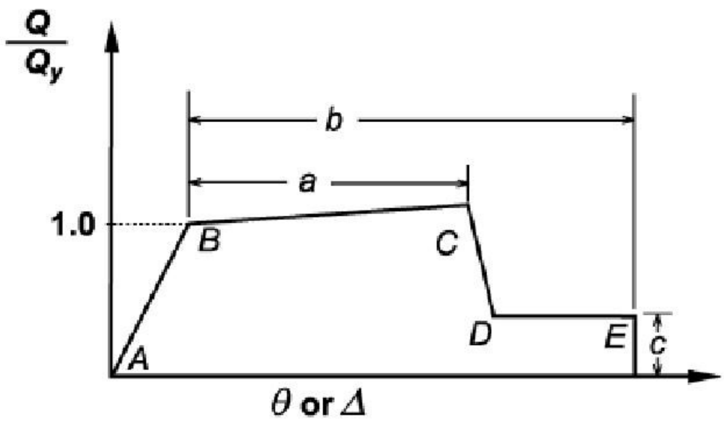

Figure 2.19. Backbone curve for nonlinear modeling.

Similar to the columns, nonlinear behavior of the beams is considered using lumped plasticity (using moment rotation hinges) as presented in Figure 2.20.

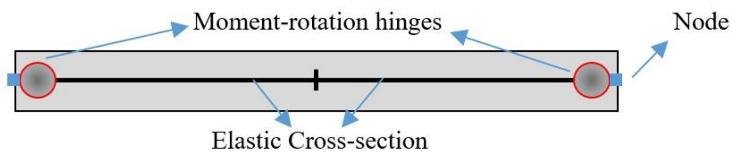

Figure 2.20. Modeling of beams using moment rotation hinges.

In compliance with ASCE 41-13, acceptance criteria and rotational capacities of the beams are defined with regard to Table 2.16.

Table 2.16. Acceptance criteria and nonlinear modeling parameters of beams.

Conditions			Plastic Rotation (rad)		Strength Loss Ratio	Performance Criteria (rad)		
$\frac{\rho-\rho'}{\rho_{bal}}$	Transverse Reinforcement	$\frac{V}{b_w h\sqrt{f_{ce}}}$	a	b	c	IO	LS	CP
≤ 0.0	Conforming	≤ 0.25	0.025	0.050	0.20	0.010	0.025	0.050
≤ 0.0	Conforming	≥ 0.50	0.02	0.040	0.20	0.005	0.020	0.040
≥ 0.50	Conforming	≤ 0.25	0.020	0.030	0.20	0.005	0.020	0.030
≥ 0.50	Conforming	≥ 0.50	0.015	0.020	0.20	0.005	0.015	0.020
≤ 0.10	Nonconforming	≤ 0.25	0.020	0.030	0.20	0.020	0.030	0.012
≤ 0.10	Nonconforming	≥ 0.50	0.010	0.015	0.20	0.0015	0.010	0.015
≥ 0.50	Nonconforming	≤ 0.25	0.010	0.015	0.20	0.005	0.010	0.015
≥ 0.50	Nonconforming	≥ 0.50	0.005	0.010	0.20	0.0015	0.005	0.010

On the other hand, there is a second approach called distributed plasticity approach (also known as fiber model) which is used to determine nonlinear behavior of structural walls. In accordance with fiber model approach force-deformation relationships of wall sections are defined as backbone curves. Moreover, the geometry of the wall sections are divided into several fibers and the corresponding uniaxial stress-strain relationship of each fiber is defined explicitly.

As mentioned, the lateral force resisting system of the sample structure consists of highly ductile structural walls. Thereby, structural walls play a significant role in terms of lateral resistance. Accordingly, modeling of their nonlinear behavior in the software is a crucial task. There are two methods available to define fiber sections in Perform3D whether as “Auto Section” or “Fixed Sections”. The limitation of “Auto Section” method is that only one type of concrete material can be used in the definition of a cross section while concrete and steel fibers as well as tributary area coordinates are assigned automatically. However, in the “Fixed Sections” method material type, area and coordinates of each fiber can be defined manually which provides the ability to model confined concrete in boundary regions and unconfined concrete in the web of structural wall sections. As a sample in Figure 2.21 and 2.22 cross section of a central core wall and its corresponding fiber model in Perform3D is presented.

Figure 2.21. Cross section of a structural wall.

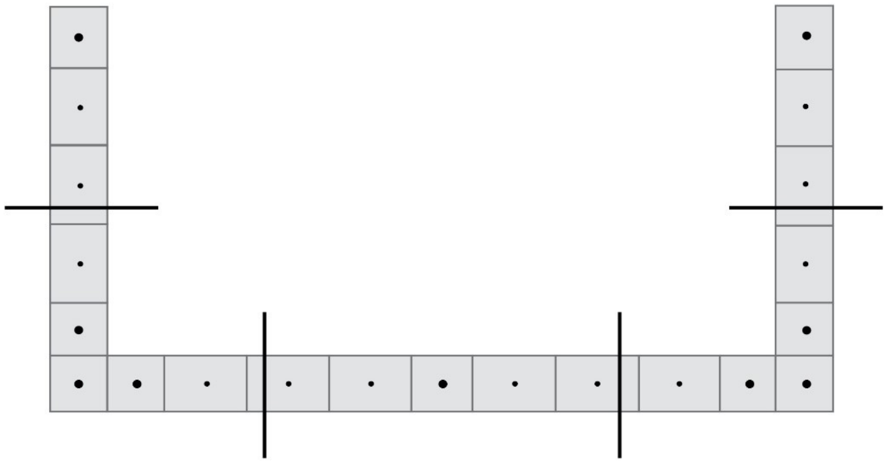

Figure 2.22. Fiber modeling of a structural wall in Perform3D.

In order to evaluate the performance level of the structure, strain gages are assigned at both ends of the structural walls. By doing so, the strain levels due to nonlinear behavior can be compared with the performance criterion introduced by TBSC 2018 in which strain limits of concrete and reinforcements is provided for 3 performance levels which is known as Immediate Occupancy (IO), Life Safety (LS), Collapse Prevention (CP).

2.3.6.3. Masses. In compliance with mass source definition in Equation 2.3 dead and reduced live loads are calculated as point masses automatically by ETABS in the linear model. Due to the complexities of mass assignment in Perform3D point masses are imported from ETABS to generate the nonlinear model.

2.3.6.4. Damping. In nonlinear analysis structural members dissipate the energy of an earthquake event by taking damage. Therefore, the members will experience inelastic range and a consistent deformation will remain in the structure. This energy dissipation is determined by a damping ratio which is used as 4.9% modal damping and 0.1% Rayleigh damping in order to consider higher mode effects in the energy absorption.

<u>2.3.6.5. Nonlinear Model Geometry.</u> As discussed, due to the difficulties of modeling procedures in Perform3D the geometry of the structure is also prepared in ETABS and exported to Perform3D (Figure 2.23(a)). The structure is considered to be fixed supported at the base level while the modeling of the foundation and soil structure interaction is neglected. Furthermore, superstructure slabs are not expected to experience a significant seismic action; therefore, they are not included in the nonlinear model. However, the nodes at each floor level of the upper system are slaved to each other. On the other hand, due to the importance of transition floor to distribute seismic actions to the perimeter walls, basement slabs are included in the model without any slaving of the nodes. Since, rigid diaphragm assumption of the basement slabs leads to have backstay effects on the structural walls. The geometry of the model imported to Perform3D is presented in Figure 2.23(b).

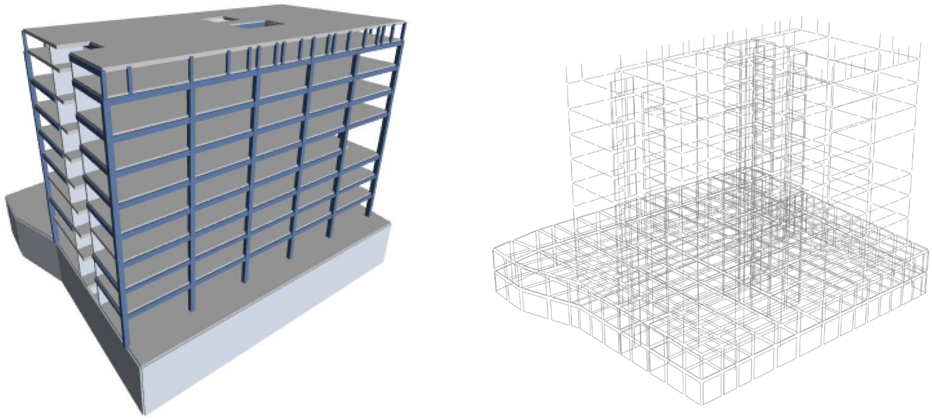

(a) (b)

Figure 2.23. Etabs linear model (a), Perform 3D nonlinear model (b).

In addition, the structural elements which is modeled for the superstructure as well as basement levels is provided as a sample story in Figures 2.24 and 2.25. The difference between superstructure stories and basement levels is that slabs of the upper system are neglected in accordance with nonlinear modeling. However, the basement slabs are modeled as elastic slabs in order to decrease the high demands due to backstay effects at basement levels.

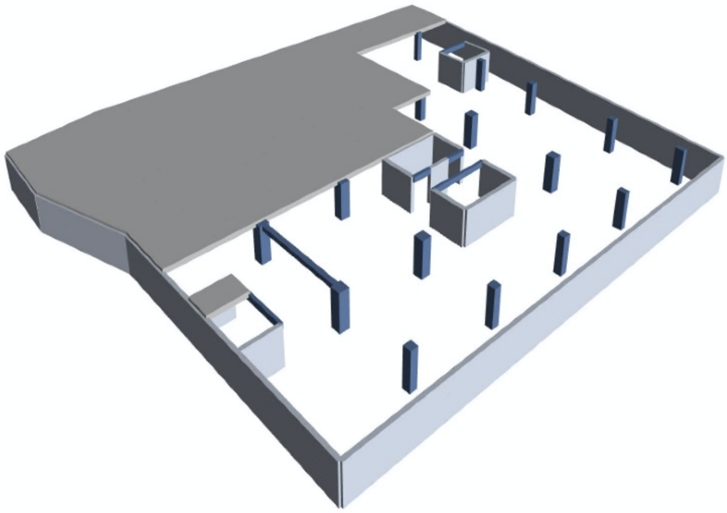

Figure 2.24. Sample basement level story.

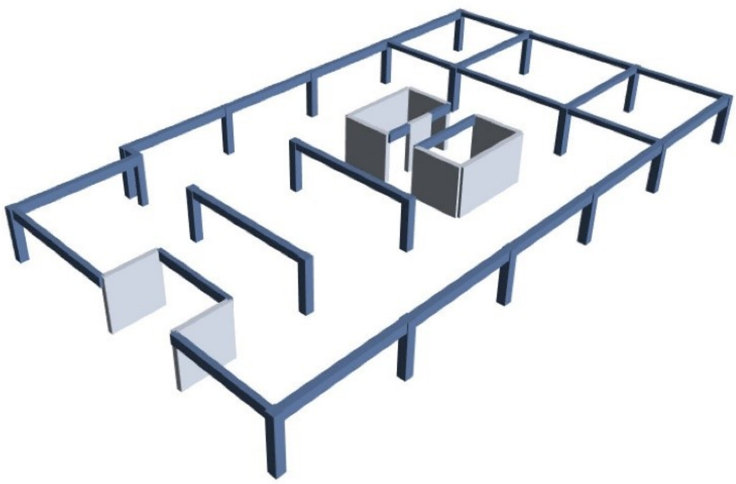

Figure 2.25. Sample superstructure story.

2.3.6.6. Seismic Hazard Definition and Ground Motion Record Selection. With respect to ground motion databases of PEER NGA WEST2 in which past earthquake records are obtained at various stations from all around the world, the classification of these records can be done with regard to their properties such as local soil conditions, fault type, distance to epicenter etc. By the use of Mean Square Error Scaling (Equation 2.40) 11 ground motion records are selected while the records are categorized with regard to Table 2.17.

Table 2.17. Record selection criteria of ground motion records.

Record Selection Criteria	
Source type	Strike slip fault mechanism (İstanbul)
Earthquake magnitude	$6.5 - 7.5$
Shear wave velocity, V_{S30}	$150 - 500$ (m/s)
Distance to closest active fault	$10 - 30$ (km)

In Mean Square Error method (MSE), with regard to the differences between spectral acceleration quantities and the target spectrum mean error is calculated at specific periods defined by the user. The records are scaled using elastic design spectrum introduced in TBSC 2018 for 2 earthquake levels of EL-1 and EL-2 as target spectra.

$$MSE = \frac{1}{m}\sum_{i=1}^{m} w_i (S_{aet} - S_{aer})^2 \tag{2.40}$$

In the direction of Equation 2.6, S_S (short period mapped spectral acceleration) and S_1 (1.0s period mapped spectral acceleration) coefficients are needed to define target elastic spectra. As mentioned, the spectral acceleration coefficients for EL-2 earthquake level is provided in Table 2.5. Accordingly, in respect of Turkish seismic map the S_s and S_1 values for EL-1 earthquake level is also obtained (Table 2.18). Moreover, the distance of the sample structure to the northern Anatolia active fault (closest active fault) is presented in Figure 2.26.

Table 2.18. Soil characteristic parameters for $EL-1$ earthquake.

Soil characteristic parameters	**Magnitude based on the location**
S_S	1.562
S_1	0.435
S_{DS}	1.562
S_{D1}	0.811
PGA	0.631(g)
PGV	39.218(cm/s)

In TBSC 2018, there are some limitations for the scaling of the records. Firstly, mean of the 11 ground motion components shall not be less than elastic design spectrum in the period range of 0.05s to 2.15s (0.2T_p to 1.5T_p in which T_p is the fundamental natural period of the structure) while minimum 0.05s accounts for basement vibration modes. Similarly, the resultant of the components in respect of SRSS combination shall not be beyond the limit of 1.3 times the elastic design spectrum in the aforementioned period range. Furthermore, the code limitation for the use of records of one ground motion from at most 3 stations has to be also satisfied. Lastly, the maximum allowable scale factor to use in the scaling of the records is considered not to exceed 10 in order to neglect small earthquake records in the analyses.The un-scaled selected records for the time history analyses is presented in Figure 2.27(a) to 2.27(v).

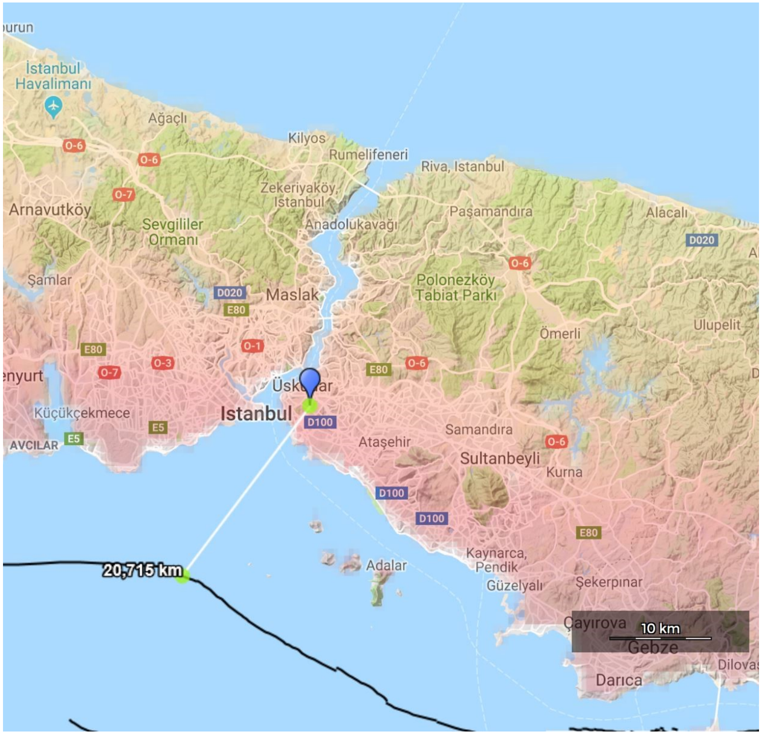

Figure 2.26. Project site distance to active fault.

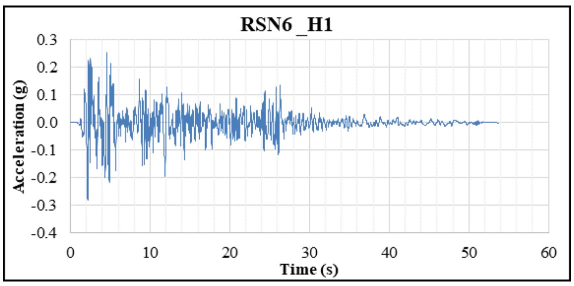

(a)

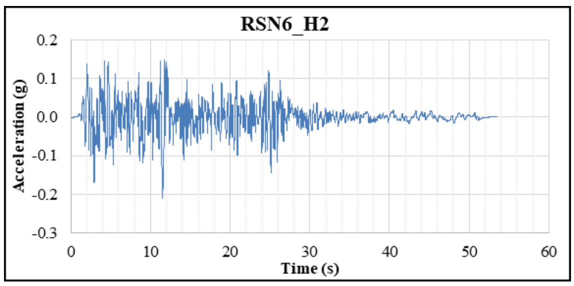

(b)

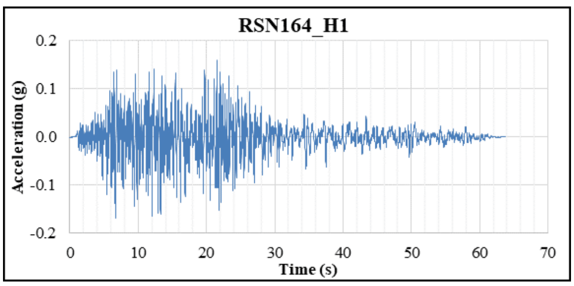

(c)

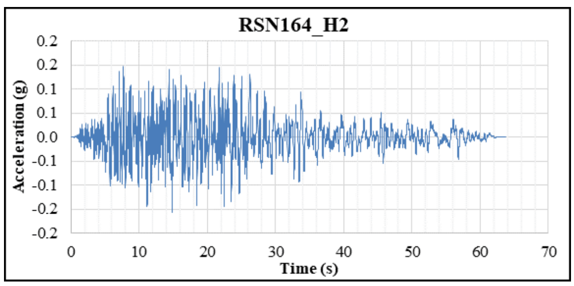

(d)

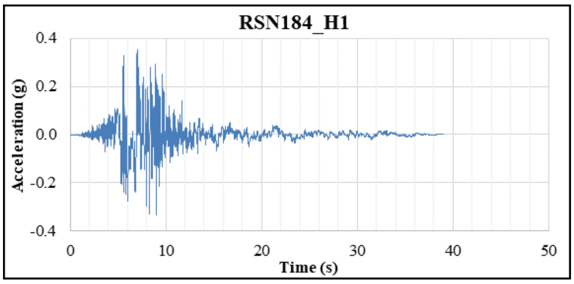
RSN184_H1
Acceleration (g)
0.4
0.2
0.0
-0.2
-0.4
0
10
20
30
40
50
Time (s)

(e)

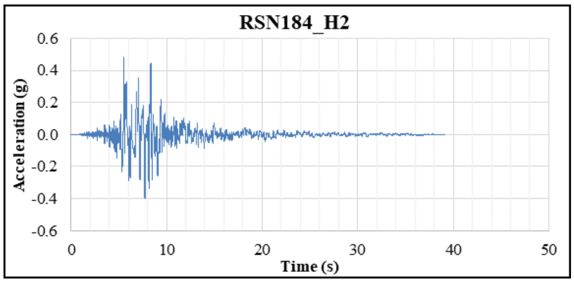
RSN184_H2
Acceleration (g)
0.6
0.4
0.2
0.0
-0.2
-0.4
-0.6
0
10
20
30
40
50
Time (s)

(f)

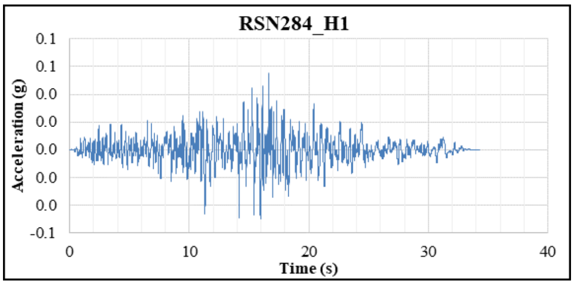
RSN284_H1
Acceleration (g)
0.1
0.1
0.0
0.0
0.0
0.0
0.0
-0.1
0
10
20
30
40
Time (s)

(g)

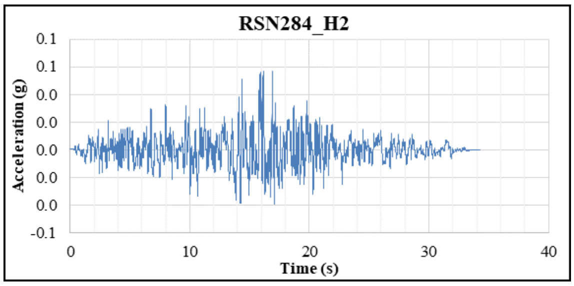
RSN284_H2
Acceleration (g)
0.1
0.1
0.0
0.0
0.0
0.0
0.0
-0.1
0
10
20
30
40
Time (s)

(h)

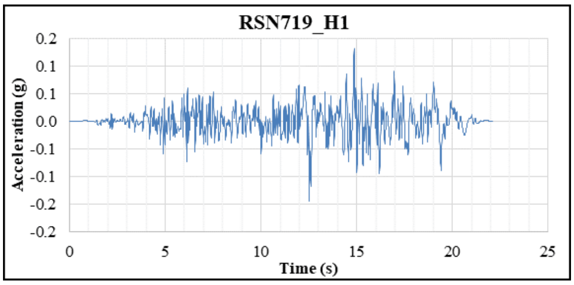
RSN719_H1
Acceleration (g)
0.2
0.1
0.1
0.0
-0.1
-0.1
-0.2
-0.2
0
5
10
15
20
25
Time (s)

(i)

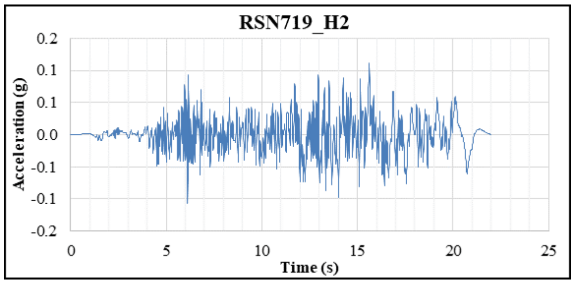
RSN719_H2
Acceleration (g)
0.2
0.1
0.1
0.0
-0.1
-0.1
-0.2
0
5
10
15
20
25
Time (s)

(j)

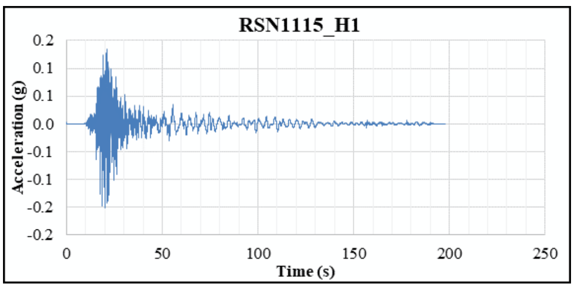
RSN1115_H1
Acceleration (g)
0.2
0.1
0.1
0.0
-0.1
-0.1
-0.2
-0.2
0
50
100
150
200
250
Time (s)

(k)

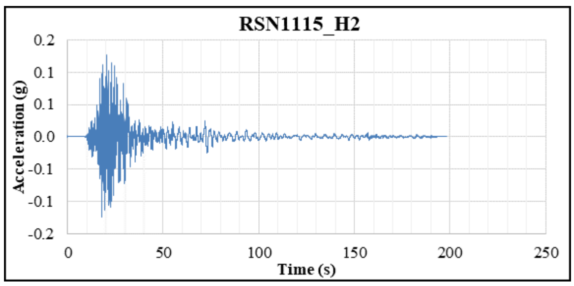
RSN1115_H2
Acceleration (g)
0.2
0.1
0.1
0.0
-0.1
-0.1
-0.2
0
50
100
150
200
250
Time (s)

(l)

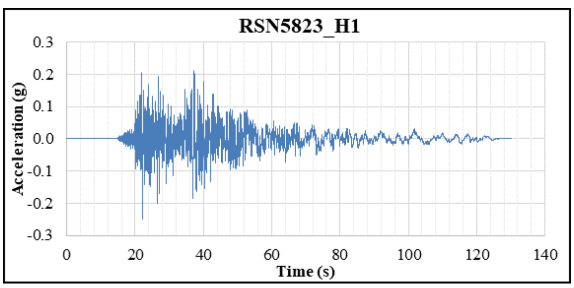
RSN5823_H1
Acceleration (g)
0.3
0.2
0.1
0.0
-0.1
-0.2
-0.3
0
20
40
60
80
100
120
140
Time (s)

(m)

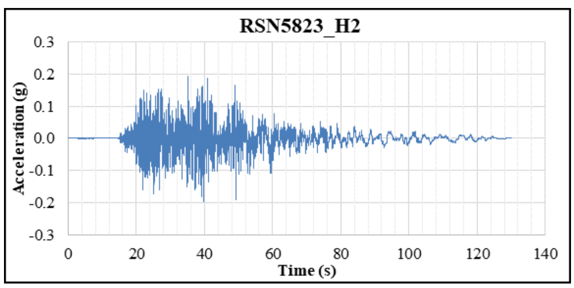
RSN5823_H2
Acceleration (g)
0.3
0.2
0.1
0.0
-0.1
-0.2
-0.3
0
20
40
60
80
100
120
140
Time (s)

(n)

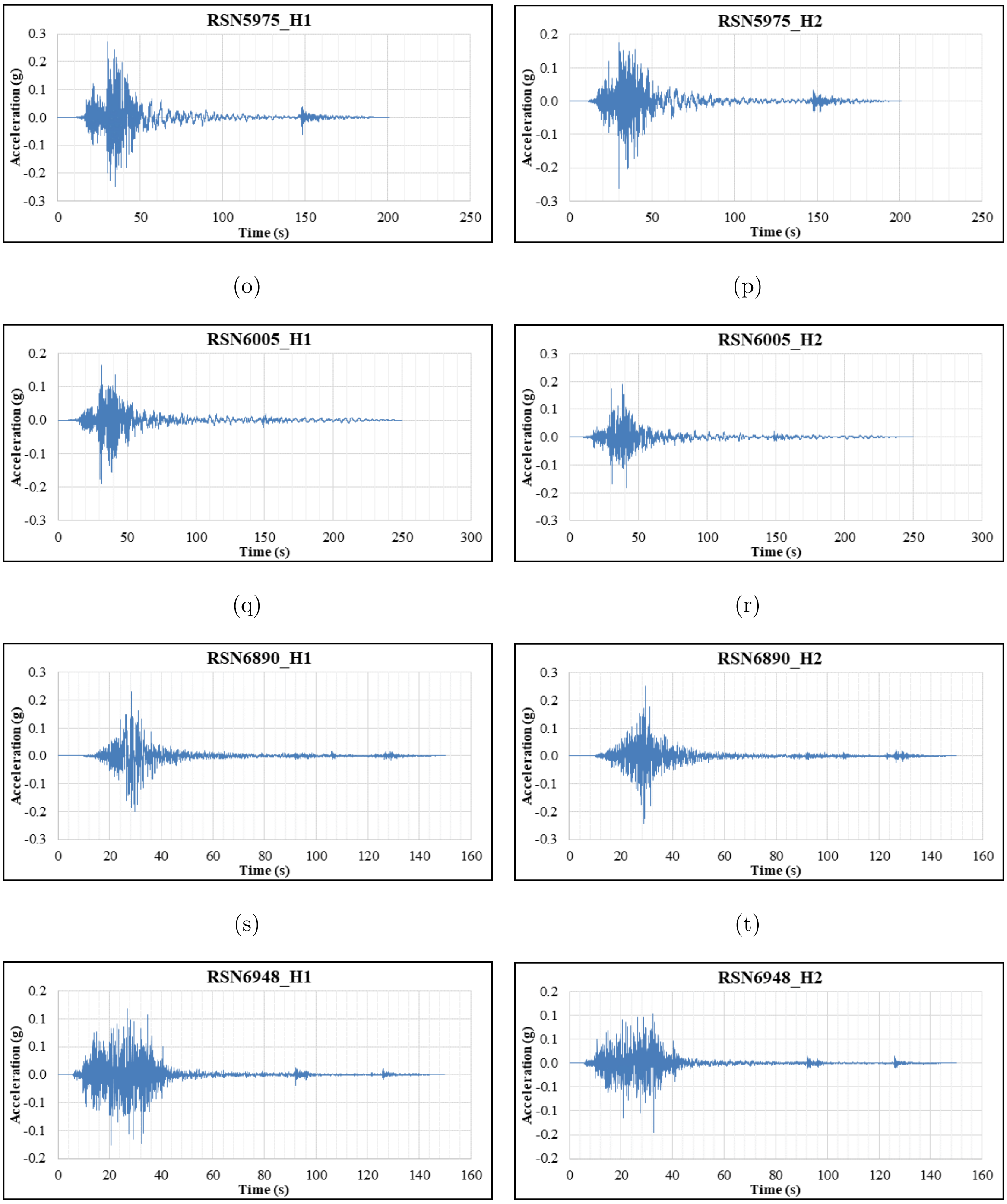

(o) (p)

(q) (r)

(s) (t)

(u) (v)

Figure 2.27. Un-scaled 11 selected ground motion records.

The properties of the selected ground motions in compliance with each earthquake level is provided in Table 2.19.

Table 2.19. Properties of selected ground motion records for EL-1 and EL-2 level earthquakes.

Record ID	Earthquake Name	EL-1 Scale Factor	EL-2 Scale Factor	Magnitude	Mechanism	R_{JB}	V_{S30}
RSN 6	Imperial Valley	2	1.518	6.95	Strike Slip	6.09	213.4
RSN 164	Imperial Valley	2.432	2.059	6.53	Strike Slip	15.19	471.5
RSN 184	Imperial Valley	3.5	1.6	6.53	Strike Slip	5.09	202.3
RSN 284	Irpinia Italy	8.677	7.348	6.9	Strike Slip	9.52	476.6
RSN 719	Superstition Hills	4.458	3.775	6.54	Strike Slip	17.03	208.7
RSN 1115	Kobe Japan	3.101	2.626	6.9	Strike Slip	28.08	256
RSN 5823	El Mayor Mexico	3	1.683	7.2	Strike Slip	18.21	242
RSN 5975	El Mayor Mexico	2.5	1.7	7.2	Strike Slip	19.12	231.2
RSN 6005	El Mayor Mexico	2.5	2.046	7.2	Strike Slip	36.15	202.9
RSN 6890	El Mayor Mexico	3.6	2.2	7	Strike Slip	17.64	204
RSN 6948	Darfield New Zealand	4.044	2.2	7	Strike Slip	30.63	481.6

In compliance with the scale factors provided in Table 2.19 the aforementioned code limitations for the scaling of the records is checked corresponding to each earthquake level. Figures 2.20 and 2.21 presents EL-1 level earthquake acceleration response spectra which is checked for mean of components not be less than elastic response spectrum while mean of the components SRSS combination is not beyond 1.3 times elastic design spectrum.

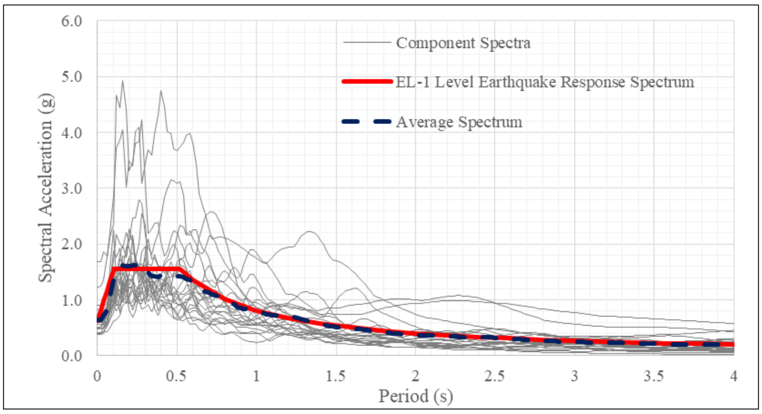

Figure 2.28. EL-1 level acceleration response spectra of selected ground motions.

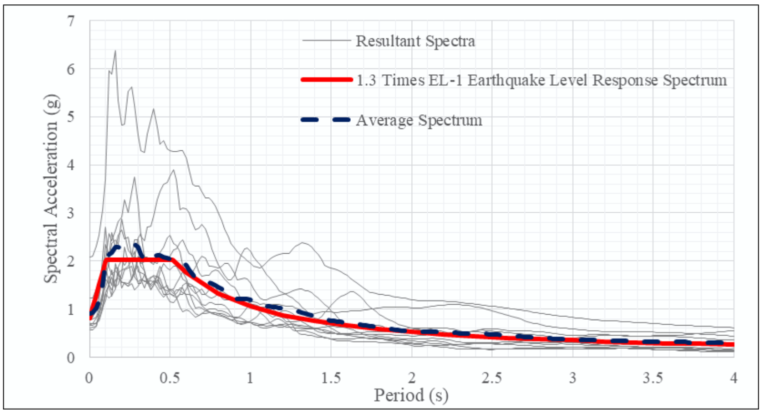

Figure 2.29. EL-1 Level SRSS acceleration spectra of selected ground motions.

Similar to the EL-1 level earthquake, the mean of acceleration spectra as well as mean of SRSS acceleration spectra is also presented for EL-2 level earthquake in Figure 2.30 and 2.31.

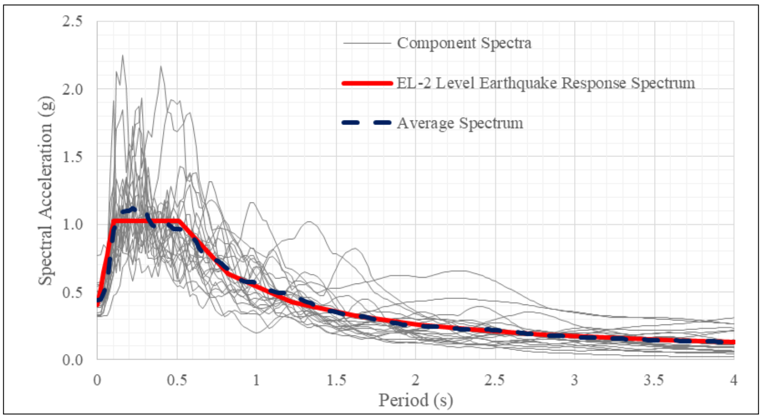

Figure 2.30. EL-2 level acceleration response spectra of selected ground motions.

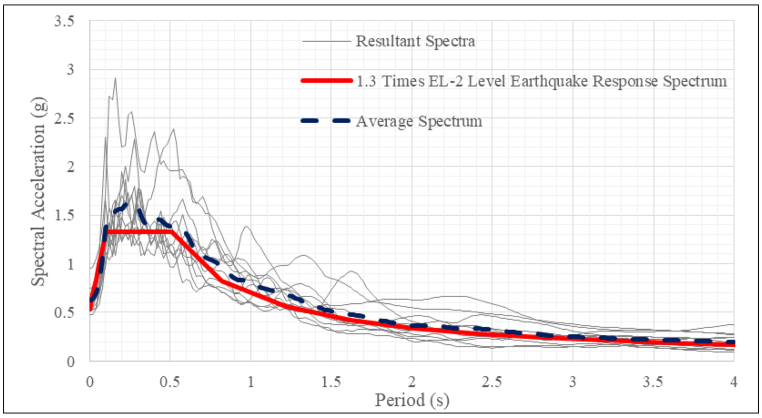

Figure 2.31. EL-2 Level SRSS acceleration spectra of selected ground motions.

3. ANALYSIS RESULTS

All of the analysis procedures described in the previous chapter are applied on the representative reinforced concrete building structure, and analysis results for selected response quantities (story shear forces and shear forces on structural walls) are compared systematically in this chapter. In addition, the performance level of the structure is also determined based on TBSC 2018 performance limits, and the NLRHA results are also compared with the design forces derived from TBSC 2018 strength-based analysis methods. The linear analysis results are obtained for the EL-2 seismicity level, which is the design earthquake level, while NLRHA results are presented for both EL-1 and EL-2 level earthquakes. For NLRHA analyses, 11 pair of ground motions are used, where each pair is also re-applied at 90-degree rotated state. Thereby, 22 nonlinear time history analyses are conducted, and average of the analysis results are presented.

3.1. TBSC 2018 Methodologies

3.1.1. Two-Stage Approach - 4.7.5 ELF Method

As discussed in the previous chapter, similar to the TEC 2007 Equivalent Static Lateral Load methodology, upper system response quantities are obtained by only considering the superstructure mass in accordance with the 4.7.5 method of TBSC 2018. Accordingly, lower portion forces based on the 4.7.5 method are derived from a simple multiplication of spectral acceleration (at $T = 0$) and lower system story masses. By doing so, lower system internal forces in compliance with ductile behavior are obtained through a linear combination of forces coming from the superstructure together with the internal forces derived from the lower system itself. Although, in order to get non-ductile internal forces of the lower system, upper portion forces are magnified by $D_{upper} = 2.5$ while lower portion forces are amplified by $\bar{D_{lower}} = 1.5$. Story shear responses in accordance with 4.7.5 method are presented in Figure 3.1 for both X and Y directions of the building.

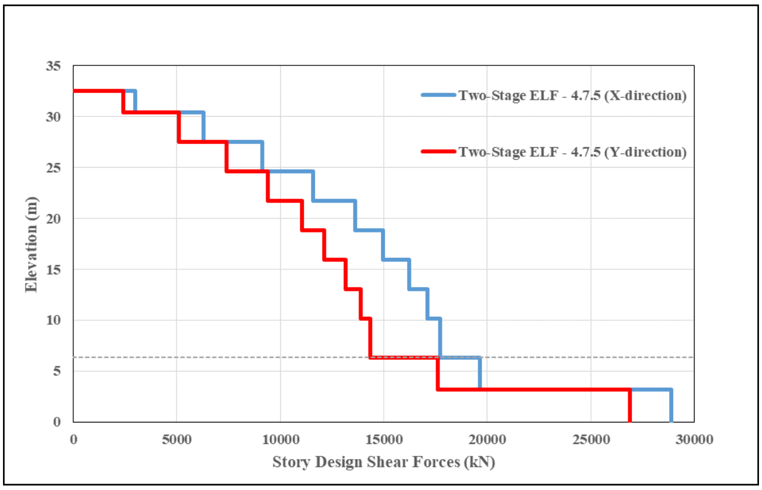

Figure 3.1. Story Forces Based on 4.7.5 Method for X and Y directions.

3.1.2. Two-Stage Approach - 4.8.5 RSA Method

The main difference between the two Response Spectrum Analysis methods in TBSC 2018 is that in the 4.3.6.2 method, the total structure mass is taken into account to calculate the upper portion internal forces. However, in the 4.8.5 method, only the upper mass is considered to obtain upper portion internal forces. In Figures 3.2 and 3.3, the results obtained using the 4.8.5 RSA method are compared with 4.7.5 ELF method, which are both based on the aforementioned two-stage approach. In compliance with two-stage approach, only upper mass is considered for the calculations of the superstructure at the first stage. Based on the upper portion response values it is observed that Equivalent Lateral Force methodology leads to obtain slightly greater response quantities in comparison to RSA methodology, as expected. On the contrary to the superstructure, it is observed that two-stage Response Spectrum Analysis of the lower portion leads to get significantly larger values of story shear in comparison to Equivalent Static Lateral Load Analysis. This is explained with regards to the flexibility and dynamic properties of the lower portion. The vibration modes of the lower portion have natural periods that correspond to large values on the reduced acceleration spectrum. Therefore, through a SRSS combination of each mode, larger values for story shear are obtained at the basement levels, compared to the Equivalent Static

Lateral Load Analysis method which assumes that the natural period is $T = 0$ for the basement.

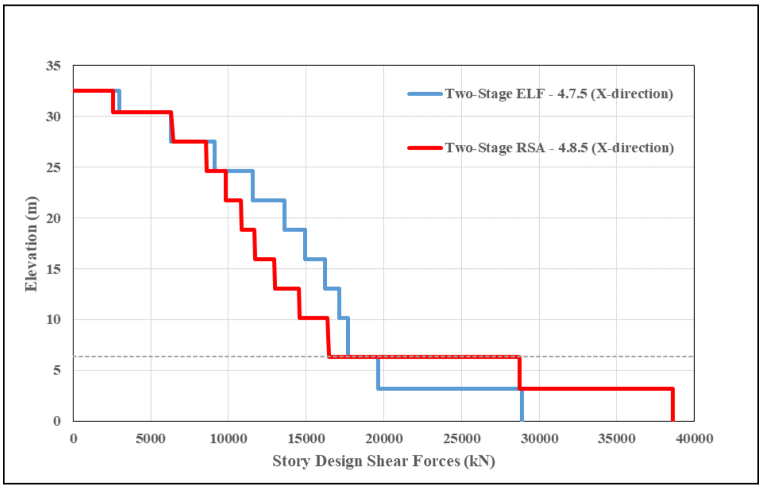

Figure 3.2. Comparison of TBSC 2018 two-stage methods (4.8.5 and 4.7.5) in X-direction.

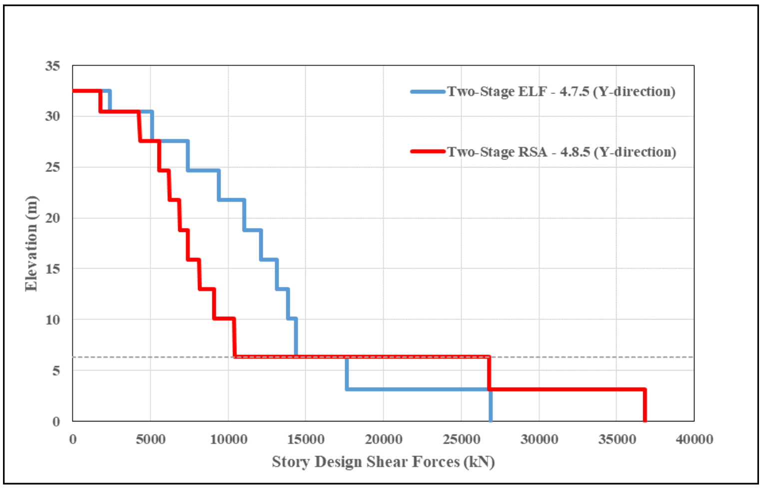

Figure 3.3. Comparison of TBSC 2018 two-stage methods (4.8.5 and 4.7.5) in Y-direction.

3.1.3. Total Structure Approach - 4.3.6.1 ELF Method

In the 4.3.6.1 method, in order to obtain the superstructure and lower portion response quantities, the total structure mass is considered. However, superstructure design forces are obtained considering to $R_a = 6$ as the reduction factor, while basement level forces are derived from a reduction factor of $(\bar{R}_a)_{lower} = 5.1$, as per the 4.3.6.1 approach. In spite of the fact that distribution of lower portion masses over total structure height based on 4.3.6.1 approach leads to reach large story shear forces on the upper system (due to definition of building height at the foundation level), the use of $(\bar{R}_a)_{lower} = 5.1$ for the lower portion causes lower quantities of story shear compared to the 4.7.5 method at the basement levels. Figures 3.4 and 3.5 presents a comparison between 4.3.6.1 and 4.7.5 methods which are the two ELF analysis approaches provided by TBSC 2018. As seen in the figure, the analysis results obtained using the 4.3.6.1 method deviates significantly from the expected distribution of story shear forces.

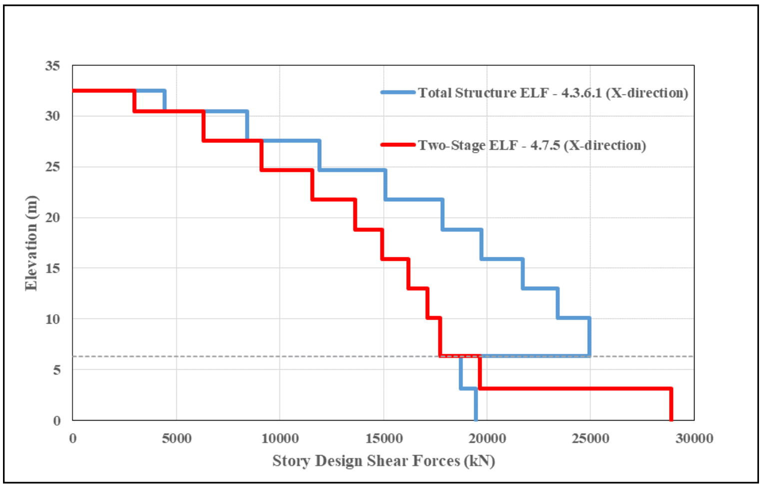

Figure 3.4. Comparison of ELF methods provided by TBSC 2018 in X-direction.

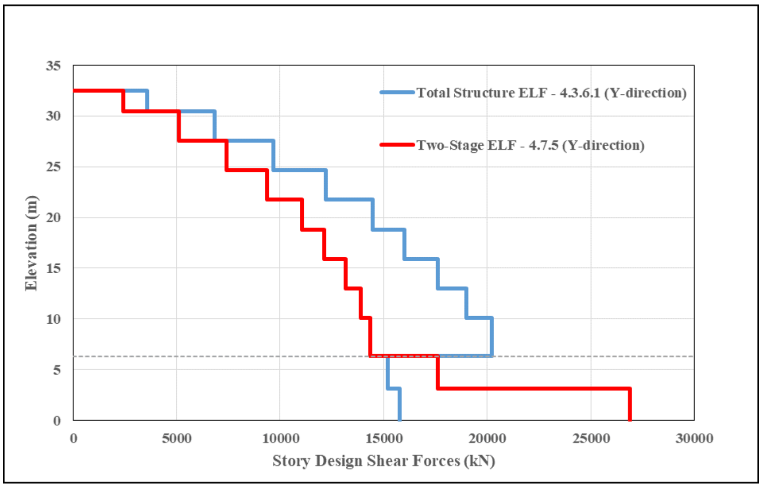

Figure 3.5. Comparison of ELF methods provided by TBSC 2018 in Y-direction.

3.1.4. Total Structure Approach - 4.3.6.2 RSA Method

In the 4.3.6.2 method, the total structure mass is considered in Modal Response Spectrum Analysis of the superstructure. Accordingly, due to the difference in mass consideration, the 4.3.6.2 method leads to slightly larger values of story shear forces for the upper portion in comparison to two-stage 4.8.5 method. In addition, for the analysis of the lower portion, there are two options in the 4.3.6.2 method related to calculating the load reduction factor for the lower portion assuming a behavior factor of $R_{lower} = 2.5$ (the simplified conservative case) or calculating it based on the modal base shear ratios for each direction. The comparison in Figures 3.6 and 3.7 indicates that 4.3.6.2 method with the simple $R_{lower} = 2.5$ assumption and and the same method based on the modal base shear ratios calculation give significantly different story shear forces at the basement levels of the building, although they are both smaller that the 4.8.5 RSA method.

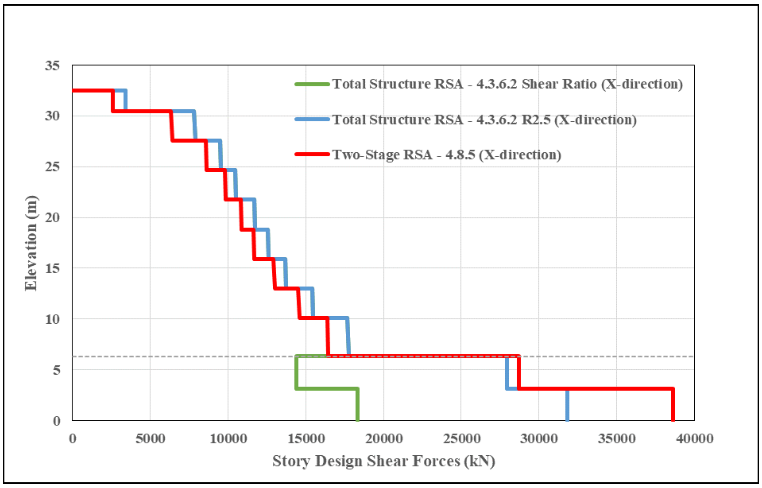

Figure 3.6. Comparison of RSA methods (4.8.5 and 4.3.6.2) based on TBSC 2018 in X-direction.

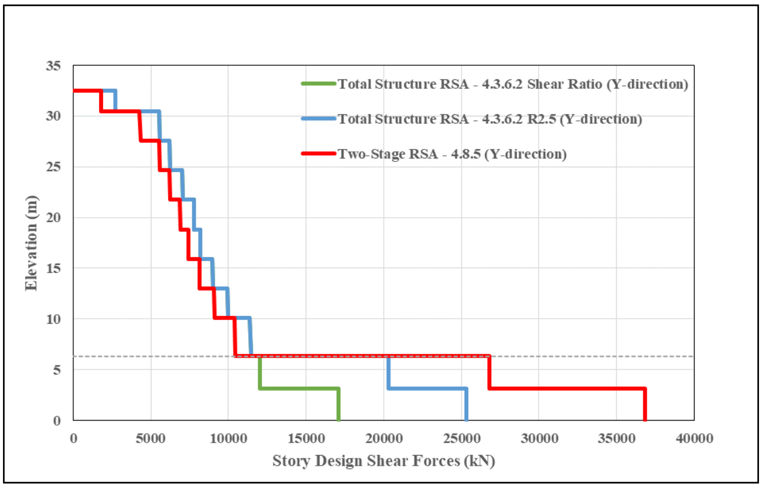

Figure 3.7. Comparison of RSA methods (4.8.5 and 4.3.6.2) based on TBSC 2018 in Y-direction.

3.1.5. Comparison of All Methods Provided by TBSC 2018

A comparison between the results derived from all of the methods recommended by TBSC 2018 is provided in this section. Due to the fact that 4.7.5 method is in the same manner as TEC 2007 ELF procedure; the 4.7.5 response quantities are considered as reference story shear forces. In accordance with Figure 3.5, it is observed that the simplified version of 4.3.6.2 (total building mass considering to $R = 2.5$ for basement levels) leads to close responses to 4.7.5. Therefore, the simplified 4.3.6.2 ($R = 2.5$) and the 4.7.5 methods are taken into account as analysis methods that are consistent with each other. On the other hand, story shear responses show that the consideration of basement-level masses in ELF analysis of the overall structure results in overestimated shear responses for the superstructure in the 4.3.6.1 method. However, the use of $(\bar{R}_a)_{lower} = 5.1$ leads to underestimated story shear forces in the lower portion. The reason why the 4.8.5 method (two stage RSA) provides very large story shears at the basement levels (compared to the 4.7.5 method) can be explained through the lower portion natural periods and the corresponding reduced spectral accelerations. The basement lateral forces are calculated during the second stage of 4.7.5 method from basement masses multiplied by a constant spectral acceleration (at $T = 0$) which is equal to $2.67 m/s^2$, whereas during the second stage of the 4.8.5 method the corresponding reduced spectral accelerations included in SRSS combination of the RSA procedure are almost twice that value. The reduced spectral accelerations corresponding to first six vibration modes of the basement are provided in Table 3.1.

Table 3.1. Basement response spectrum modal information.

Mode	**Period (s)**	**Spectral Acceleration** (m/s^2)
1	0.099	5.81
2	0.083	5.35
3	0.059	4.64
4	0.057	4.56
5	0.056	4.55
6	0.050	4.34

Furthermore, the 4.3.6.2 method, in which the earthquake load reduction factors for the basement are obtained based on modal base shear ratios, results in underestimated story shear forces for the lower portion.

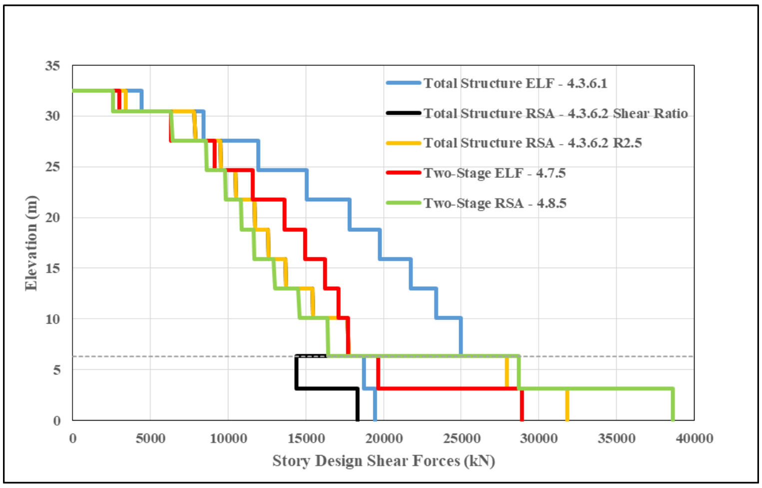

Figure 3.8. Comparison of all methods based on TBSC 2018 methodologies for X-direction.

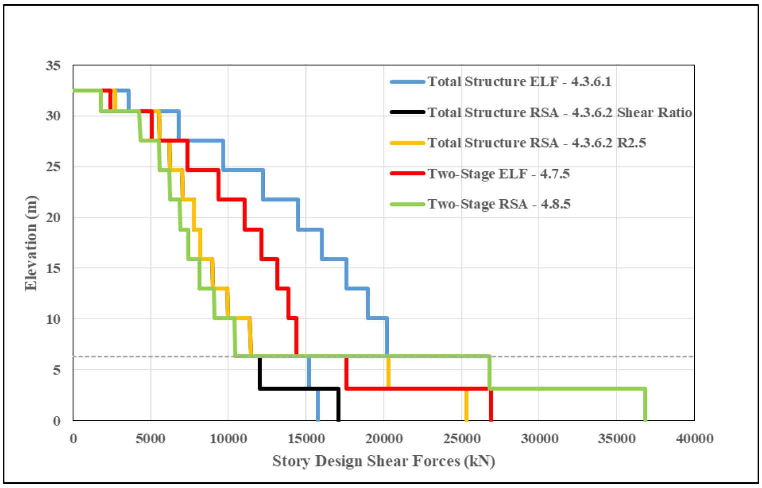

Figure 3.9. Comparison of all methods based on TBSC 2018 methodologies for Y-direction.

3.2. TEC 2007 Methodologies

The analysis results obtained using the approaches specified in TEC 2007 are presented in this section. As discussed previously, the ELF method in TEC 2007 is identical to the TBSC 2018 4.7.5 approach for both the superstructure and the basement of the building. However, TEC 2007 analyses are conducted considering uncracked sections while the TBSC 2018 method is applied based on cracked sections for which the stiffness modifiers are defined using Table 4.2 of the code (use of effective cross section rigidity). Moreover, in compliance with TEC 2007, the lateral loads are considered to be applied to the upper and lower portion simultaneously while a linear load combination is used for the application of the TBSC 2018 method. Using this linear combination will lead to backstay effects in the structural walls when the lateral loads on are applied separately. Story design shear forces in accordance with TEC 2007 methods are compared with the 4.7.5 method of TBSC 2018 in Figures 3.10 and 3.11. Based on the figure, it is observed that uncracked section assumption which results in shorter fundamental natural periods increases the corresponding spectral accelerations; thereby, story shear forces are increased, as expected. Other than that, the TEC 2007 and the TBSC 2018 Two-Stage ELF methods provide analysis results that are consistent with each other.

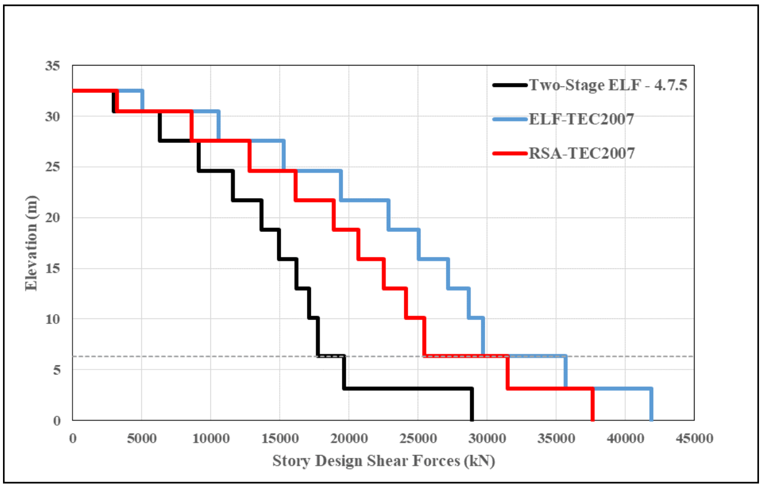

Figure 3.10. Comparison of story design shear forces based on TEC 2007 methodologies for X-direction.

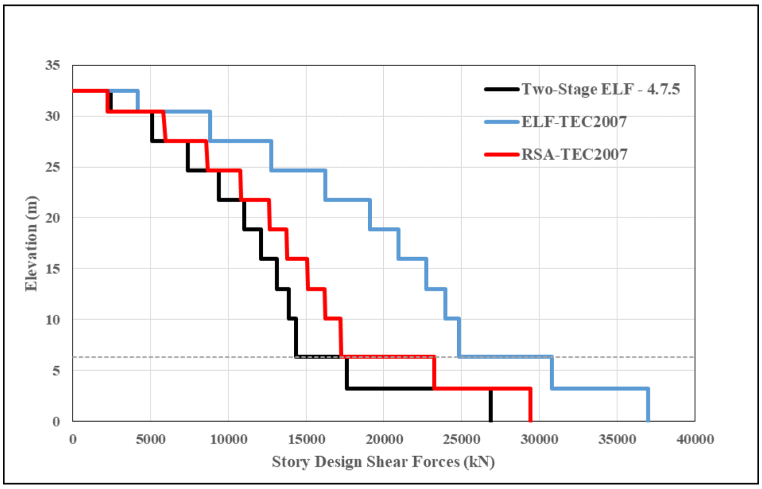

Figure 3.11. Comparison of story design shear forces based on TEC 2007 methodologies for Y-direction.

3.3. ASCE 7-10 Methodology

As mentioned, a two-stage analysis is specified in ASCE 7-10 for buildings with rigid basement levels. A two-model approach is used to obtain the seismic actions on each portion. The superstructure is considered as a separate fixed-supported model in which the internal forces are calculated using the ELF or RSA methods described in the code. In following, the support reactions obtained at each of 6 DOFs at base level supports of the upper system model are applied statically to the top elevation of the lower system model, in opposite direction. Subsequently, an ELF procedure is conducted for the lower system model. Therefore, the internal forces of the lower system are obtained by a linear combination of the statically applied forces and moments from the upper structure and lower portion's ELF analysis results itself. Story design shear forces based on ASCE 7-10 approaches are provided in Figures 3.12 and 3.13 while the results are compared with 4.7.5 method which is considered as the reference method in TBSC 2018. In accordance with Figures 3.12 and 3.13, in terms of the ELF procedure, the ASCE 7-10 method gives larger story shear forces in the superstructure, due to the fact that fixed supported superstructure consideration decreases the fundamental natural period of the structure; therefore, the upper system is subjected to larger spectral accelerations corresponding to the decreased natural period. In conclusion, the ASCE 7-10 methods give consistent analysis results with the 4.7.5 Two-Stage ELF method in TBSC 2018.

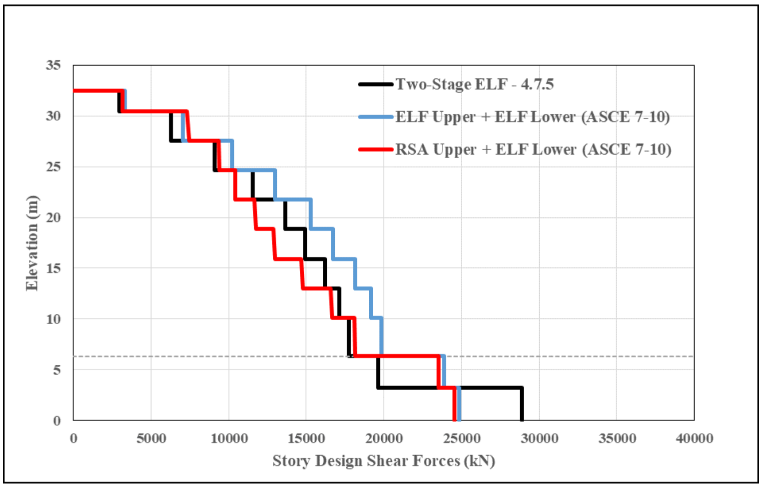

Figure 3.12. Comparison of story design shear forces based on ASCE 7-10 methods in X-direction.

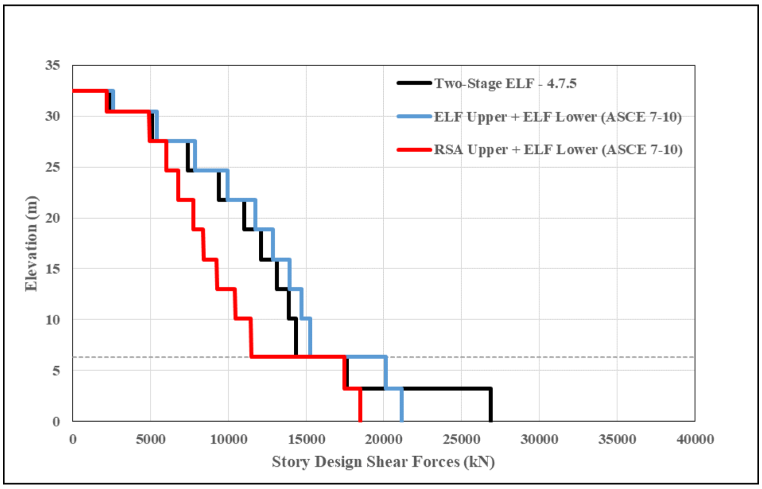

Figure 3.13. Comparison of story design shear forces based on ASCE 7-10 methods in Y-direction.

3.4. Eurocode 8 Methodology

In Eurocode 8, basement floors are assumed to be infinitely rigid in lateral direction. Moreover, the earthquake forces acting on the rigid basement levels are assumed to be fully-resisted by the rigid perimeter basement walls. Therefore, basement level masses are neglected in the analysis of the total structure. In terms of the behavior factor, structural elements at basement levels are designed using the same behavior factor as the superstructure (e.g., $R = 6$) also considering capacity design principles for brittle failure modes, and the foundation elements can be designed for low ductility class ($R = 1.5$ for reinforced concrete buildings). As shown in Figures 3.14 and 3.15, in the Eurocode 8 method, below the transition floor between the upper and lower structure, story shear forces remain constant since the mass of the basement floors is neglected in the analysis. Accordingly, basement-level story shear forces are much smaller that the 4.7.5 method in TBSC 2018. However, the total base shear transmitted to the foundation, calculated using a coefficient of $R = 1.5$ in the Eurocode 8 ELF method, is consistent with the 4.7.5 Two-Stage ELF method in TBSC 2018.

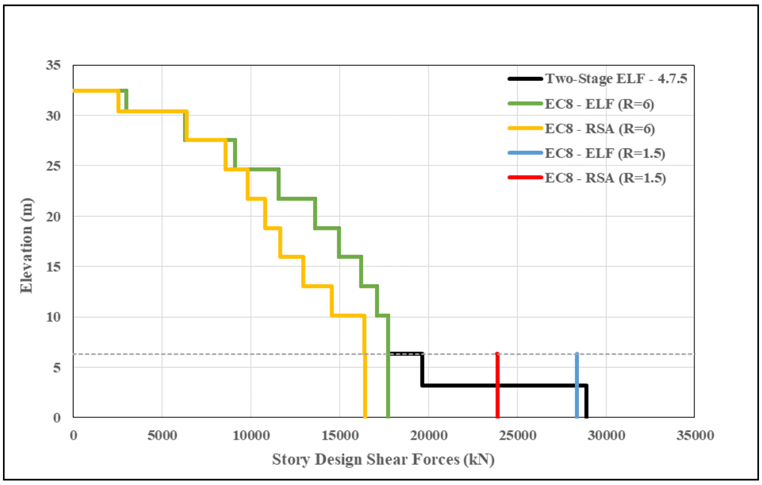

Figure 3.14. Comparison of Eurocode 8 approaches in X-direction.

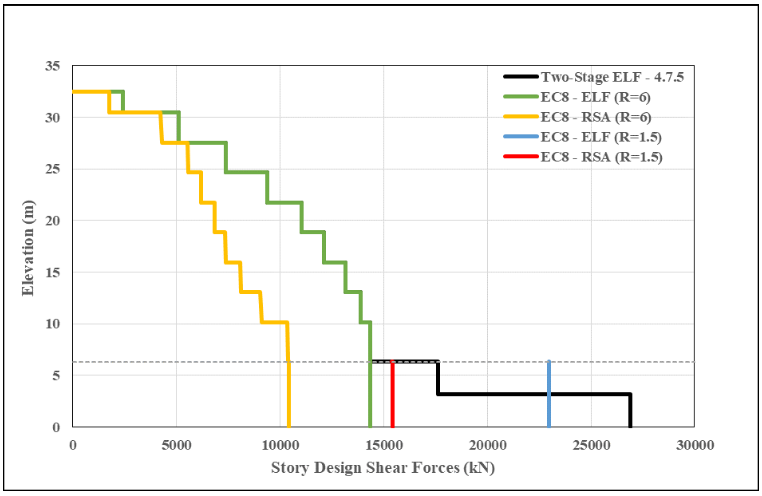

Figure 3.15. Comparison of Eurocode 8 approaches in Y-direction.

Moreover, the results of the superstructure is as same as the 1st stage of TBSC 2018 reference method (4.7.5) in which only upper mass is considered for the application of ELF procedure.

3.5. Comparison of Story Shear Forces with NLRHA Results

In order to check the reliability of the results obtained from the linear methods of analysis for design, they are compared with the nonlinear response history analysis results obtained for the building investigated. In Figure 3.16 and Figure 3.17, nonlinear analysis results under the EL-1 and EL-2 level earthquakes are compared with the linear analysis methods (under reduced earthquake actions) described in TBSC 2018, in terms of the story shear responses (amplified considering structural over-strength) along the total height of the structure. Based on the results presented in Figures 3.16 and 3.17, it can deduced that all of the linear analysis methods of TBSC 2018 provide safe predictions of story shear responses for the superstructure, with magnitudes even larger that the NLRHA results under the EL-1 earthquake level, while only the 4.7.5 Two-Stage ELF and the simplified 4.3.6.2 Total Structure (simplified for $R = 2.5$) methods give consistent results at the basement levels with the NLRHA results under the EL-2 earthquake level. It is also clear from the figure that the 4.3.6.1 Total Structure ELF method largely overestimates the story shear forces for the upper structure and severely underestimates the story shear forces in the basement, the detailed (not simplified) 4.3.6.2 Total Structure RSA method also severely under-predicts the story shear forces in the basement, and the 4.8.5 Two-Stage RSA method significantly overestimates the story shear forces on the basement levels under the EL-2 level (design level) earthquake.

These comparisons indicate that only the 4.7.5 Two-Stage ELF and the simplified 4.3.6.2 Total Structure (simplified for $R = 2.5$) methods provide reasonable estimations of the global earthquake force (story shear) demands acting on the structure, along both the upper portion and the lower basement portion. However, what is more relevant for design of the basement levels is the internal forces developing in the structural members (structural walls and columns), since the majority of those story shear force demands will be resisted by the perimeter basement walls. Therefore, in the following section, the design-level shear forces on the structural walls are presented, in which back-stay effects on wall shear forces are also noticeable.

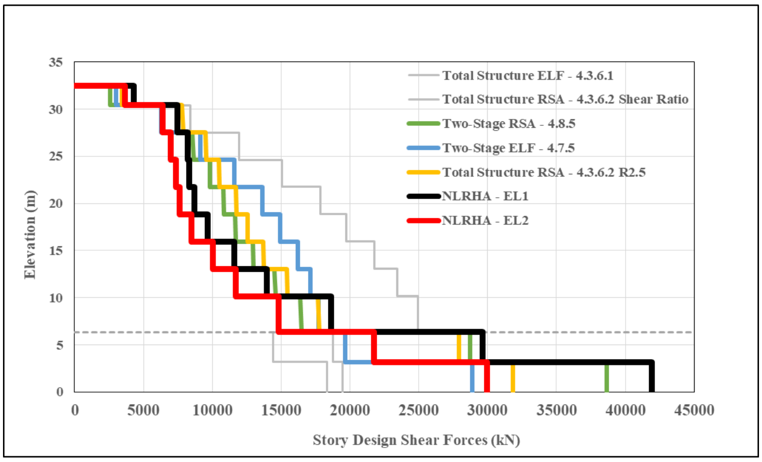

Figure 3.16. Comparison of linear and nonlinear results based on TBSC 2018 in X-direction.

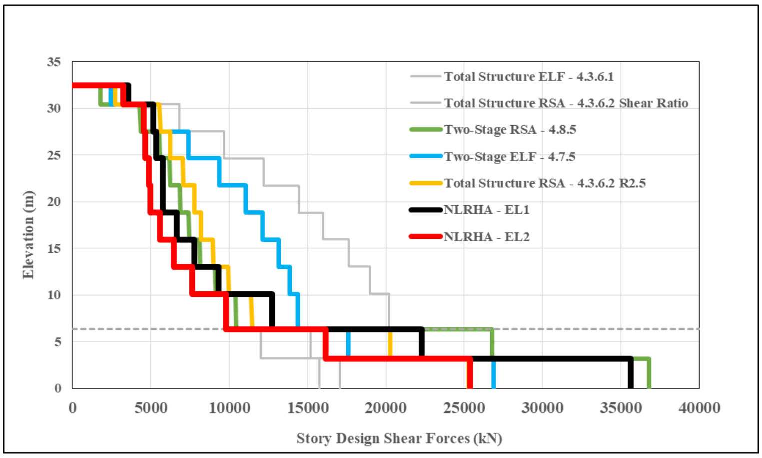

Figure 3.17. Comparison of linear and nonlinear results based on TBSC 2018 in Y-direction.

3.6. Comparison of Internal Shear Forces on Structural Walls with NLRHA Results

Following comparison of the story shear forces presented in the previous section, the internal shear forces on structural walls (amplified considering over-strength) obtained using the linear analysis methods in TBSC 2018 and NLRHA of the building (under EL-2 and EL-1 earthquake levels) are compared in this section. Internal shear forces on only the U-shaped walls (entire cross-section) are investigated for demonstrative purposes. The wall nomenclature on the plan view of the building is shown in Figure 3.18.

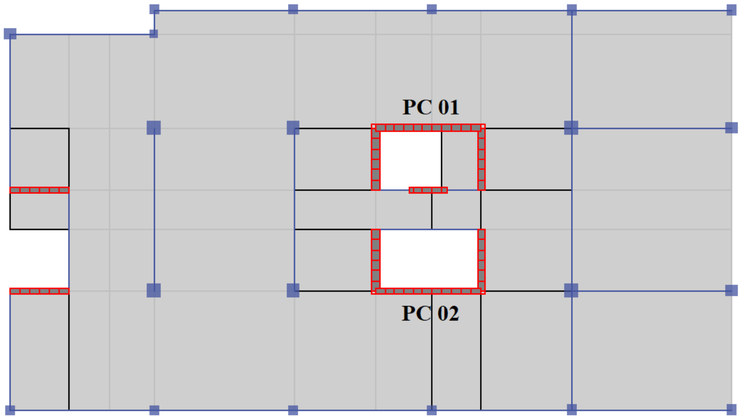

Figure 3.18. Wall numbers on the plan view.

Due to back-stay effects in the rigid basement levels, the internal shear forces on the structural walls obtained using the linear analysis methods specified in the code, are not consistent with NLRHA results at basement levels. For example, while using the two-stage analysis methods in TBSC 2018, when lateral forces are applied to the superstructure (during the first stage) back-stay effects lead to internal shear forces developing in the walls at the basement levels that are in opposite direction to those developing during the 2nd stage of loading (lateral forces applied on the basement levels). Therefore, linear summation of the internal shear forces obtained from the 1st stage of loading, with those obtained from the second stage may result in small internal shear force resultants on the walls at the basement levels. This phenomenon will be demonstrated in the following analysis results. The internal shear forces developing in the U-shaped core walls PC01 and PC02 are compared in Figure 3.19 and Figure 3.20, respectively. In the comparisons, the internal shear forces obtained from the linear analysis methods of TBSC 2018 are design-basis shear forces, meaning that they are amplified by 1.2 times the structural over-strength coefficient (1.2D), as specified in the seismic code for obtaining the design shear forces on structural walls. Comparison of the code-specified linear and nonlinear analysis results indicates that along both directions of the walls, the methods of linear analysis recommended in this study (the 4.7.5 Two-Stage ELF and the simplified 4.3.6.2 Total Structure RSA method with

$R = 2.5$) provide reasonable estimates of wall shear forces along the upper portion of the building. However, back-stay effects on the walls at the lower rigid portion create inconsistencies between the linear and nonlinear analysis results, creating discrepancies in the wall shear forces along the basement levels. Wall shear forces in the basement are underestimated compared to the nonlinear analysis results, especially when the the 4.7.5 Two-Stage ELF method is used in analysis, due to the opposite direction of wall shear forces obtained from the first and second stages of analysis, as described in the previous paragraph.

Therefore, based on the analysis results presented, it is recommended in this study that a constant design-basis shear force is used for shear design of structural walls along the basement levels, for which the design shear force obtained from the analysis (using either the 4.7.5 Two-Stage ELF method or the simplified 4.3.6.2 Total Structure RSA method with $R = 2.5$) cannot be taken smaller that the design shear force obtained at the base of the upper structure, for a depth of at least two basement story heights, as shown by the dashed lines in Figures 3.19 to 3.22.

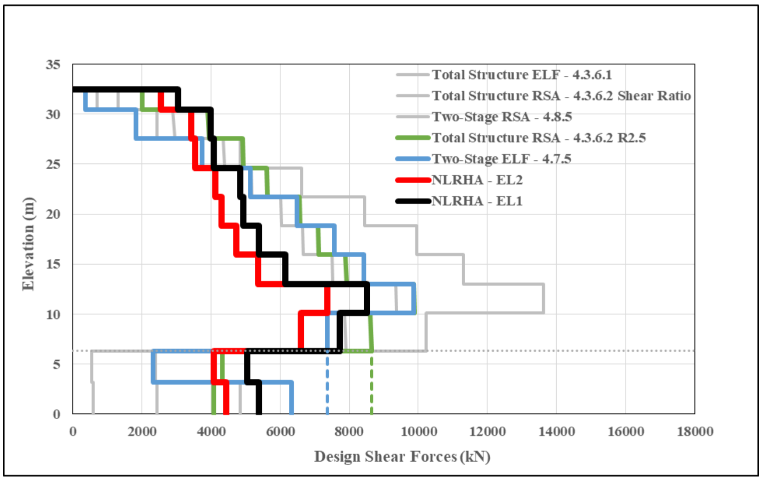

Figure 3.19. Comparison of design shear forces of PC01 in X-direction.

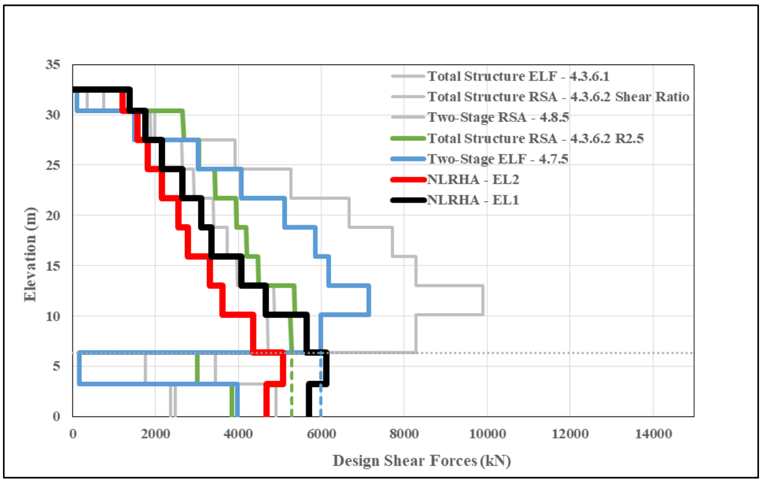

Figure 3.20. Comparison of design shear forces of PC01 in Y-direction.

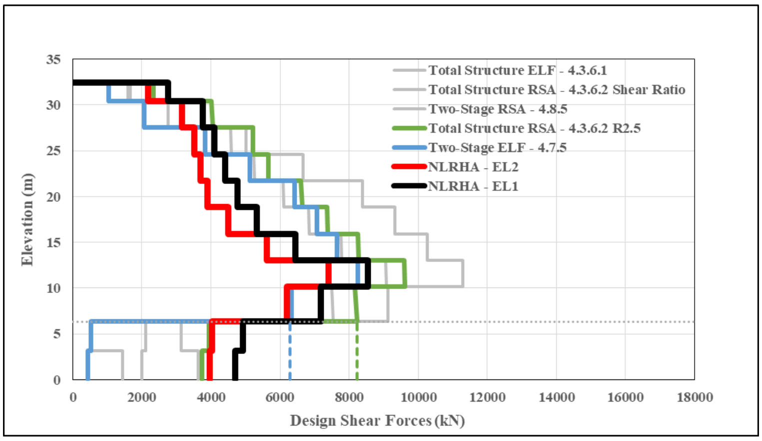

Figure 3.21. Comparison of design shear forces of PC02 in X-direction.

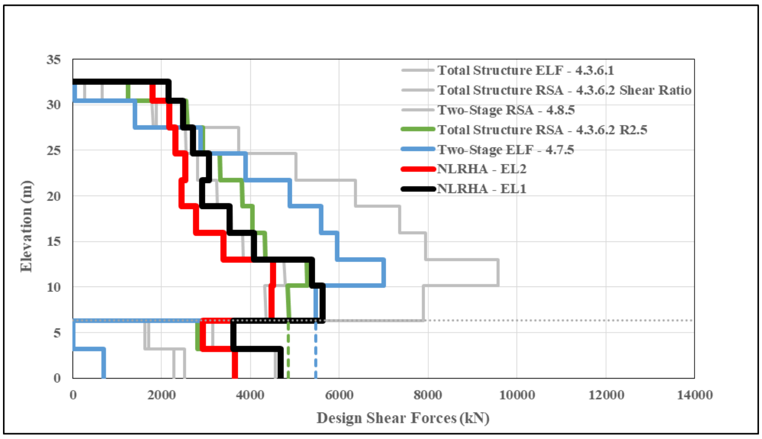

Figure 3.22. Comparison of design shear forces of PC02 in Y-direction.

4. SUMMARY AND CONCLUSIONS

4.1. Summary

In this study, a representative reinforced concrete building structure with rigid basement levels is analyzed based on TBSC 2018 strength-based analysis approaches. In compliance with TBSC 2018, two general approaches are introduced for the analysis of structures with basement levels. To begin with, a two-stage approach is provided in which the superstructure is analyzed by ignoring the basement story masses, but using a unified analysis model that also includes the basement levels. Therefore, not the mass but the stiffness of the basement levels are accounted for in the analysis model. The two-stage approach provides the ability to calculate the earthquake loads on the basement levels separately, but using a single analysis model. With regard to two-stage approach in TBSC 2018, based on the building height, either an Equivalent Lateral Load procedure (Section 4.7.5) or Modal Response Spectrum Analysis procedure (Section 4.8.5) can be applied.. Contrary to ASCE 7-10 and TEC 2007, it is permitted to perform a RSA procedure for the analysis of the rigid lower portion in the 4.8.5 method. On the other hand, a Total Structure approach is provided as an alternative analysis method in TBSC 2018 for buildings with rigid basement levels. Similarly to the Two-Stage Analysis approach, the Total Structure can be used in either Equivalent Lateral Load analysis (Section 4.3.6.1) or Response Spectrum Analysis (Section 4.3.6.2) Despite the fact that there is not a clear statement on mass considerations in the 4.3.6.1 and 4.3.6.2 methods, the total structure mass is taken into account in this study for the analysis of the superstructure as well as basement levels. In addition, despite the fact that 4.3.6.1 method is allowed for the analysis of the structures with basement levels, it is more suitable to use this approach for the analysis of mixed (along height) structural systems in which the upper and lower portion R factors (behavior factors) are close to each other. Therefore, the unexpected base shear values for the rigid lower portion which is obtained based on 4.3.6.1 method can be explained by this phenomenon. Finally, regarding the 4.3.6.1 method, the code intent is to obtain a specific reduction factor of $(\bar{R}_a)_{lower}$ in order to get lower portion design loads. Accordingly, the aforementioned coefficient is not only affected by the ratio of the upper-structure and lower-structure elastic base shear values but also the R and D values of the upper and lower structures. Similarly, in respect of 4.3.6.2 method $(\bar{R}_a)_{lower}$ coefficient is calculated at each mode for each direction in order to obtain a reduced spectral acceleration diagram corresponding to relevant direction while a conservative approach is also provided in which a behavior factor of $R = 2.5$ is taken for the total structure.

Furthermore, main differences between TBSC 2018 and previous Turkish seismic code TEC 2007 are observed. Firstly, in contrast with TEC 2007, element sections are considered to be cracked sections in TBSC 2018, which means that effective stiffness modifiers are used for the structural elements. Therefore, appropriate stiffness modifiers have to be applied to the corresponding elements in respect of Table 4.2 in TBSC 2018 code. Accordingly, due to the elongation in fundamental natural period of the structure because of the reduction in lateral stiffness, corner period criterion is increased from T_a to T_b which is utilized to calculate $R_a(T)$ (spectral acceleration reduction coefficient). Respectively, incorporation of over-strength factor in the calculation of $R_a(T) = 2$ based on TBSC 2018 indicates the importance of structural over-strength which provides the permission to reduce design loads. Moreover, in spite of the fact that 4.7.5 method in TBSC 2018 is defined in identical manner to the ELF procedure in TEC 2007, in which lower portion base shear is obtained through a multiplication of basement floor masses by a spectral acceleration corresponding to $T = 0$, there is not a clear distinction between ductile and non-ductile behavior for the rigid lower system in TEC 2007. However, in accordance with TBSC 2018 specific over-strength factor of D is introduced to consider non-ductile behavior of the rigid lower portion while TEC 2007 intent is to reduce superstructure forces by $R_a(T) = 2$ in order to determine non-ductile response values of the lower system.

Besides, a two-stage analysis approach based on ASCE 7-10 is performed and methodological differences with TBSC 2018 approaches are identified. In compliance with the two-stage analysis method in ASCE 7-10, for structures composed of a vertical combination of a flexible upper system which is supported by a rigid lower portion it is permitted to perform a two-model analysis. However, there are some limitations in which the structure has to comply with all in order to be able to use two-stage analysis. At the first stage the flexible superstructure is modeled as a fixed supported structure in which it can be analyzed in respect of whether ELF or RSA procedure. Secondly, the lower structure is modeled in a separate model. In contrast with TBSC 2018, the lower portion model can only be analyzed using an Equivalent Static Lateral Load procedure, while the response quantities coming from the superstructure model have to be also considered simultaneously. Therefore, the response quantities obtained whether from ELF or RSA procedure for each joint at the base level of the superstructure model are assigned statically to the corresponding nodes in the lower portion model while the values are amplified by the ratio of R/ρ of the upper portion over R/ρ of lower portion.

Furthermore, the Eurocode 8 approach is utilized for the analysis of the representative structure. Accordingly, basement level masses are ignored in the analysis of the total structure. This approach assumes that the earthquake loads acting on the rigid basement levels are fully resisted by the rigid perimeter walls. Therefore, an identical base shear is transferred from the upper portion to the lower portion of the structural system (excluding the perimeter walls). Design of the basement levels can be done considering the behavior factor defined for the upper portion, also considering capacity design principles for brittle failure modes, and the foundation elements can be designed for low ductility class ($R = 1.5$ for reinforced concrete buildings).

Ultimately, response quantities obtained from linear analysis methods of TBSC 2018 are compared to Nonlinear Response History Analysis results for the building investigated. Nonlinear modeling and response history analysis of the structure is conducted in accordance with TBSC 2018 specifications. In addition, the performance level of the structure is evaluated based on story drift ratios, as well as strain limits provided in TBSC 2018 for longitudinal strains in structural walls. The performance evaluation of the structure is presented in APPENDIX A and B of this thesis.

4.2. Conclusions

In light of analyses results obtained using various approaches used in this study, the following conclusions can be drawn:

- A safe and code-compliant design is expected be based on reasonable and consistent structural analysis results. However, the earthquake demands obtained in compliance with the alternative analysis methods specified in TBSC 2018 for the rigid basement levels of building structures incorporate not only uncertainties and difficulties in application, but also show too much scatter in the analysis results, which may potentially lead to either an unsafe or an overly-conservative design of the basement levels.

- In accordance with shear responses, 4.3.6.1 ELF method leads to obtain underestimated base shear values for the lower portion which are almost half of the results derived from 4.8.5 RSA method due to the use of $(\bar{R}_a)_{lower}$ in the calculations of basement levels. Although, the inclusion of basement masses in the calculations of the superstructure results in overestimated design forces for the upper system. Therefore, the use of 4.3.6.1 method is not recommended especially for the analysis of the structures having rigid lower portion. Accordingly, based on TBSC 2018 handbook it is asserted that 4.3.6.1 method is better to use for the analysis of mixed structures having close R factors.

- As demonstrated in this study, the permission to conduct a RSA procedure for the basement levels of a building with respect to the 4.8.5 RSA method (Two-Stage Approach) in TBSC 2018 may lead to overestimated basement story shear force values, which significantly exceed the quantities derived from the alternative (and traditional) 4.7.5 ELF procedure (Two-Stage Approach), and NLRHA results. This is because the fundamental vibration modes of the basement correspond to large spectral acceleration values on the reduced acceleration spectrum of TBSC 2018.

- The 4.3.6.1 ELF method (Total Structure Approach) leads to underestimated story shear values for the basement levels, which are almost half of the results derived from the traditional 4.7.5 ELF method (Two-Stage Approach) due to the calculated value of a $(\bar{R}_a)_{lower}$ for the basement levels. In contrast, the inclusion of basement masses in the ELF calculations for the superstructure results in overestimated story shear forces for the upper portion. The 4.3.6.2 RSA method (Total Structure Approach) also underestimates story shear values at the basement levels when detailed load reduction factor calculations are made (according to the ratio of base shears of the superstructure and total structure) are performed for the basement levels. The use of the 4.3.6.1 method or the detailed 4.3.6.2 method is not recommended for the analysis of the structures having rigid basement levels. These methods are more suitable for the analysis of mixed (along building height) structural systems having close R factors.

- The 4.3.6.2 RSA method, in which a complex calculation of $(\bar{R}_a)_{lower}$ is made for each mode in each direction, the use of base shear ratios for the calculation of the reduction factor ($(\bar{R}_a)_{lower}$) is not consistently meaningful. The calculated reduced spectral acceleration values corresponding to the basement vibration modes (small periods) of the building are supposed to have values that are compatible with the behavior coefficient defined for the basement ($R = 2.5$), whereas analysis results obtained using the 4.3.6.2 RSA method show that the reduced spectral acceleration values for small periods may occasionally correspond to behavior coefficients closer to $R = 6$, which is more representative of the superstructure, contrary to what is expected.

- Due to the fact that the 4.7.5 method of analysis in TBSC 2018 is identical to the ELF procedure provided by previous Turkish seismic code (TEC 2007), the 4.7.5 method can still be considered as the conventional analysis method for design of low or medium rise building structures (for which the ELF method can be applied) with basement levels. However, for Response Spectrum Analysis purposes, the 4.3.6.2 method in TBSC 2018 is recommended in this study, with the condition that the $R = 2.5$ simplification is used to calculate the load reduction factors at the basement levels. Results obtained with the 4.7.5 and the simplified 4.3.6.2 methods were found to be consistent with Nonlinear Response History Analysis results obtained for the building investigated.

- Due to backstay effects on structural walls, even the recommended 4.7.5 and simplified 4.3.6.2 methods may result in underestimated design shear forces on structural walls at the basement levels. Therefore, a design-level shear force envelope is recommended for structural walls in basement levels, for which the design shear force obtained from analysis cannot be taken smaller than the design shear force obtained at the base of the upper structure, for a depth of at least two basement story heights.

4.3. Recommendations for Future Studies

With regards to the scope of this thesis, the following recommendations can be made for future studies:

- The methodologies introduced by TBSC 2018 have to be applied to various structural configurations with different dynamic properties and configurations in order to further validate the results.

- A clear clarification of mass considerations has to be introduced in the 4.3.6.1 method of TBSC 2018 which is provided specifically for the analysis of mixed-along-height structures in which the building composed of a vertical combination of two structures with different R and D values.

- A more reliable design-level shear force envelope needs to be defined for the shear design of structural walls, specifically for buildings having basement levels in which there is a possibility of backstay effects.

REFERENCES

1. Turkish Building Seismic Code, *Specifications for Structures to be Built in Disaster Areas*, Disaster and Emergency Management Presidency, Ankara, 2018.

2. Building Research Institute (P) Ltd., *Seismic Resistant Design*, 2018, `https://www.buildingresearch.com.np/services/erd/erd4.php`, accessed at May 2018.

3. Zafar, A., *Response Modification Factor of Reinforced Concrete Moment Resisting Frames in Developing Countries*, M.Sc. Thesis, University of Illinois at Urbana-Champaign, Urbana, Illinois, USA, 2009.

4. Branci Taeb, B. S., "Accounting for Ductility and Over-strength in Seismic Design of Reinforced Concrete Structures", *Proceedings of the 9th International Conference on Structural Dynamics*, 2014.

5. ASCE/SEI American National Standards Institute (ANSI), *Minimum Design Loads for Buildings and other Structures*, ASCE SEI $7-10$, American Society of Civil Engineers, Reston, VA, 2010.

6. Michael Allen, Ngai-Chi Chung, Alfred Tran, Daniel Zepeda, "Two-Stage Analysis:Implentation Challenges", *Conference Paper*, p. 10.1061/9780784412848.192, 2013.

7. Xiaoli Yuan, *Simplified Seismic Design for Mid-Rise Buildings with Vertical Combination of Framing Systems*, Ph.D. Thesis, University of Waterloo, Ontario, Canada, 2016.

8. D.-G. Lee H.S. Kim, Min Hah Chun, "Efficient Seismic Analysis of High-Rise Buildings Considering the Basements", *Elsevier Science Ltd. Journal of Engineering Structures*, Vol. 24, pp. 613–623, 2002.

9. Thanasis Papageorgiou, Charis J. Gantes, *Mixed-in-Height Concrete-Steel Buildings Under Seismic Actions: Modeling and Analysis*, Beer M., Kougioumtzoglou l., Patelli E., Au IK.(eds) Encyclopedia of Earthquake Engineering, Springer, Berlin, Heidelberg, 2014.

10. Computers and Structures Inc, *Etabs Ultimate v 16.2.1*, 2018, Extended 3D Analysis of Building Structures, Computers and Structures, Inc., California, USA.

11. Turkish Standards Institute, *Design Loads for Buildings*, TS498, Turkish Standards Institute, Ankara, 1997.

12. Turkish Standards Institute, *Requirements for Design and Construction of Reinforced Concrete Structures*, TS500, Turkish Standards Institute, Ankara, 2000.

13. Computers and Structures Inc, *CSI KNOWLEDGE*, 2018, Computers and Structures Inc.,California, USA.

14. Disaster and Emergency Management Presidency, *Turkish Earthquake Hazard Map*, 2018, `https://tdth.afad.gov.tr/`, accessed at May 2019.

15. Turkish Building Earthquake Code Educational Handbook, *Specifications and Sample Applications*, Union of Chambers of Turkish Engineers and Architects, Chamber of Civil Engineers, Ankara, 2018.

16. Turkish Earthquake Code, *Specifications for Structures to be Built in Disaster Areas*, Disaster and Emergency Management Presidency, Ankara, 2007.

17. Eurocode European Comisssion Joint Research Centre, *Seismic Design of Buildings Worked Examples*, 2012, publication Office of the European Union, Italy.

18. Computers and Structures Inc, *Perform 3D V7.0.0*, 2018, Nonlinear Analysis and Performance Assessment for 3D Structures, California, USA.

19. ASCE/SEI Seismic Rehabilitation Committee, *Seismic Evaluation and Retrofit of*

Existing Buildings, ASCE SEI 41−13, American Society of Civil Engineers, Reston, VA, 2014.

APPENDIX A: INTER-STORY DRIFT CONTROLS BASED ON TBSC 2018

In this section, inter-story drift ratios obtained from NLRHA results are evaluated with regard to TBSC 2018 limits. The performance limits are classified as Immediate Occupation (IO), Life Safety (LS) and Collapse Prevention (CP). In accordance with TBSC 2018, under EL-1 earthquake level maximum inter-story drift derived from one ground motion (out of $2 \times 11 = 22$ ground motions) shall not exceed 0.045 while the mean of inter-story drifts obtained from all of ground motions shall be less than 0.03. Inter-story drift values are obtained from 3 stations which is defined in the nonlinear model. In Figure A.1, the location of the stations are presented. Respectively, for each station at each floor level inter-story drifts are obtained for X and Y directions (H1 and H2 directions).

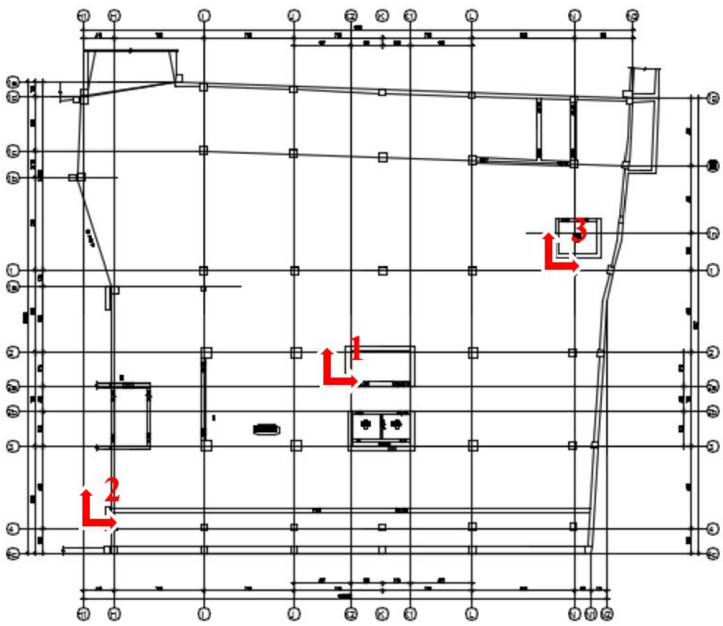

Figure A.1. Location of inter-story drift ratio reading stations.

Although in some cases, under the EL-1 level earthquake outlier results can be observed in the analysis results, which exceed the upper limit of the code. However, the target performance level of the building (Collapse Prevention under the EL-1 level earthquake) can be deemed acceptable, considering inter-story drift ratios.

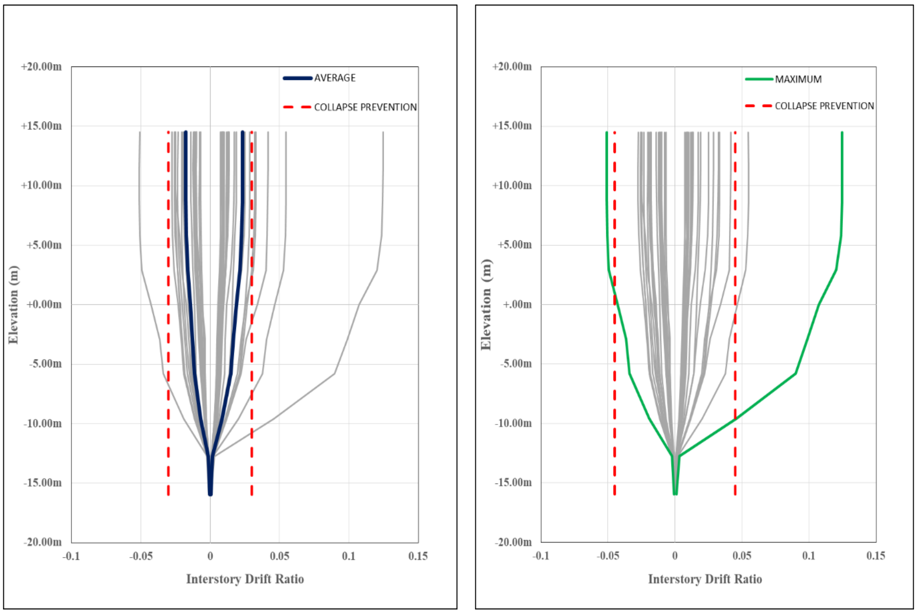

(a) (b)

Figure A.2. Station 1 inter-story drift controls for H1 direction.

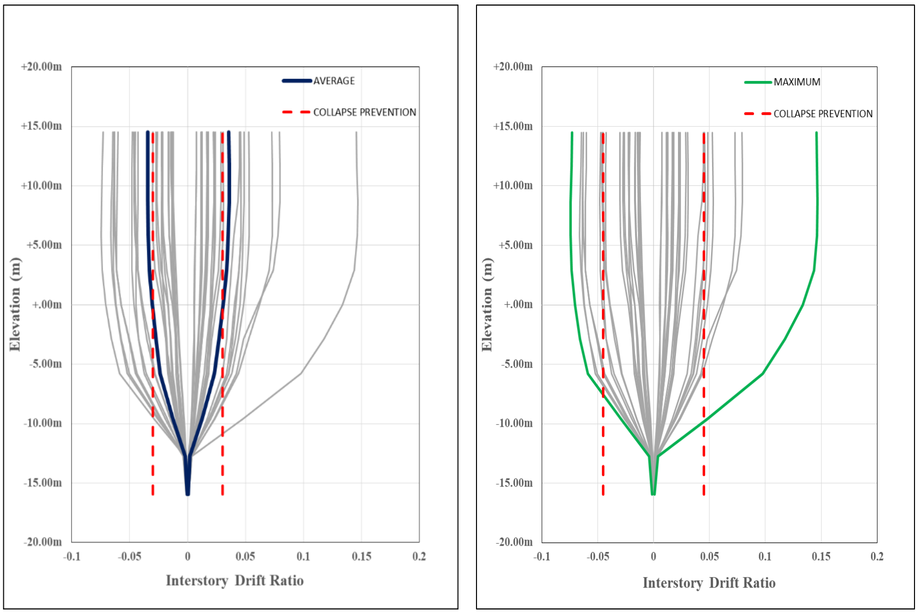

(a) (b)

Figure A.3. Station 1 inter-story drift controls for H2 direction.

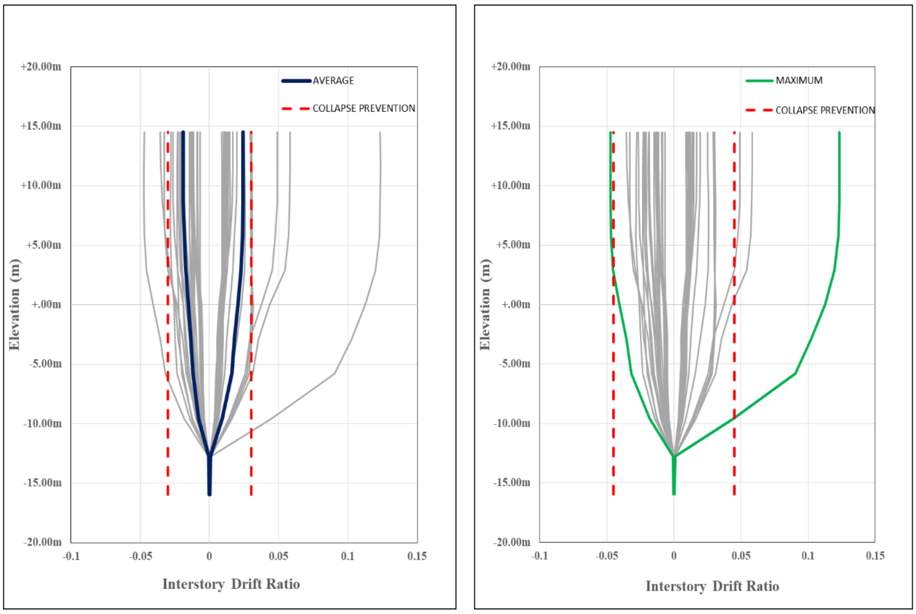

(a) (b)

Figure A.4. Station 2 inter-story drift controls for H1 direction.

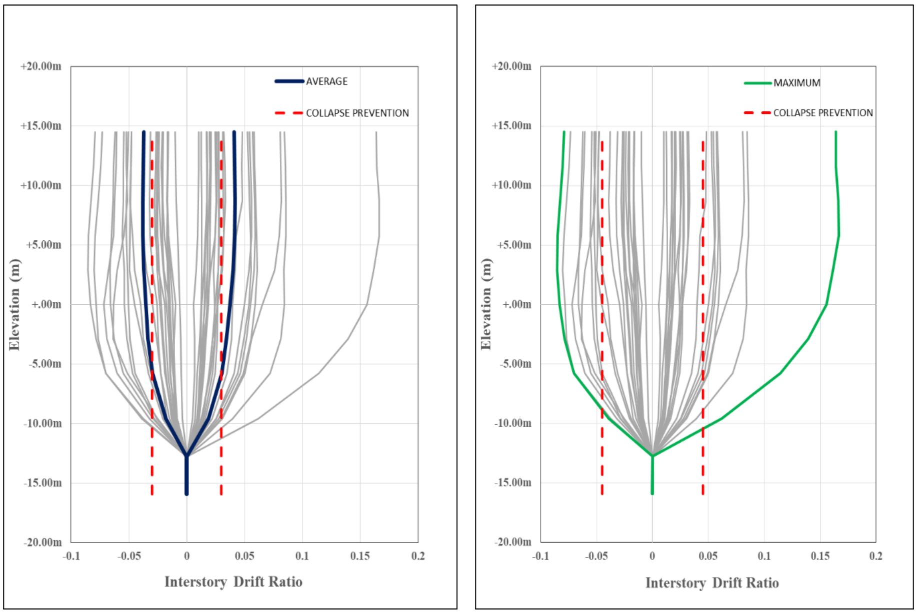

(a) (b)

Figure A.5. Station 2 inter-story drift controls for H2 direction.

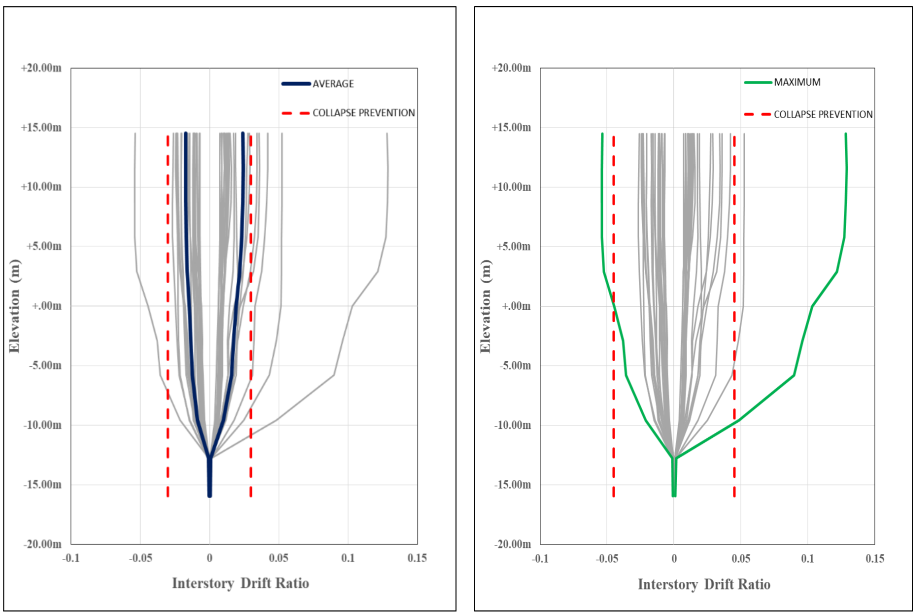

(a) (b)

Figure A.6. Station 3 inter-story drift controls for H1 direction.

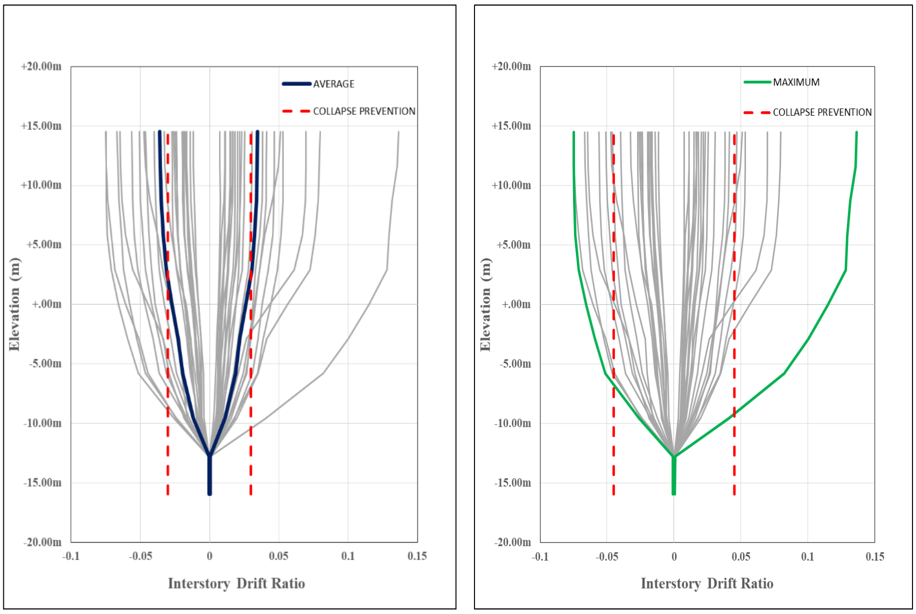

(a) (b)

Figure A.7. Station 3 inter-story drift controls for H2 direction.

APPENDIX B: STRAIN CONTROLS BASED ON TBSC 2018

Longitudinal strains on structural walls are also evaluated with regards to the TBSC 2018 performance limits, for 3 performance limits of IO, LS and CP. The strain gages are defined at the both ends of structural walls as shown in Figure B.1. Thereby, 14 strain gages are specified. Accordingly, strain limits corresponding to performance levels with regard to TBSC 2018 is provided in Table B.1. In terms of longitudinal strains on structural walls, the building satisfies the Life Safety performance level under the EL-1 level earthquake.

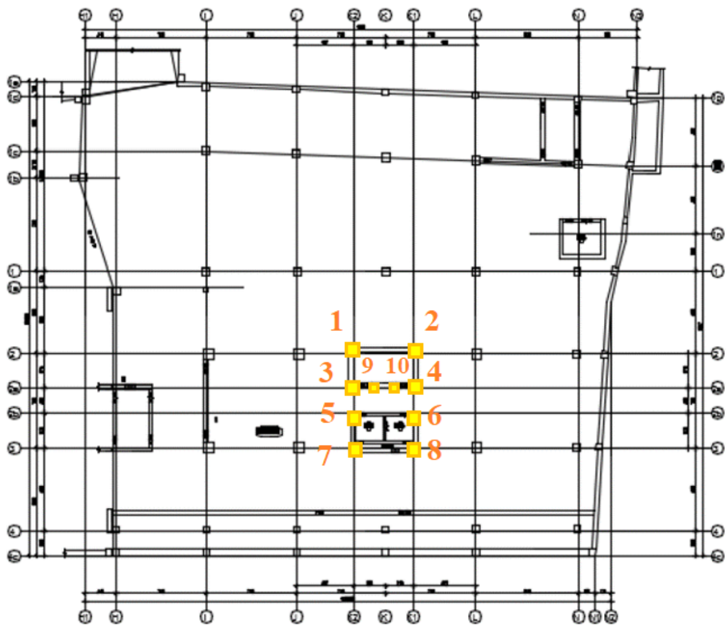

Figure B.1. Location of strain gauges.

Table B.1. Strain limits corresponding to performance levels based on TBSC 2018.

Performance Levels					
Reinforcement			**Concrete**		
Positive IO	Positive LS	Positive CP	Negative IO	Negative LS	Negative CP
0.0075	$0.75\epsilon_s^{(CP)}$	$0.4\epsilon_{su}$	0.0025	$0.75\epsilon_c^{(CP)}$	0.018
0.0075	0.024	0.032	−0.0025	−0.0135	−0.018

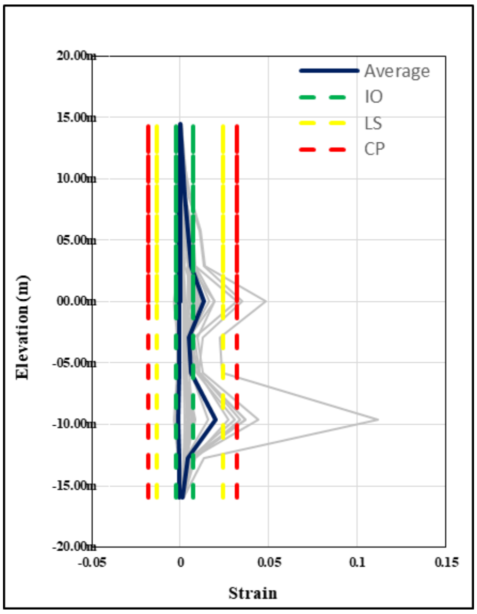

(a) SG01

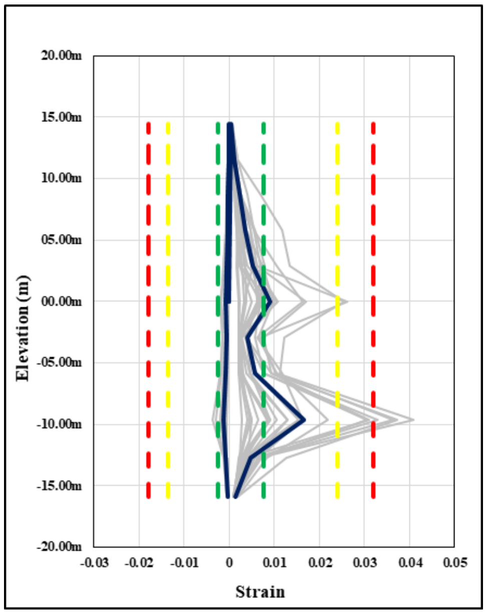

(b) SG02

Figure B.2. SG01 and SG02 strain evaluation.

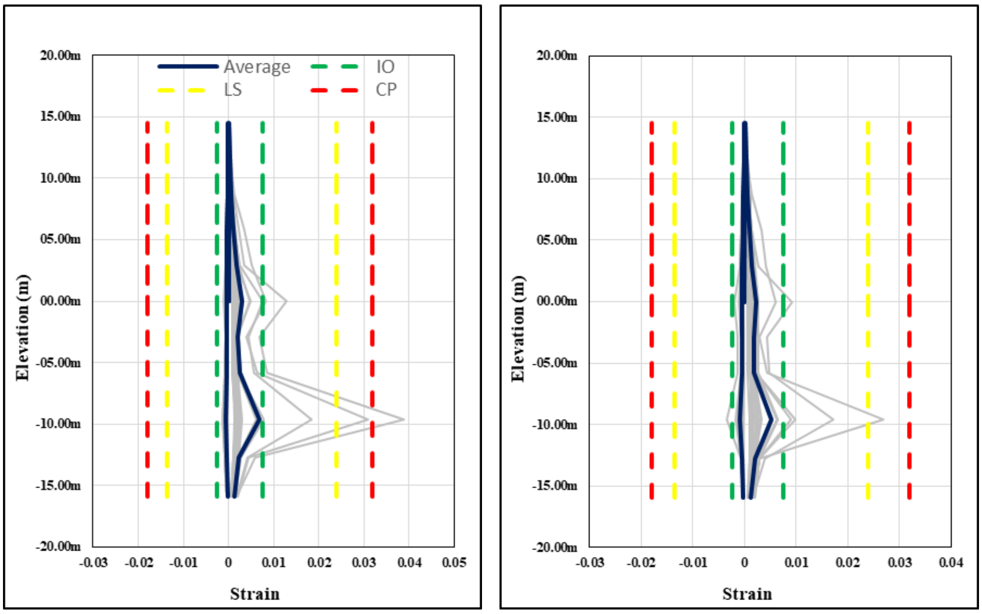

(a) SG03 (b) SG04

Figure B.3. SG03 and SG04 strain evaluation.

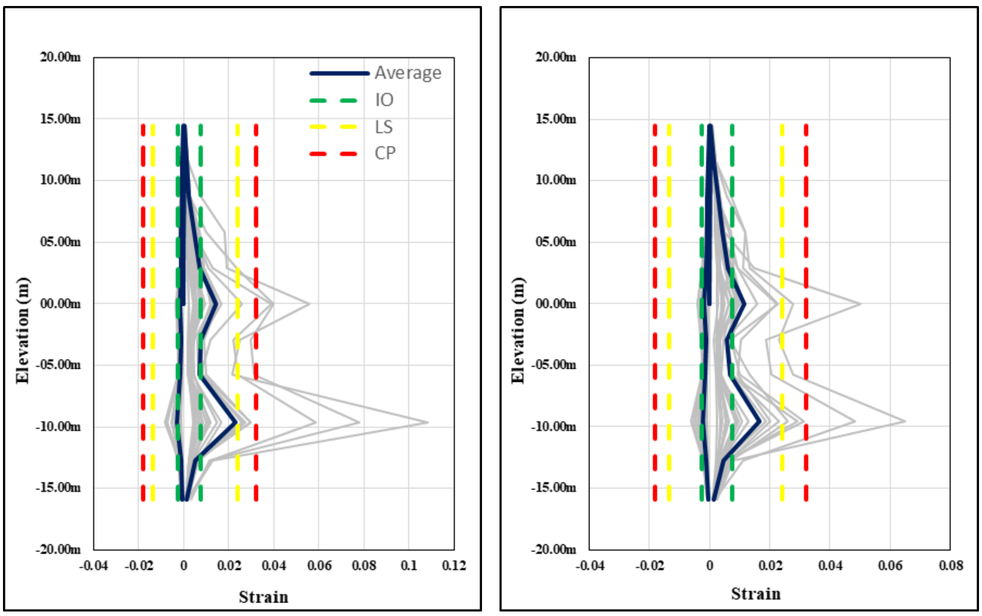

(a) SG05 (b) SG06

Figure B.4. SG05 and SG06 strain evaluation.

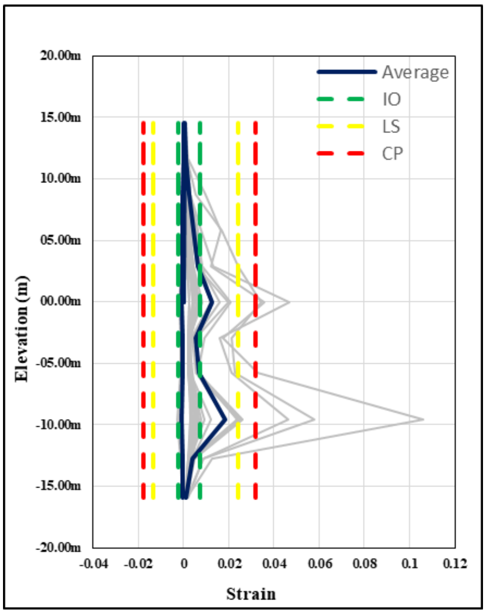

(a) SG07

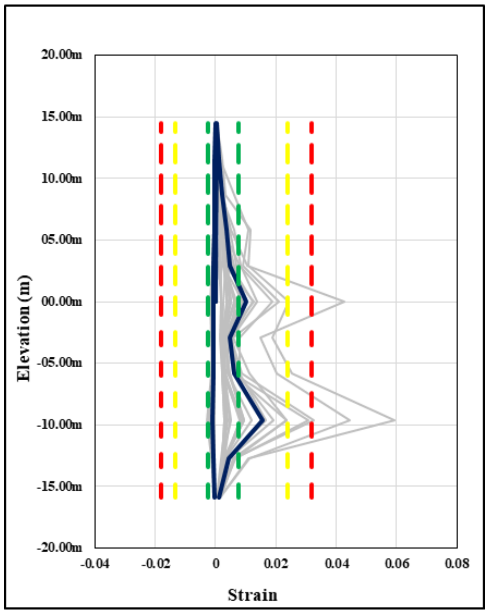

(b) SG08

Figure B.5. SG07 and SG08 strain evaluation.

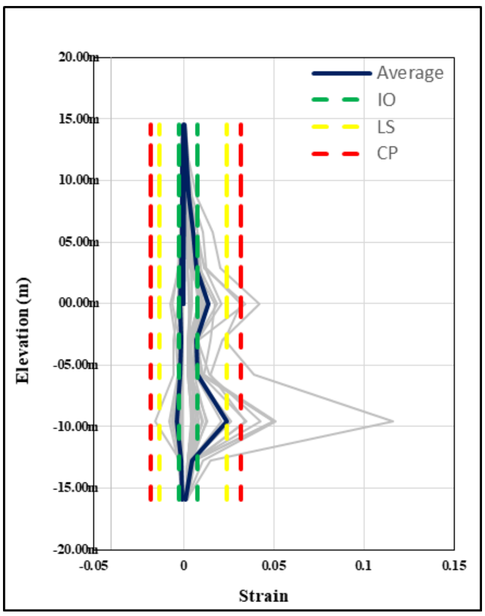

(a) SG09

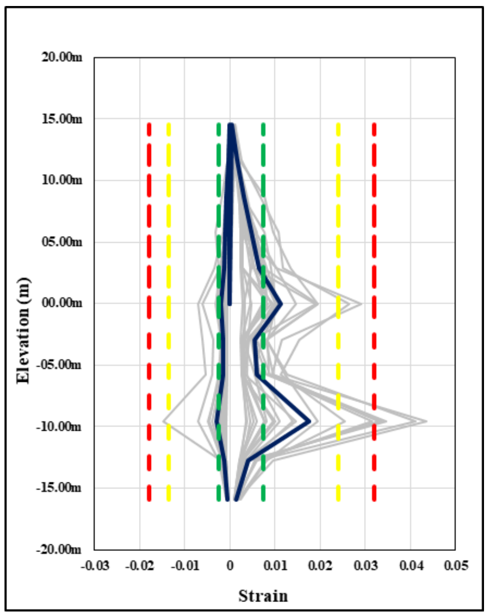

(b) SG10

Figure B.6. SG09 and SG10 strain evaluation.